

Dissertation  
submitted to the  
Combined Faculties for the Natural Sciences and for Mathematics  
of the Ruperto-Carola-University of Heidelberg, Germany  
for the degree of  
Doctor of Natural Sciences

presented by  
Christian Guijarro Řezniček  
born in: Gijón, Spain

# Detection of pollutants in aquatic media using a cell-based sensor

Referees: Prof.Dr. Stefan Wöfl  
Prof.Dr. Michael Wink

# Contents

<b>1</b>	<b>Introduction</b>	<b>1</b>
1.1	Environment . . . . .	1
1.2	Biological-based detection systems . . . . .	3
1.2.1	Biological recognition element . . . . .	4
1.2.2	Transducers . . . . .	6
1.3	Bringing water quality monitoring and biosensors together . . . . .	7
1.4	Model pollutants . . . . .	8
1.4.1	2-Aminoanthracene (2-AA) . . . . .	8
1.4.2	Chlorpyrifos . . . . .	10
1.4.3	3,3',5,5'-Tetrabromobisphenol A (TBBPA) . . . . .	11
1.4.4	4-methylbenzylidene camphor (4-MBC) . . . . .	12
1.5	Detection of estrogen acting xenobiotics . . . . .	14
1.6	The logistical challenge: preservation and transport of a biosensor . . . . .	15
1.6.1	Preservation and protection of cells from temperature fluctuations . . . . .	16
1.6.2	Packaging for transportation . . . . .	18
1.7	The aim . . . . .	19
<b>2</b>	<b>Experimental</b>	<b>21</b>
2.1	Materials . . . . .	21
2.1.1	Chemicals and reagents . . . . .	21
2.1.2	Nutrient media and buffers . . . . .	22
2.1.3	Cytotoxicity assay . . . . .	22
2.1.4	Devices . . . . .	22
2.2	Methods . . . . .	23
2.2.1	Cell culture . . . . .	23
2.2.2	Storage and conservation . . . . .	24
2.2.3	The cell based sensor system . . . . .	24
2.2.4	The sensor chip . . . . .	25
2.2.5	Measurements with the cell based-sensor system . . . . .	27
2.2.6	Cell viability assays . . . . .	28

2.2.7	Functional data analysis, prediction of a chemical pollutant in a sample	29
<b>3</b>	<b>Results</b>	<b>31</b>
3.1	Toxicity measurements using a cell-based sensor system . . . . .	31
3.1.1	Single measurements . . . . .	31
3.1.2	Cell viability measured by an end-point assay, prove of concept . . . . .	37
3.1.3	Simultaneous detection of organic pollutants . . . . .	39
3.1.4	Coexposure of organic pollutants to RLC-18 cells analyzed by MTT . . . . .	43
3.2	Prediction of chemicals in the sample, functional data analysis . . . . .	46
3.2.1	Identification of a polluted sample . . . . .	47
3.2.2	Identification of a concrete chemical in a polluted sample . . . . .	49
3.2.3	Identification of a concrete chemical in mixed samples . . . . .	51
3.3	Proliferation promoting chemicals . . . . .	55
3.3.1	Presence of the ER $\alpha$ in MCF-7 cells . . . . .	56
3.3.2	Cell seeding for a proliferation analysis . . . . .	57
3.3.3	Proliferation analysis of MCF-7 cells after exposure to estrogen (17 $\beta$ -estradiol) . . . . .	58
3.3.4	Proliferation analysis of MCF-7 cells after exposure to TBBPA . . . . .	61
3.4	Overcoming challenges . . . . .	65
3.4.1	Preservation and transport of cell-loaded chips . . . . .	65
3.4.2	Water kills cells, <i>no longer</i> . . . . .	71
<b>4</b>	<b>Discussion</b>	<b>80</b>
4.1	Characteristics of a cell line to suit detection layer requirements . . . . .	80
4.2	Solubility and Sensitivity . . . . .	81
4.3	Beyond acute toxicity of single exposure . . . . .	83
4.4	The long way towards an application . . . . .	84
<b>5</b>	<b>Outlook</b>	<b>86</b>
<b>A</b>	<b>Using other solvents instead of DMSO</b>	<b>87</b>
A.1	Polyethylene glycol (PEG) . . . . .	87
A.2	Saponin . . . . .	88
<b>B</b>	<b>PBS to impede the toxic effect of water</b>	<b>90</b>

# List of Tables

2.1	List of chemicals and reagents . . . . .	21
2.2	List of Nutrient Media and buffers . . . . .	22
2.3	Cytotoxicity assays . . . . .	22
2.4	List of devices . . . . .	22
2.5	Specifications of the Bionas 2500 Analyzing System . . . . .	25
3.1	Overview over the pollutant pairs and the employed concentrations . . . . .	40
3.2	List of models. . . . .	46
3.3	State of gelatin/DMEM mixture dependent on the temperature . . . . .	66
4.1	Solubilities of 2-AA, Chlorpyrifos, TBBPA and 4-MBC in water . . . . .	82

# List of Figures

1.1	Conventional methods to control water quality . . . . .	2
1.2	Schematic overview of the components of a biosensor . . . . .	3
2.1	Cell lines used as detection layer . . . . .	23
2.2	2500 Analyzing System by Bionas GmbH . . . . .	24
2.3	Overview of a cell-based sensor chip . . . . .	26
3.1	Detection of Chlorpyrifos using RLC-18 cells as the sensitive layer . . . . .	32
3.2	Detection of TBBPA using RLC-18 cells as the sensitive layer . . . . .	33
3.3	Detection of 4-MBC using RLC-18 cells as the sensitive layer . . . . .	34
3.4	Detection of 2-AA using RLC-18 cells as the sensitive layer . . . . .	35
3.5	Cell viability of RLC-18 cells after single exposure determined by MTT . . . . .	38
3.6	Detection of Chlorpyrifos and TBBPA using RLC-18 cells as the sensitive layer	41
3.7	Detection of 4-MBC and TBBPA using RLC-18 cells as the sensitive layer . . .	42
3.8	Cell viability of RLC-18 cells after coexposure determined by MTT . . . . .	44
3.9	Prediction of an undefined pollutant in a sample, model quality and validation .	48
3.10	Prediction of chlorpyrifos, TBBPA and 4-MBC as single pollutants, model quality and validation . . . . .	50
3.11	Prediction of chlorpyrifos and TBBPA if present in a mixed sample, model quality and validation . . . . .	51
3.12	Prediction of 4-MBC and TBBPA if present in a mixed sample, model quality and validation . . . . .	53
3.13	Estrogen Receptor ( $\alpha$ -ER) in MCF-7 cells . . . . .	56
3.14	Estrogen Receptor ( $\alpha$ -ER) in RLC-18 cells . . . . .	57
3.15	Comparison of the cell confluency between a chip ready to test the impact of a chemical and a proliferation analysis . . . . .	57
3.16	Detection of a proliferation promoting substance, estrogen, during an exposure time of 3 days using MCF-7 as the detection layer . . . . .	59
3.17	Detection of a proliferation promoting substance, estrogen, during an exposure time of 6 days using MCF-7 as the detection layer . . . . .	60
3.18	Detection of an endocrine disrupting substance, TBBPA . . . . .	62

3.19	Cell viability of MCF-7 cells after exposure to TBBPA determined by calcein assay . . . . .	63
3.20	Physiological viability of RLC-18 cells after 1 day storage at 4°C in gelatin . .	67
3.21	Physiological viability of RLC-18 cells after 3 days storage at 4°C in gelatin . .	68
3.22	Physiological viability of RLC-18 cells after 7 days storage at 4°C in gelatin, transportation from Munich to Heidelberg and 3 days storage at 4°C . . . . .	70
3.23	RLC-18 cells as biological detection layer for water quality control: survival analysis . . . . .	72
3.24	Impact of tap water and rain water on RLC-18 cells after 10h exposure time . .	74
3.25	Impact of water from the river Isar (Munich) on RLC-18 cells . . . . .	75
3.26	Detection of Ni <sup>2+</sup> in tap water using RLC-18 cells as the sensitive layer . . . .	77
3.27	Suitability of RLC-18 as the detection layer for a 1 week long measurement . .	79
4.1	Reliability of RLC-18 cells as the detection layer for the detection of pollutants in aqueous media . . . . .	81
A.1	Effect of the solvent PEG on RLC-18 cells compared to DMSO . . . . .	88
A.2	Efect of the solvent saponin on RLC-18 cells . . . . .	89
B.1	Application of PBS with or without Ni <sup>2+</sup> for 10 minutes . . . . .	91

# List of Abbreviations

2-AA	2-Aminoanthracene
4-MBC	4-methylbenzylidene camphor
ATP	Adenosine Triphosphate
BenMen	Benign Meningioma Cells
BSA	Bovine Serum Albumin
CTRL	Control
DMSO	Dimethyl Sulfoxide
DMEM	Dulbecco's Modified Eagle Medium
DSMZ	Deutsche Sammlung von Mikroorganismen und Zellkulturen
E2	17- $\beta$ Estradiol
EDTA	Ethylenediaminetetraacetic Acid
EFSA	European Food Safety Authority
EPA	Environmental Protection Agency
ER	Estrogen Receptor
EU	European Union
FCS	Fetal Calf Serum
FGLM	Functional Generalized Linear Model
FGM	Functional Generalized Model
h	Hour
Hepes	N-(2-hydroxyethyl)piperazine-N'-(2-ethanesulphonic) acid
IDES	Interdigitated Electrode Structure
ISFET	Ion-Sensitive Field-Effect Transistors
M	Molar
MCF-7	Michigan Cancer Foundation-7
min	Minute
MTT	3-(4,5-dimethylthiazol-2-yl)-2,5-phenyltetrazolium bromide
PBS	Phosphate Buffered Saline
RLC-18	Rat Liver Cells
RM	Running Medium
RT	Room Temperature
TBBPA	3,3',5,5'-Tetrabromobisphenol A
TX	Triton-X
UV	Ultraviolet
WHO	World Health Organization



## Abstract

Water is a precious good which in good quality we need essentially to survive. In this work a novel method for the detection of bioactive pollutants in aqueous media will be presented. It is based on a sensor system, which uses mammalian cells, RLC-18 (rat liver cells) or MCF-7 (breast cancer cell line) as the detection layer for harmful substances. With these mammalian cells as the sensing layer a metabolically active sensor interface will become available reflecting the physiology of living organisms. In this work the cell layer is cultured on a multi-electrode silicon chip and the response of the cells to toxic substances is monitored by recording morphological changes, oxygen consumption, as well as the acidification properties of the cells.

Until now there is no easy-to-use system that can detect the overall toxicity of a water sample. Analytical chemistry can be used to detect chemical substances at very low levels, down to few picograms. However, only substances known to be harmful will be analyzed in dedicated protocols. New, unknown chemicals or derivatives can be present unnoticed. For this work, four known organic pollutants were chosen as model substances to test the sensitivity and reliability of the developed system: 2-Aminoanthracene (2-AA), a heterocyclic amine used in dyes, drugs, inks and plastics; chlorpyrifos, an organophosphate insecticide; 3,3',5,5'-Tetrabromobisphenol A (TBBPA), a flame retardant; and 4-methylbenzylidene camphor (4-MBC), an ultraviolet filter. RLC-18 cells were exposed to these chemicals in single and combinatorial measurements. These measurements revealed, which physiological parameters were targeted, and at which time point during treatment the toxic effect occurred. Cotreatment with various combinations showed how the chemicals interacted with each other either by reinforcing their toxicity or mitigating it. Moreover, also cell promoting effects of certain substances could be detected using this system. Proliferating effects could indicate hormonal activities of the pollution. In this context, the focus was on compounds mimicking the effect of estrogen, which can be detected using MCF-7 cells as the detection layer since this cell line expresses the estrogen receptor and shows hormone dependent growth.

Due to the different options for the interaction of pollutions, a more dedicated analysis was required. In order to predict the presence of a pollutant in a sample, even in the presence of another compound that could suppress the expected physiological effect, an algorithm using functional data analysis was designed and an analytical protocol including analysis software was developed.

A major problem was the maintenance of the cell layer, to make it suitable for application in the field. For this a gelatinous medium was developed to protect the cells against impacts, dehydration and temperature variations during storage and transportation. This gel medium permitted the storage of cell loaded chips at 4°C for up to one week. Moreover, it could be demonstrated that, with some optimization, this system can be used to analyze natural water samples from different sources.

Taken together, the cell-based detection system developed in this work could be used for the detection of pollutants with acute toxicity and other biological activity. With this work, it could be shown that a future cell based sensor system should be an ideal toxicity monitor, to continuously record, in “real time”, the quality of inshore waters as a reliable toxicity meter.

## Zusammenfassung

Wasser ist ein kostbares Gut, welches wir in guter Qualität zum Überleben brauchen. In dieser Arbeit wird ein Sensorsystem zur Erkennung bioaktiver Schadstoffe in wässrigen Medien vorgestellt. Dieses System basiert auf Säugerzellen, RLC-18 (Leberzellen aus der Ratte) oder MCF-7 (humane Brustkrebszellen), die als Detektorschicht zur Erkennung von Gefahrenstoffen dienen. Der metabolisch aktive Sensor stellt die Schnittstelle zu der Zellulären Detektorschicht dar und spiegelt die Physiologie lebender Organismen wider. Diese Schicht lebender Zellen wird auf der Oberfläche eines Silizium-Chips kultiviert, dessen Elektroden Veränderungen in der Morphologie, Atmung und Ansäuerung der Zellen misst.

Bis jetzt gibt es kein einfach zu bedienendes System, welches die allgemeine Toxizität einer Wasserprobe analysiert. Analytische Chemie kann verwendet werden um Substanzen im Picogramm-Bereich zu detektieren. Neuartige Substanzen oder Derivate herkömmlicher oder neuartiger Substanzen bleiben somit unerkannt. Für diese Arbeit wurden vier organische Substanzen ausgewählt, um die Sensitivität und Zuverlässigkeit des Systems zu ermitteln: 2-Aminoanthracen (2-AA), ein heterozyklisches Amin welches in Farben, Tinte und Plastik vorkommt; Chlorpyrifos, ein Insektizid aus der Gruppe der Organophosphate; 3,3',5,5'-Tetrabromobisphenol A (TBBPA), ein Flammenschutzmittel; und 4-methylbenzyliden Campher (4-MBC), ein Filter gegen UV-Strahlung. RLC-18 Zellen wurden diesen Chemikalien in Einzel- und Kombinationsmessungen ausgesetzt. Die Messungen zeigten welche physiologischen Parameter angegriffen sowie der Zeitpunkt des Wirkungseintritts. Die Kombinationsmessungen zeigten, wie die Substanzen miteinander interagieren und den Effekt auf den Zellmetabolismus entweder verstärken oder hemmen können. Der Wachstumsfördernde Effekt mancher Substanzen, wie Hormone, kann durch dieses Systems ebenso detektiert werden. In diesem Zusammenhang wurden MCF-7 Zellen als Detektorschicht verwendet um Östrogenähnliche Substanzen zu erkennen, da diese den Östrogenrezeptor exprimieren.

Um ein Gefahrstoff erkennen zu können, welches den physiologischen Effekt eines zweiten Stoffes tarnt wurde ein Algorithmus basierend auf funktionaler Datenanalyse programmiert.

Eine große Herausforderung stellte die Aufrechterhaltung der Zellschicht dar um diese in einen Einsatzort zu verwenden. Ein gelartiges Medium wurde entwickelt um die Zellen gegen Stöße, Austrocknung und Temperaturschwankungen während des transports zu schützen. Darüber hinaus ermöglicht dieses Gel auch die Lagerung eines mit Zellen bewachsenen Chips bis zu einer Woche bei 4°C. Als letztes wurde das System dahingehend optimiert, dass Wasserproben ohne Extraktion oder Aufkonzentrierung der darin vorhandenen Substanzen gemessen werden können.

Das hier entwickelte und vorgestellte System könnte zur Erkennung biologisch aktiven Gefahrstoffen mit akuter Toxizität verwendet werden. Diese Arbeit zeigt das in der Zukunft ein Zellbasiertes Sensorsystem zur Überwachung der Wasserqualität in Echtzeit verwendet werden könnte.

# Chapter 1

## Introduction

### 1.1 Environment

Industrial chemicals, pharmaceutical drugs, personal care products, pesticides, herbicides and chemical additives have in common that their production is increasing continuously because we human need them more and more. But at the same time all these anthropogenic substances challenge the environment and some of them may represent an ecological and/or human-health risk. One of the main concerns is that these compounds end up in soil, ground and inshore waters like pointed out in *Science*, vol. 295, pg. 2209, 22 March 2002. Humans may come in contact with these chemicals directly or via the food chain as described in Ritter et al. (2002) and Eltzov and Marks (2011). Some contaminants can be localized in their source and thus may be controllable at the local level. Others can be found in remote areas far away from their source of origin and travel long distances through long-range transport (Evans et al., 2005). These organic pollutants retain their toxicity and still degrade after several decades. Special effort is being put on reducing circulating organic pollutants. So does the United Nations Environmental Programme (UNEP) on a global scale, the Water Framework Directive (WFD) in the European Union and the U.S. Environmental Protection Agency (EPA) within the boundaries of the United States.

Even if certain water quality parameters, like oxygen deficiency or phosphate concentration, have ameliorated over the last decades in the European Union (Fuerhacker, 2009), there are still contaminants, mainly organic pollutants, whose short and/or long-term consequences are yet not completely known and remain still to be elucidated (Eltzov and Marks, 2011).

More over, it is conceivable the existence and presence of new chemicals or still unknown

degradation products thereof which remain yet undetectable for conventional analytical methods.

Conventional analytical methods are a prime reason for having lunched this PhD thesis. Analytical methods are good if not fantastic, precise, sensitiv and reliable. In fact, the accuracy how the German Government takes care about the inshore waters within its frontiers is remarkable and worth to venerate in the following sentences.

In regular time intervals, maximal once per month, workers from the State Office for Environment, for example the bavarian, take water probes from a river, lake, water treatment plant, groundwater etc (see figure 1.1 A). Temperature, pH value and turbidity of the water are determined on site<sup>1</sup>. For a detailed and precise determination of its costitution the water sample is taken to an analytical laboratory. The samples must first be prepared for an analysis, relevant compounds are extracted from the sample, cleaned up and enriched. Then they can be quantified using gaschromatograhy or liquidchromatography. An inorganic (see figure 1.1 A), organic (see figure 1.1 B) and biological (see figure 1.1 C) analysis is performed<sup>2</sup>.

The biological analysis ensures that the biotop is not altered, the organisms behave in a healthy manner and the concentration and variety of plancton remains constant.

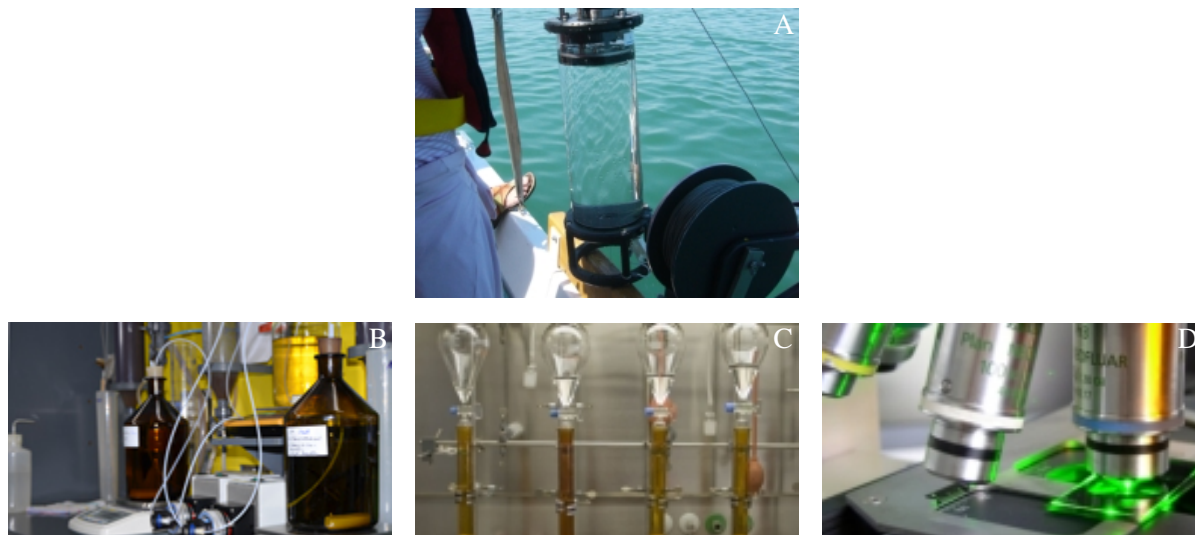


Figure 1.1: How the quality of water is monitoed nowadays. A water probe is taken from with a scoop (A), after storage, cleaning up, sample enrichment an analytical inorganic (B), organic (C) and biological (D)analysis is performed to determine the composition of the sample and detect and quantify possible pollutants present in the probe.

---

<sup>1</sup>Source: Bavarian State Office for Environmen, [http://www.lfu.bayern.de/wasser/gewaesserqualitaet\\_seen/untersuchungsprogramme/index.htm](http://www.lfu.bayern.de/wasser/gewaesserqualitaet_seen/untersuchungsprogramme/index.htm) (Jun. 26, 2014)

<sup>2</sup>Source: Bavarian State Office for Environmen, [http://www.lfu.bayern.de/analytik\\_stoffe/index.htm](http://www.lfu.bayern.de/analytik_stoffe/index.htm) (Jun. 26, 2014)

In this way the governmental monitoring program tries to cover all possible sources of pollutants ranging from metals to organic species like pesticides, synthetic materials, detergents and solvents.

But more than 100,000 different chemical are produced in the European Union<sup>3</sup>, stored, used and disposed of. There are several thousands of kilometers of rivers, thousands of lakes, billions of cubic meters water in Europe. Even if all States have a good running water quality monitoring program, covering the detection of every single substance is a huge challenge.

The question is, if it is possible, not to replace conventional analytical methods and strategies, but to improve them, and to back up them. The scope is to get information about imminent danger faster. If a sudden threat happens it is better to react instantly. For this purpose, biological-based sensors are promising tools.

## 1.2 Biological-based detection systems

The International Union of Pure and Applied Chemistry (IUPAC) defines a biosensor as a device that transforms biological or biochemical information into an analytically usefull signal (Thévenot et al., 2001). The structure of a biosensor may be divided in the biological detection layer, and a transducer (see figure 1.2 for an schematic diagram). The analytes bind to the biological detection layer. This binding evokes a biological alteration of the sensing layer causing

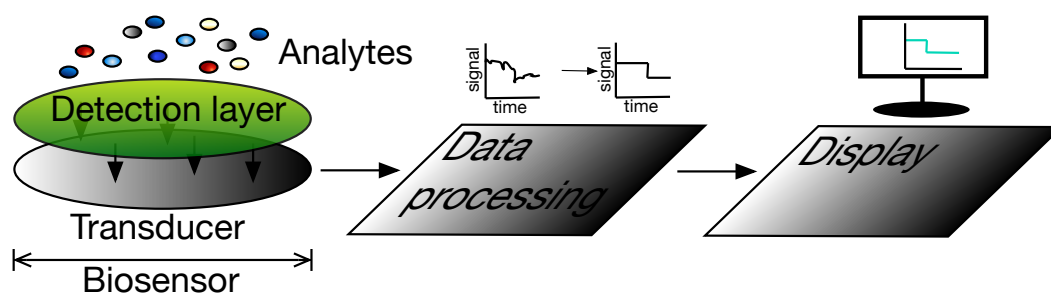


Figure 1.2: Schematic overview of the components of a biosensor. The analytes bind to the biological detection layer causing its alteration. The biological signal is relaid to the transducer which converts it to a electronical read-out ready to be processed. The ongoing measurement can be followed in real time.

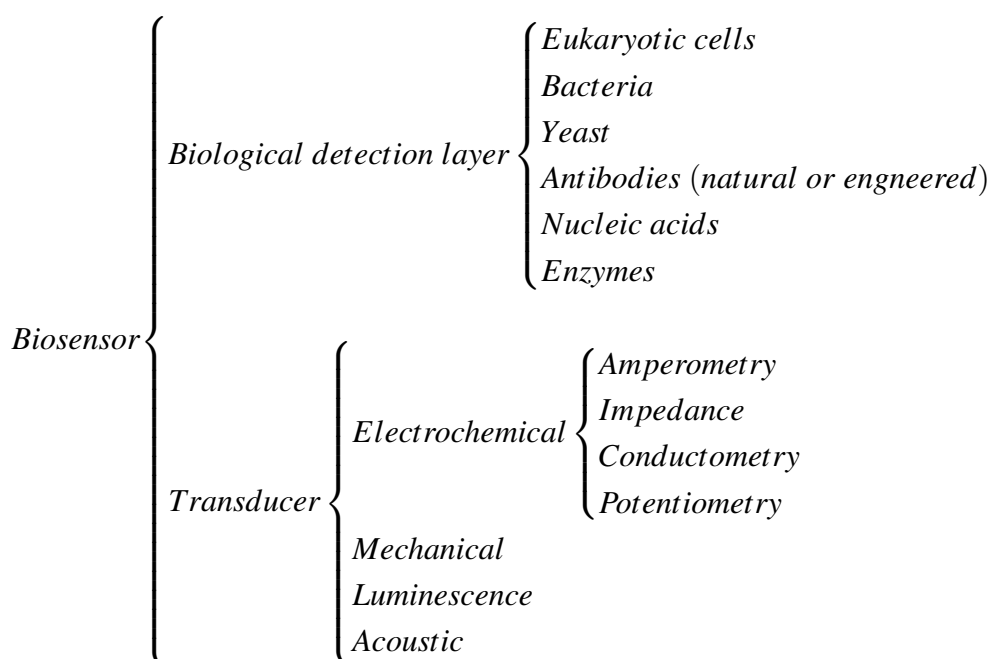
---

<sup>3</sup>Source: Bavarian State Office for Environmen, [http://www.lfu.bayern.de/analytik\\_stoffe/analytik\\_org\\_stoffe\\_leistungsspektrum/index.htm](http://www.lfu.bayern.de/analytik_stoffe/analytik_org_stoffe_leistungsspektrum/index.htm) (Jun. 26, 2014)

a physical or chemical response which is transferred to the transducer (Eltzov and Marks, 2011). The transducer interpretes this chemical or physical signal and converts it into a read-out which can be processed by a data analysis software (Ronkainen et al., 2010). Finally, the events taking place on the biosensor are displayed in a comprehensible manner on a screen.

There are actually a variety of biosensors being developed and proven for functionality and efficacy. The classification of them takes place on the basis of the nature of the used detection layer and the method used to transduce the biological signal into an electrical read-out.

The following scheme depicts the most widely used detection layers and transducers:



In the next two subsections all these possibilities are going to be explained and defined briefly .

### 1.2.1 Biological recognition element

The biological recognition element is the layer directly interacting with the target analyte(s). The choice of this layer will determines the selectivity of the sensor and up to a certain point the choice of the transducer since not all biological signals can be relaid, read and interpreted by all transducer technologies. Whole-cells as well as molecules can be used as the detection layer. Bacteria and yeast have gained in importance in the last decade. Mainly because they allow easily and efficiently the transfection of a reporter gene encoding luciferase or green fluorescence protein (GFP) (Burbaum and Sigal, 1997; Scheirer, 1997; Su et al., 2011). Technically speaking, the sensing element is the regulatory protein or the promoter sequence. This sequence

accounts for the selectiveness of the assay (Ramanathan et al., 1998; Eltzov and Marks, 2010). Only the contaminants able to activate the regulatory protein(s) which in turn activate the reporter genes will be detected.

The third and last possibility of a whole-cell biosensor is the use of eukaryotic cells, specially mammalian cell lines (Alborzinia et al., 2011). The advantage of biosensors using mammalian cells over those using bacteria or yeasts is that their response to toxic compounds may resemble more the one of humans. More over, only by using this living component it is possible to obtain functional information (Bousse, 1996).

Another possibility instead of using whole-cells is the usage of biomolecules. Enzymes for instance have been used for the detection of glucose (in this specific case the glucose oxidase) (Clark and Lyons, 1962). This biosensor from 1962 represents the first in history and the emerging of a new technology. But the use of other enzymes like tyrosinase has enabled the detection of environmental pollutants like diuron and atrazine (Anh et al., 2004), also pathogens in food and methamphetamine in human urine could be detected using enzymes as the sensing layer of a biosensor (Yagiuda et al., 1996).

A high selectivity is accomplished by using antibodies against a specific antigen. The affinity constant of the binding between an antibody and an antigen is of the order of  $10^6$  (Eggins, 2002). This high affinity and selectivity has made it feasible to detect analytes in the concentration range of just a few pM (Senveli and Tigli, 2013). The drawback of using antibodies as the biological recognition element in a biosensor is the fact that the synthesis of an antibody against a certain antigen is fairly difficult, time-consuming and costly (Subramanian, 2004).

Nucleic acid layers are another featured biological recognition element. Here, 20–40 basepair single-stranded DNA segments are immobilized on the sensor surface. These segments have the ability to selectively bind the target DNA (Bartlett, 2008). One way to visualize the binding of the target segment is to use a redox active label. The immobilized segment is by design shorter than the target strand. This leaves a segment where a short DNA probe containing an electroactive species can bind. Amperometry (see section below 1.2.2) enables the measurement of the current due to the oxidation of the label (Takenaka et al., 2000).

After the analyte has been bound or detected by the biological recognition layer, the biological has to be converted into a signal that can be interpreted and analyzed. This job is performed by a transducer.

### 1.2.2 Transducers

The transducer converts the biological signal relayed by the biological sensing layer to a more or less interpretable read-out (more or less because usually a correct interpretation is enabled not before a downstream data processing system analyzes the data). There are several possibilities to convert the biological signal to an electrical read-out.

For whole-cell-based sensors an amperometric transducer monitors the changes in current generated by an electrochemical oxidation or reduction of an electroactive species like oxygen. The redox reaction and the subsequent current results from the maintenance of a constant potential at the working electrode with respect to a reference electrode (Ronkainen et al., 2010). This technique enables for example the monitoring of oxygen consumption.

Electrical impedance spectroscopy measures charge transfer processes occurring at electrode-electrolyte interface and thus characterizes the dielectric properties of a biological system (Lagarde and Jaffrezic-Renault, 2011). A cell consists, very simplified, of a nucleus, a conducting cytoplasm and a thin insulating cell membrane. If the cells are exposed to an electric field the cell behaves due to the cell membrane as an insulating object. The electric field is prevented to penetrate the cell (Sun et al., 2010). The electrical impedance reflects the disruption of an electric field by an intact cell membrane. Therefore this transducer enables to track micromotion, cell attachment and spreading, cell concentration and growth and apoptosis (Giaever and Keese, 1993; Xiao and Luong, 2003; Hong et al., 2011).

Conductometry measures changes in the electrical conductivity of a solution while its composition is changing in the course of the time due to a chemical reaction (Ronkainen et al., 2010). The sensing layer is often composed of enzymes whose charged products alter drastically the conductivity of the solution (Muhammad-Tahir and Alocilja, 2003).

A potentiometric transduction detects the difference of potential between the electrode where the cells are immobilized and a reference electrode while a negligible current is flowing between them (Lagarde and Jaffrezic-Renault, 2011). The classical glass pH-electrode works in this manner as well as  $\text{Ca}^{2+}$ ,  $\text{Na}^{+}$  and  $\text{Cl}^{-}$  detectors (Eggins, 2002).

Mechanical sensing uses in essence biomolecules immobilized on a cantilever. In case of a static cantilever the binding of the target analyte to the biomolecule causes it to bend. A second modality is a resonant device where the binding produces an alteration in the deflection frequency of the cantilever (Senveli and Tigli, 2013). The bending or resonance characteristics are the read-out of these biosensors. This principle is mainly used for molecule-based sensors.



Since bioluminescens have come on the scene of biosensors, it has been widely used for water monitoring purposes. Mainly light-producing bacteria have been engineered using recombinant DNA (Kim and Gu, 2003). This method takes advantage of the specific gene activation of certain contaminants. A DNA segment encoding for example luciferase or green fluorescence protein is placed downstream of the target promoter. The binding of an analyte to an extra- or intracellular receptor will activate the corresponding molecular pathway leading to the transcription of a light producing protein (Bhattacharyya et al., 2005; Eltzov and Marks, 2011). This light emission is detected and evaluated.

Typical acoustic sensing consists in an immobilized receptor molecule layer. Acoustic waves are propagated through the solid substrate of the sensor. If a molecular recognition and binding to the target analyte happens, a shift in the resonance frequency will occur (Saitakis and Gizeli, 2012). This transducer technology has been also used to study eukaryotic cell attachment and spreading. Also morphological changes due to cytoskeleton impairment or cell to cell contact variations after drug application has been studied (Marxer et al., 2003; Braunhut et al., 2005).

### **1.3 Bringing water quality monitoring and biosensors together**

This introductory chapter was opened arguing how and why conventional analytical methods for water quality monitoring could be improved (section 1.1). Next up, we presented, defined and explained what a biosensor is. Now it is time to bring these two issues together rounding out the motivation of this thesis.

As referred before, new chemicals and materials are being synthesized with more and less biodegradable intermediates. This evolution in synthetic materials should be accompanied by an evolution in detection systems.

Novel and skilful chemical, physical and biological detection systems for environmental monitoring (Ho et al., 2005; Lieberzeit and Dickert, 2007, 2009; Jimenez-Jorquera C, 2010) try already to counteract this global request. These multiselective approaches detect a variety of chemicals whether in gases or in an aqueous phase. But selectivity means that they are limited to only a certain amount of substances.

This study was carried out using a technology switching from selective and single substance detection towards overall toxicity detection systems. This could enable rapid quality assessment of inshore waters as complex matrices and specify the toxic effects for living organisms

which get in contact with these media. The physiological parameters of the cellular detection layer –metabolism, mitochondrial integrity and cell-morphology– are the electrical read-out of this system and indicate the point of action of the pollutant or the mixture of pollutants present in the sample.

First tests have been run using this system with samples containing heavy metals like  $\text{Ni}^{2+}$  and  $\text{Cu}^{2+}$  showing the potential of this technology for the discrimination of a clear and polluted sample (Kubisch et al., 2012a). Now it is time to extend the spectrum of detectable substances and improve the system towards a water applicability.

## 1.4 Model pollutants

In Europe the Water Framework Directive defines a number of biological, chemical and physical parameters that should be part of broad range monitoring programs with a focus on 33 priority chemical substances. Two of the listed priority substances were also chosen for this work: 2-Aminoanthracene, a polyaromatic hydrocarbon and derivative of anthracene, and chlorpyrifos, a pestizide.

The flame retardant 3,3',5,5'-Tetrabromobisphenol A (TBBPA) was also tested as it is a wide used chemical and meanwhile present in many products of our daily life.

The fourth substance, also an organic one, is 4-methylbenzylidene camphor (4-MBC). It is a UV-filter and due to the intense public dicussion about its toxicity it was also taken into account in this study.

### 1.4.1 2-Aminoanthracene (2-AA)

2-Aminoanthracene is a heterocyclic amine synthesized for a variety of industrial purposes like dyes, drugs, inks, plastics and agricultural chemicals (Boudreau et al., 2006). It can also be produced naturally and unintended during the frying of meat and burning of tobacco. This occurs mainly by nitration of a polycyclic aromatic hydrocarbons (PAHs). Therefore other combustion processes occurring in vehicles, aircrafts, industries or wood burnings are as well sources to produce 2-AA (Baker et al., 2001).

Due to the easy exposure of human to 2-AA and in general to many other heterocyclic amines, these chemicals have become of public interest. The World Health Organization describes in an official document, Environmental Health Criteria 229 written by J. Kielhorn among others, in

detail their sources of exposure, environmental consequences and effects on laboratory animals and humans (WHO, 1998).

Ambient air monitoring in selected urban environments around the world like St. Louis, Missouri, USA; Tokio, Japan; Florence, Italy; Copenhagen, Denmark; Bayreuth, Germany; Damascus, Syria has revealed the presence of heterocyclic amines. Also in the amazon forest near biomass burning were particles of heterocyclic amine detected (WHO, 1998).

Although the presence of these chemicals seem to be ubiquitous present in ambient air their presence in water has fortunately not become so critical. 2-AA and in general all heterocyclic amines are insoluble in water, therefore transportation along long distances or filtration into the groundwater is less likely (WHO, 1998).

The concern and worry about 2-AA and probably the main reason why this chemical is included in the European Water Framework Directive is because it is well known to act as potent carcinogen in animal models and to cause mutations at multiple sites (Carrière et al., 1992; Windmill et al., 1997; Gato et al., 2012). 2-AA itself is not the carcinogenic agent. As well as nearly all other known polycyclic amines, 2-AA requires metabolic activation by cytochrome P450 (CYP) enzymes to more reactive metabolites in order to exhibit carcinogenicity (Shimada and Fujii-Kuriyama, 2004). It has been shown that CYP1A2 converts heterocyclic amines to N-hydroxylated metabolites that are subsequently modified by phase II enzymes, such as acetyltransferase and sulfotransferase, to ultimate carcinogens (Shimada and Fujii-Kuriyama, 2004; Jemnitz et al., 2004).

Unfortunately only few studies report about the toxicity arising from 2-AA behind mutagenicity and carcinogenicity. Boudreau et al. (2006) show necrotic changes in cells of the pancreas after chronic dietary exposure of rats to 2-AA as well as diabetic-like symptoms. Intraperitoneal injection of 2-AA (5 mg per week during up to 9 weeks) led to reversible serum enzyme levels including alkaline phosphatase, total protein, albumin, and globulin. More over irreversible histologic liver changes were observed, hepatocyte hypertrophy and biliary hyperplasia (Baker et al., 2001).

The here presented biosensor and detection system allows to figure out more precise details about the point of action since the morphology, respiration and metabolism are monitored in real time while the chemical is applied to the cells.

## 1.4.2 Chlorpyrifos

Chlorpyrifos is an organophosphate insecticide used in the European Union mainly in vineyards (European Food Safety Authority 2011). It was included in Annex I to Directive 91/414/EEC on 1 July 2006 by Commission Directive 2005/72/EC. Its approval was only provisionally with an expiration date scheduled first until the 30<sup>th</sup> of June 2016 and prolonged recently until the 31<sup>th</sup> of January of the year 2018 (Commission Implementing Regulation (EU) No 762/2013).

The use of chlorpyrifos and in general of organophosphate pesticides is controversial since risk assessment studies point to imminent health risk for humans and animals and cannot exclude a potential damage of this substances if present in the environment (European Food Safety Authority 2011 and U.S. Environmental Protection Agency 2000, 2011).

The primary mechanism of action of chlorpyrifos is the inhibition of the acetylcholinesterase (AChE) in target tissues by its oxon metabolite (Eaton et al., 2008). The Neurotransmitter acetylcholine is degraded by extracellular AChE. Inhibition of AChE leads in consequens to an accumulation of ACh in the presynaptic space and thus to an over-stimulation of muscarinic and nicotinic receptors (Nicholls et al., 251; Costa, 2006). Acute poisoning with chlorpyrifos leads therefore to the “cholinergic syndrom” which is characterized by sweating, salivation and gastrointestinal motility, diarrhea, profound bronchial secretion, bronchoconstriction, miosis, tremors and muscular twitching (Hsieh et al., 2001).

The toxicity of chlorpyrifos needs, as well as the one from 2-AA, the bioactivation of a member of the cytochrome P450 superfamily to a more potent AChE inhibitor, chlorpyrifos-oxon. This reaction consists in an oxidative desulfuration by the CYP2B6 which take mostly place in the liver (Tang et al., 2001; Foxenberg et al., 2011; Khokhar and Tyndale, 2012).

The cholinergic syndrome follows an acute intoxication of chlorpyrifos (Jokanovič and Kosanovič, 2010) but the main discussion of the use of chlorpyrifos are the neurodevelopmental effects that may cause this pesticide. It has been shown that neurodevelopmental disorders are caused below AChE-inhibition threshold and therefore for the most part asymptomatic (Slotkin, 2004). Several studies in humans, animal models and cell culture have shown that prenatal exposure to chlorpyrifos alters the proper development of the central nervous system. This disorders concern cognitive development, perceptual reasoning and intellectual development (Engel et al., 2011; Bouchard et al., 2011). Higher prenatal exposure to Chlorpyrifos declined the intelligence quotient in 7 years old children, on average, by 1.4% and Working Memory Index scores

by 2.8% (Rauh et al., 2011). This could be accounted by structural changes in the developing human brain as reported in Rauh et al. (2012) and by deficits in the number of neurons and/or glia cells (Garcia et al., 2005; Roy et al., 2005; Mauro and Zhang, 2007). The molecular mechanism how chlorpyrifos acts is yet not complete understood and still to be elucidated but a recent study has shown, that chlorpyrifos targets genes regulating the cell cycle and apoptosis in the developing brain (Slotkin and Seidler, 2012).

All this facts make chlorpyrifos an interesting substance to account for in the present study. Pesticides are by definition in direct contact with the environment. Rainfall flushes them into circumjacent rivers and lakes and transport them many kilometers from their original source away. They can filtrate into the soil and reach in this manner the groundwater (Eltzov and Marks, 2011).

### **1.4.3 3,3',5,5'-Tetrabromobisphenol A (TBBPA)**

Many articles and objects we use in our daily life, like clothing, furniture, electronics, computers and vehicles, are composed of polymers. Given that most of them are petroleum based they are inflammable. In order to fulfill fire safety regulations and hence minimize the risk of a fire, flame retardants are added during the manufacturing and production process of textiles, plastics, wood and paper (Alaee et al., 2003). Flame retardants are materials added or applied to a material to increase the fire resistance of that product (WHO, 1995).

The World Health Organization (WHO) lists approximately 75 chemicals which are used as flame retardants (WHO, 1997). Flame retardants can be inorganic compounds like antimony oxide ( $\text{Sb}_2\text{O}_3$ ) as well as organic compounds. The latter group can be divided into organohalogen compounds, organophosphate esters and nitrogen containing chemicals which are less common (WHO, 1997, 1998).

In this study we will dwell on a particular chemical within the group of organohalogen compounds, tetrabromobisphenol A (TBBPA). Currently, it is the most heavily produced flame retardant in the world (Betts, 2013) with an annual worldwide market demand of more than 120.000 tons (de Wit et al., 2010). Its primary use is in printed electronic circuit boards but it is an additive in several other polymers. The relevance of TBBPA relies not only in its huge industrial usage but rather on the fact that TBBPA and its metabolites are released into the environment and can be found in the air, soil and in sediments (Birnbaum and Staskal, 2004).

Similar as chlorpyrifos, TBBPA is categorized as a persistent organic pollutant that does not degrade for several years. More over it bioaccumulates and was found in fish liver and human tissues and breast milk (Shen et al., 2012; Meijer et al., 2014).

Toxicological studies of TBBPA reveal adverse effects consisting in the impairment of the central and peripheral nervous system and disruption of thyroid homeostasis (Hendriks et al., 2012; Meijer et al., 2014). The developing brain is the major affected by its exposure. Dingemans et al. (2011) reviews structural and functional alterations in the brains of animals exposed to polybrominated diphenyl ethers like TBBPA. Changes in the expression of genes and proteins involved in synapse and axon formation, neuronal morphology, cell migration, synaptic plasticity, ion channels, and vesicular neurotransmitter release have been documented. More over, TBBPA has been shown to induce oxidative stress by the formation of reactive oxygen species (ROS) (Reistad et al., 2005, 2007).

A last concern is the endocrine disrupting property of TBBPA. The flame retardant competes with  $17\beta$ -estradiol for binding to the sulfotransferase. This enzyme adds a sulfate molecule to a estradiol molecule getting it ready to eliminate it from the body. This leads to raising levels of estradiol in the body (Betts, 2013). On top of this Samuelsen et al. (2001) reports the competitive binding of brominated analogs of bisphenol A to the estrogen receptor using MCF-7 cells. The potential of binding the estrogen receptor decreased with increasing bromo-substitutions. The potential of inducing cell growth is therefore higher for bisphenol-A than for TBBPA but still present.

### 1.4.4 4-methylbenzylidene camphor (4-MBC)

Camphor is a natural product derived from the wood of the camphor laurel (*Cinnamomum camphora* L.) tree. It is commercially available and its usage comprises medical and aromatic purposes as well as a flavouring ingredient in food (Chen et al., 2013). It is also used for the home treatment of colds in the form of inhalands or camphorated oil (Jochen and Theis, 1995) and as a topical analgesic in liniments and balms (Xu et al., 2005). Dietary exposure to camphor arises from the consumption of foods flavoured by using either herbs (e.g. basil, coriander, marjoram, rosemary, sage), their essential oils or the chemically defined flavouring substance d-camphor. The available data on toxicity of camphor are limited. Sporadic cases of seizures have been reported in children after acute ingestional, inhalatory or dermal exposure

(Khine et al. (2009)). The symptoms comprises convulsion, lethargy, ataxia, nausea, vomiting and coma (Zuccarini, 2009; Manoguerra et al., 2006). The US Food and Drug Administration (FDA) settled the maximal permitted concentration for over-the-counter products containing camphor to 11% (FDA, 1983) and the European Food Safety Authority (EFSA) suggests that the maximum levels should be set to 2 mg/Kg bodyweight on a single day over all age groups to ensure human healthiness after dietary exposure (Aguilar et al., 2008).

One of its derivatives is 4-methylbenzylidene camphor that is used in the cosmetic industry for its ability to protect the skin against Ultraviolet (UV) light, specifically UV B. Some of its tradenames include Eusolex 6300 from the company Merck KGaA and Parsol 5000 from DSM. The increasing production of UV absorbers for cosmetic and technical purposes has led to the presence of this chemicals in the environment. 4-MBC was found in surface waters (Balmer et al., 2005), particularly in the effluents of sewage treatment plants (Plagellat et al., 2006). Since UV filters are not only used for cosmetic reasons but also as UV stabilizers in plastics, clothing, curtains and food (Kawamura et al., 2003), we humans are in constantly contact with this substances in our daily life. Janjua et al. (2004) has shown that the sunscreens benzophenone-3, octyl-methoxycinnamate and 4-methylbenzylidene camphor are absorbed through the skin, show a systemic level in the plasma and their metabolites can be detected in urine after whole-body topical application in humans. This UV filters used in sunscreens and specially 4-MBC are under suspicion of having endocrine activity and therefore to alter the physiological levels of the reproductive hormones follicle-stimulating hormone (FSH), luteinizing hormone (LH), testosterone and estradiol. Several studies have shown that 4-MBC unfolds estrogenic activity (Schlumpf et al., 2001, 2004a, 2004; Klammer et al., 2005; Kunz et al., 2006) and displays also an anti-androgenic effect (Ma et al., 2003; Schreurs et al., 2005). More over interference of 4-MBC with the thyroid axis was observed *in vitro* (Schlumpf et al., 2004) and *in vivo* (Maerkel et al., 2007).

4-MBC is only approved in Europe and due to the ongoing risk concerns the Danish Environmental Protection Agency recommends not to use 4-MBC for children younger than 12. The Danish authorities requested in 2001 the European Commission for a safety evaluation of the UV filter 4-MBC. In particular they expressed their concern on the calculation of a margin of safety when used by children due to its potential effects on the thyroid gland. More over

based upon the publication of Schlumpf et al. (2001), in which the potential estrogenic effect of 4-MBC was studied, the European Commission's Scientific Committee on Cosmetic Products and Non-Food Products (SCCNFP) considered a safety evaluation under investigation by M. Schlumpf and representatives from industry (including Merck KGaA). The Committee drew the conclusion that the allowed UV filters in sunscreen products in the European Union have no estrogenic effect that could harm human health (European Union, 2001).

Concerning thyroid axis alteration or interference, the SCCNFP concluded in the year 2004 that the available data in rat analysis is difficult to interpret. Nevertheless the results suggest an interference of 4-MBC in thyroid hormone metabolism reasoned by increased TSH in combination with elevated levels of triiodothyronin and tetraiodothyronin (T<sub>3</sub>,T<sub>4</sub>), enlarged thyroids and thyroid proliferation. The committee stated that “the current use of 4-Methylbenzylidene camphor in sunscreen products **poses a reason for concern**” (European Union, 2004) but was also of the opinion that a safe use of a maximum concentration of 4% 4-MBC in sunscreens cannot be established (European Union, 2006).

## **1.5 Detection of estrogen acting xenobiotics**

Xenobiotics are chemical substances present within an organism but not naturally occurring or synthesized by it and therefore not supposed to be there (de Bolster, 1997). Environmental pollutants are also potential xenobiotics since they can enter the human organism through the food chain, inhalation, or through the skin (Eltzov and Marks, 2011).

Some of these xenobiotics have the ability to activate cellular pathways mimicking endogenous molecules. The activation of these pathways out of time or in excess can lead finally to health implications. The proper functioning of the endocrine system is particularly sensitive to xenobiotics. Some of them are able to alter or disrupt the pathways of reproductive hormones like FSH, LH, androgen and estrogen (Jeffries et al., 2011; Banerjee et al., 2013) as well as those from the hypothalamic–pituitary–thyroid axis, thyrotropin-releasing hormone (TRH), thyroid-stimulating hormone (TSH), triiodothyronine (T<sub>3</sub>) and thyroxine (T<sub>4</sub>) (Schlumpf et al., 2004; Maerkel et al., 2007; Leung et al., 2013).

In section 1.4.3 and 1.4.4 it was mentioned that TBBPA and 4-MBC have been shown to



bind the estrogen receptor acting as an agonist. Estrogen regulates a variety of cell functions including proliferation, differentiation, adhesion, migration, cell-cell interaction, and apoptosis (Edwards, 2005; Banerjee et al., 2013).

High estrogen levels in serum are associated with a 2-2.5% greater risk of breast cancer development and 60-70% of breast cancers expressing the estrogen receptor are estrogen signaling driven (Caldon, 2014).

Since the body does not differentiate between endogenous estrogen and a chemical that “is only acting as estrogen”, all these estrogen-like xenobiotics represent a health risk and potential carcinogenic substances. The here being presented biosensor, opens the possibility to detect those whose physiological alterations lead to a faster or uncontrollable cell proliferation. A higher respiration rate and a higher metabolic rate is expected if cells are growing faster on the chip. More over, a higher covering of the chip surface while cells are proliferating will change the impedance measured by the IDES electrode. In section 3 we will deliberate if a faster proliferation can be appreciated with a biosensor after application of  $17\beta$ -estradiol and some chemicals under suspicion of having estrogen-like activity.

## **1.6 The logistical challenge: preservation and transport of a biosensor**

The interaction between the analyte and the detection layer is of course a fundamental topic during the development of a biosensor. The biological layer must be sensitive enough to detect the target analytes and one has to take care that the biological signal produced after the binding or interaction is converted in a reasonable read-out.

At a practical level there are other concerns to consider. For example, a client, owing and using a detection system, but without a cell culture laboratory in his background, has to receive per mail a chip loaded with (living) cells. More over the customer has to be able to store the chip if its usage is not immediate without owning a laboratory equipment. One storage possibility would be a 4°C refrigerator.

All in one, the cells must be encapsulated in a medium or substance which shields impacts, provides them with enough nutrients and protects them from fluctuations of the temperature and dehydration.

### **1.6.1 Preservation and protection of cells from temperature fluctuations**

Nowadays cell preservation and transportation is performed mainly at subzero temperatures using cryoprotective substances. Cryopreservation is the use of very low temperatures to preserve structurally intact living cells and tissues (Pegg, 2007). The most commonly used cryoprotective substances are glycerol and DMSO (Pegg, 1976). In this way, cells can be transported and conserved at  $-90^{\circ}\text{C}$  in cell culture medium supplemented e.g. with 10% bovine serum and 10% DMSO. Cryoprotective substances have the ability to reduce the amount of intra- and extracellular ice formed just by increasing the concentration of solutes in the system (Pegg, 2002). The risk of cellular damage arises first from the toxicity of the cryoprotective substance and second, from the tradeoff between intracellular freezing and the concentration of solutes (Armitage, 1987; Pegg, 2007).

Cryopreservation is a complex but very good understood process. It has an established position in medicine as well as in biology for the conservation of cells and some tissues. Nevertheless for our purpose it is insufficient since:

1. the target tissue is a two dimensional monolayer and not a suspension,
2. there is no warranty for subzero temperatures and far less for  $-90^{\circ}\text{C}$  in the target place,
3. the silicium based sensor chip will break at very low temperatures,
4. we can not run the risk that cells die after the freezing/thawing procedure,
5. the cell-loaded chip is going to be placed in the measuring system without pretreatment.

This means that we need to avoid the use of toxic preservation substances in order to ensure healthy and reliable physiological parameters.

This requirements imply that there is a need for a procedure that allows to keep a cellular monolayer alive and maintain its full functional capacity at temperatures ranging between  $4^{\circ}\text{C}$  and  $25^{\circ}\text{C}$ . The nutritive and biochemical environment has to be ensured. Mechanical load needs also to be overcome since shipping or transportation is a matter of stress for the cells. The

monolayer is not allowed to slide over the surface of the chip or detach from its surface. For all these reasons cryopreservation and vitrification are not the right choice. The latter process denotes the process of cooling down tissues or cultured cells or whole organs to subzero temperatures without phase change (Han and Bischof, 2004; Bagchi et al., 2008). Vitrification avoids ice formation which is why this procedure claims to be gentler for the cells as described in Fahy et al. (2009).

The task was to look for hypothermic preservation without a freezing/thawing procedure. In hypothermic preservation, the cellular metabolism within a tissue is reduced due to storage temperatures ranging between 4 and 10°C (Han and Bischof, 2004). In fact it is possible to maintain cells at these low temperatures. In the early eighties James H. Southard, Folkert O. Belzer and colleagues were working on a cold-storage solution – the University of Wisconsin (UW) Solution – that was thought to improve preservation of the liver and pancreas (Belzer and Southard, 1980; Belzer et al., 1983). At that point of time, these organs countenanced only a preservation for 4 to 8 hours. This time constrain seriously limited the distance from which organs could be procured to the place they needed to be transplanted. The result was a three day successful preservation of dog pancreas (Wahlberg et al., 1987) and kidney (Ploeg et al., 1988) and a two day dog liver (Jamieson et al., 1988) preservation. A possible reason for the successfully results of UW solution is the usage of lactobionic acid and raffinose, a trisaccharide, to suppress hypothermically induced cell swelling (Southard and Belzer, 1995). But this is not the only reason, also the presence of adenosine in a concentration of 5 mmol/L (Ono et al., 1995) contributes substantially to the improved preservation. In fact, most organs loose 95% of its initial amount of ATP (Southard and Belzer, 1995) and the values of adenosine diphosphate and adenosine monophosphate decreased to approximately 25% of original values by 24 hours in cultured human cardiomyocytes (Fremes et al., 1991c). Without doubt a supply of this nucleoside is a welcome clue for the organ preservation industry, leading in the above mentioned case of human cardiomyocytes to a stable morphology and a near to perfect  $\beta$ -adrenergic response (Fremes et al., 1991c).

To conclude we state that organ preservation techniques has been improved to supply demand and cultured cells can be also stored for a at least 2 days at 4°C (Fremes et al., 1991a,b).

So we now know that it is posible to keep cells at 4°C. But what about higher temperatures? García et al. (2008) showed that cultured human articular chondrocytes could be stored at roomtemperature (in their case 18°C-24°C) for up to 30 days. They found out that cell viability ranged

between 91% and 100% after 15 days (using HAM-12 medium, results turned out to be not so satisfying using DMEM with this cellline) and between 6% and 95% after 30 days.

This means that cells can survive temperature variations within a wide interval. It is only a matter of the right medium that feeds and protects them.

### 1.6.2 Packaging for transportation

Not only the question of the right medium to overcome temperature fluctuations and allow storage at 4°C needs to be circumvented. Also the packaging for transportation and the question of a substance that protects the cells from mechanical stress remains open.

A colloidal or gelatinous substance could be promising for this intention. A fibrin-based gel matrix has been used as carrier for hepatocytes in culture (Bruns et al., 2005). In this manner cells could be transplanted into the liver in animal models. There is a trend towards encapsulating cells in a three dimensional hydrogel for tissue engineering applications. The used gels provide an environment similar as the one experienced *in vivo* and may allow intact physiological function of the cells (Hunt and Grover, 2010). The use of encapsulated cells or tissue in a sponge-like material evolved from the idea of developing man-made organs or tissues. Particularly, the use of patient's own cells is a revolutionary strategy for organ regeneration and wound healing. Cells are isolated from a small biopsy from the patient, cultured *ex vivo* and injected back to the patient (Marler et al., 1998). A variety of tissues like arteries, skin, cartilage, bone, ligament, and tendon are engineered in this manner (for an exemplary paper see Service (2000)). During this procedure, cells are incorporated in a three dimensional polymer scaffold. This scaffold acts as an extracellular matrix, deliver the cells to the appropriate tissue or organ and provides space for the formation of new tissue (Lee and Mooney, 2001). Critical is the choice of the polymer being used since it has to mimic the extracellular matrix and be biocompatible.

This tissue engineering procedure was adapted to immobilize and protect the cellular monolayer of the biosensor used here. Actually, hydrogels from natural polymers as well as from synthetic polymers are used for tissue engineering. The latter ones comprise polyacrylic acid and its derivatives, polyethylene oxide and its copolymers, polyvinyl alcohol, polyphosphazene,

polypeptides (Lee and Mooney, 2001). The most frequently used natural polymers are agarose, alginate, chitosan, collagen, fibrin, gelatin and hyalauronic acid. Among all these biopolymers we focused on alginate, fibrin and gelatin since these have been tested with hepatocytes before (Hunt and Grover, 2010). Due to proteolytic enzymes, fibrin can degrade rapidly in the presence of mammalian cells (Ye et al., 2000). So does alginate, even if its mechanical properties can be controlled and tailored by the molecular weight of the polymer, amount of cross-linking species and concentration of cross-linking cations like  $\text{Ca}^{2+}$  (Hunt et al., 2010).

Due to the fast degradation of alginate and fibrin, gelatin was used as the protecting medium. Gelatin is formed from the hydrolysis of collagen. It solves in aqueous media at  $60^\circ\text{C}$  and it gels when it cools down to roomtemperature (Young et al., 2005). The solidification temperature depends on the concentration of gelatin used. Lower concentrations need lower temperatures to solidify. That means, that it is possible to tailor the solidification state of the gel by regulating the concentration of gelatin used. A solid state below  $25^\circ$  and a liquid state above  $30^\circ\text{C}$  is desired because the measuring system runs at  $37^\circ\text{C}$ . Therefore, a cell-loaded chip stored at  $4^\circ\text{C}$  could be taken out of the refrigerator and placed without pretreatment into the system. The inherently temperature of the system would melt the gelatine and replace it by the running medium of the system or a water probe.

## 1.7 The aim

The aim of the current thesis is to drive this technology step by step towards a real application as a monitoring system for the quality of fresh water.

First, the sensitivity of the system will be evaluated by testing it with four organic model substances with industrial and environmental relevance. Then and in order to ascertain the contaminant present in the sample, a self-designed software based on functional data analysis is going to be presented. Also the physiological read-out provided by the system is going to be used to identify the nature of the compound. This will be relevant for compounds promoting proliferation.

If the goal in a near future is to bring this technology or method close to an application, there

are some challenges which must be faced. The difficulties to deliver a chip loaded with living cells had to be overcome and maybe the most important challenge is the fact that pure water kills cells due to the difference of osmolarity between the intracellular and the extracellular medium and the lack of nutrients. This means that the system had to be adapted in a way that a clean and crystal water probe did not kill the cells.

# Chapter 2

## Experimental

### 2.1 Materials

#### 2.1.1 Chemicals and reagents

2-Aminoanthracene, C <sub>14</sub> H <sub>11</sub> N	Sigma Aldrich (Steinheim, Germany)	#A38800
Alexa Fluor <sup>®</sup> 488 donkey anti-rabbit	Life Technologies (Darmstadt, Germany)	#A-21222
Anti-Estrogen Receptor $\alpha$ Antibody, rabbit monoclonal	Merck Millipore (Darmstadt, Germany)	#04-227
Bovine Serum Albumin (BSA)	Sigma Aldrich (Steinheim, Germany)	#A2153
Chlorpyrifos, C <sub>9</sub> H <sub>11</sub> Cl <sub>3</sub> NO <sub>3</sub> PS	Sigma Aldrich (Steinheim, Germany)	#45395
Clearmount Mounting Solution	Life Technologies (Darmstadt, Germany)	#00-8110
4',6-diamidino-2-phenylindole (DAPI)	Life Technologies (Darmstadt, Germany)	#D1306
Dimethyl sulfoxide, C <sub>2</sub> H <sub>6</sub> OS	Sigma Aldrich (Steinheim, Germany)	#D8418
D-(+)-Glucose, C <sub>6</sub> H <sub>12</sub> O <sub>6</sub>	Sigma Aldrich (Steinheim, Germany)	#G8270
4-Methylbenzylidene camphor, C <sub>18</sub> H <sub>22</sub> O	Sigma Aldrich (Steinheim, Germany)	#78551
Nickel(II) chloride, NiCl <sub>2</sub>	Sigma Aldrich (Steinheim, Germany)	#339350
Paraformaldehyde, HO(CH <sub>2</sub> O) <sub>n</sub> H	Sigma Aldrich (Steinheim, Germany)	#158127
Sodium hydroxide, NaOH	Sigma Aldrich (Steinheim, Germany)	#5881
3,3',5,5'-Tetrabromobisphenol A, (CH <sub>3</sub> ) <sub>2</sub> C[C <sub>6</sub> H <sub>2</sub> (Br) <sub>2</sub> OH] <sub>2</sub>	Sigma Aldrich (Steinheim, Germany)	#330396
Triton X-100, C <sub>14</sub> H <sub>22</sub> O(C <sub>2</sub> H <sub>4</sub> O) <sub>n</sub>	Sigma Aldrich (Steinheim, Germany)	#93443
Water (HPLC grade), H <sub>2</sub> O	Sigma Aldrich (Steinheim, Germany)	#34877

Table 2.1: List of chemicals and reagents used

### 2.1.2 Nutrient media and buffers

Dulbecco's MEM (DMEM)	Biochrom (Berlin, Germany)	#FG 1445
DMEM w/o phenol red	Biochrom (Berlin, Germany)	#F 0475
DMEM powder	Biochrom (Berlin, Germany)	#T 041-01
Fetal bovine serum (FBS)	Biochrom (Berlin, Germany)	#S 0615
FBS hormon-free	Biochrom (Berlin, Germany)	#S3113
Phosphate buffered saline (PBS)	Biochrom (Berlin, Germany)	#L 1825
Penicillin/Streptomycin	BioWhittaker (Heidelberg, Germany)	#12001-350
Trypsin/EDTA	Biochrom (Berlin, Germany)	#L 2163
L-Glutamine	Biochrom (Berlin, Germany)	#K 0282
Hepes	BioWhittaker (Heidelberg, Germany)	#CC-5024

Table 2.2: List of Nutrient Media and buffers

### 2.1.3 Cytotoxicity assay

Cell Proliferation Kit I (MTT)	Roche (Mannheim, Germany)
Calcein AM Cell Viability Assay	Biotium (Hayward, USA)

Table 2.3: List of cytotoxicity assays

### 2.1.4 Devices

Centrifuge	Heraus Multifuge 1S-R	Thermo Scientific (Schwerte, Germany)
Laminar flow hood	Hera Safe	Thermo Scientific (Schwerte, Germany)
Photometer	FLUOstarOPTIMA	BMG Labtechnology (Offenburg, Germany)
Incubator	CO <sub>2</sub> Air-Jacket Incubator	NuAire (Plymouth, USA)
Light microscope	Axiovert 40 CFL	Zeiss (Wetzlar, Germany)
Cell-sensor system	AS 2500	Bionas (Rostock, Germany)

Table 2.4: List of devices



## 2.2 Methods

### 2.2.1 Cell culture

Four different cell lines were tested and used: RLC-18, rat embryonal liver cells (figure 2.1 a); MCF-7, human breast adenocarcinoma (figure 2.1 b); BenMen, human benign meningioma cells (figure 2.1 c); 8-MG-BA, human glioma cells (figure 2.1 d).

All cells were purchased from DSMZ (German Collection of Microorganisms and Cell Lines, Braunschweig, Germany) and grown at 37°C in 5% CO<sub>2</sub> in a humidified atmosphere. Cells were cultivated in DMEM, supplemented with 10% FBS, 100 units/mL penicillin and 100 µg/mL streptomycin.

Beyond that, MCF-7 were cultivated with hormone free medium if used for experiments concerning the estrogen-like activity of a compound. For this, the regular DMEM was replaced by DMEM without phenolred and supplemented with 10% hormon free FBS, 100 units/mL penicillin and 100 µg/mL streptomycin 3 passages prior to perform the experiment .

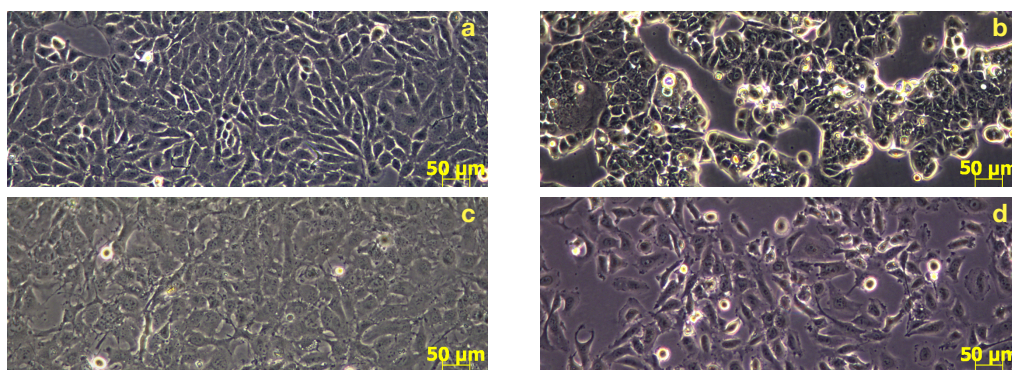


Figure 2.1: Cell lines tested or used as the detection layer, a) RLC-18, b) MCF-7, c) BenMen, d) 8-MG-BA.

To conclude which cell line is the most adequate all cell lines were tested for sensitivity and reliability twice with the following compounds: NiCl<sub>2</sub>, 2-AA, chlorpyrifos, TBBPA and 4-MBC. The cell line had to be sensitive against the compound and show the same result every time tested. Moreover a cell line had to be reliable after having passed a freezing/thawing procedure.

RLC-18 turned out to be the most promising cell line as the detection layer for our cell-based sensor system. Therefore all further experiments were performed with this cell line. More

over, MCF-7 was also used since it possesses the estrogen receptor needed to detect and attest estrogenic activity.

### 2.2.2 Storage and conservation

The storage of all all cell lines was achieved by suspending a centrifuged pellet in freshly mixed cryostorage medium (80% DMEM; 10% FCS and 10% DMSO) and stored at  $-80^{\circ}\text{C}$ . If cells were required, frozen cells were thawed, washed twice with nutrient medium and cultivated as described above.

### 2.2.3 The cell based sensor system

The cell based sensor system used here is the 2500 Analyzing System developed by Bionas GmbH (see figure 2.2). The system houses 6 biomodules and each of them holds a metabolic chip for measuring the impedance as well as the changes in oxygen concentration (respiration rate) and the pH (acidification rate) over the time. The sensor chip will be explained more in detail in the next section.

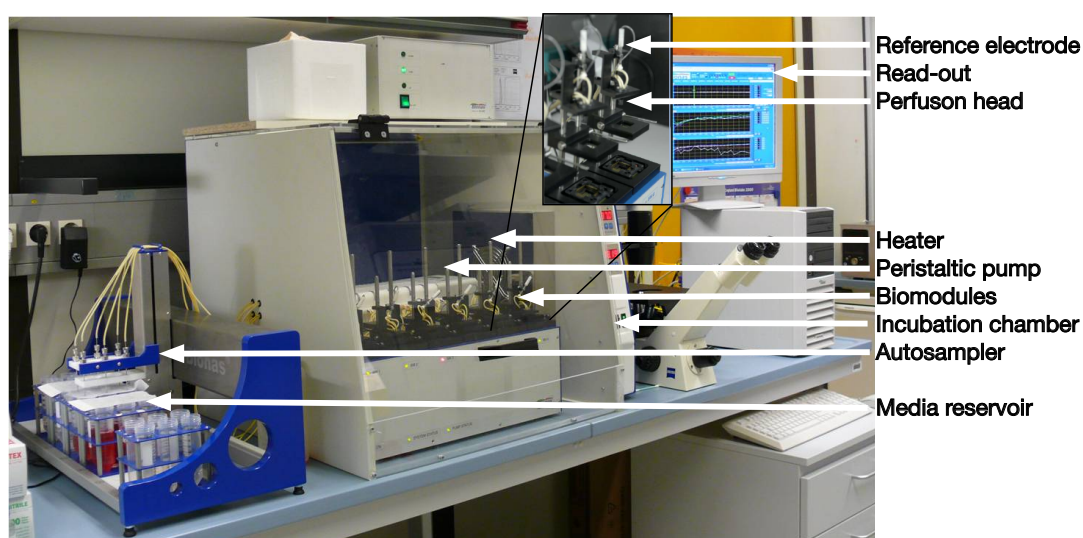


Figure 2.2: 2500 Analyzing System by Bionas GmbH

The whole setup is covered with an incubation hood and constantly heated at  $37^{\circ}\text{C}$ . The system is equipped with an autosampler for automatic medium or probe supply and operates in a stop/go modus (Ceriotti et al., 2007). During the go phase, a perfusion head pumps fresh medium over the cells on the sensor chip. After 3 min, the pump stops for 3 min. Due to the

metabolic activity of the cells the pH value of the medium decreases as well as the oxygen concentration. The acidification and respiration rates are calculated from the slope of the pH value and oxygen concentration which decreased over the time. Specifications of the sensor system are listed in table 2.5.

Parameter	Description
Chip radius	4.75 mm
Growth area	70.88 mm <sup>2</sup>
Chip volume	≈122 μL
Test volume between sensor surface and perfusion head	≈5.85 μL
Flow-through height between sensor surface and perfusion head	83 μm
Number of electrodes	1 IDES, 2 Clark, 5 ISFET
Reference electrode	Ag/AGgCl
Frequency	10 kHz
Clark electrode	Palladium
ISFET gate	Silicon nitride (Si <sub>3</sub> N <sub>4</sub> )
Passivation	Silicon Oxide (SiO <sub>2</sub> )
Flow rate	56 μL/min
Media osmolarity	270-340 mOsmol/Kg
Incubation temperature	37°C
Tube material	polyetheretherketon (PEEK)
Tube diameter	0.9-1.02 mm

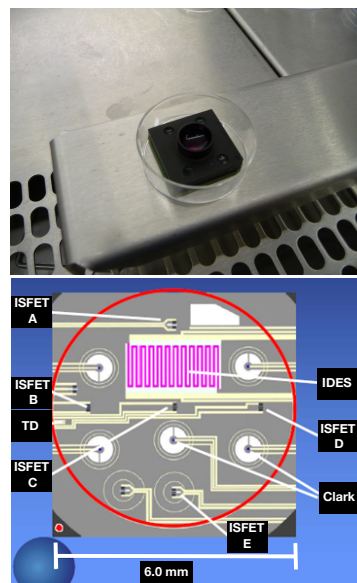


Table 2.5: Specifications of the Bionas 2500 Analyzing System. Picture of the housing of the chip (upper picture) and detail view of the surface of the chip (bottom)

### 2.2.4 The sensor chip

Three types of electrodes cover the surface of the chip beneath the cells. They allow the measurement of the physiological parameters and thus the viability status of the cells.

In this section the functioning of the electrodes is going to be explained as well as how the cells are seeded on the chip surface.

#### The electrodes

Interdigitated electrode structures (IDES, figure 2.3) measure the cellular impedance. The cell membrane is a strong insulator. If a current is applied they will disable the current flow in a passive way and the impedance will decrease (Ehret et al., 1998). For the detection of the oxy-

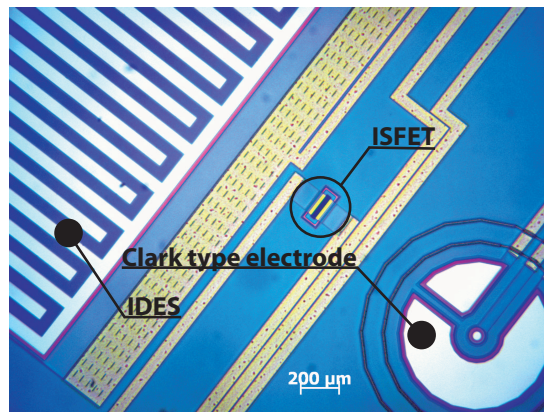


Figure 2.3: Microscopical image of a cell-based sensor chip. Interdigitated electrodes (IDES) measure the impedance under and across the cell layer. This provides information about the strength of attachment to the surface and thus about the morphological integrity. Clark-type electrodes measure oxygen consumption and ion-sensitive field effect transistors (ISFET) detect pH changes in the extracellular medium, i.e. metabolic activity. In total one ID electrode, five Clark electrodes and five ISFET electrodes cover the surface of the physiological sensor.

gen consumption two of the in total five integrated Clark-type electrodes (figure 2.3) are used (Ceriotti et al., 2007). The measurement of the  $O_2$  concentration is based on an amperometric transduction. A constant potential is applied on a *Pt* based working electrode which leads to the reduction of oxygen. The resulting current is directly correlated to the consumption rate of the electroactive species  $O_2$  (Thévenot et al., 2001; Holenya et al., 2014). Five ion-sensitive field-effect transistors (ISFETs, figure 2.3) measure the pH value of the extracellular medium. In this potentiometric measurement a drain current is maintained at a constant value. This leads to a potential difference which varies with change in activity of the sensed ion species, in this case  $H_3O^+$  (Thévenot et al., 2001; Covington, 1994).

Recording of cell impedance, extracellular acidification rate and respiration rate provides all information about morphological status and metabolic activity of the cellular layer. Cellular metabolism is in touch with the production and excretion of acid waste products like lactate and  $CO_2$  and the consumption of oxygen. Oxygen consumption reflects almost exclusively mitochondrial activity, while cellular acidification is the result of oxidative and non-oxidative pathways (Wolf et al., 1998).

### Cultivation on the metabolic Chip

The same growth conditions were used for the cultivation of cells on the sensor chip (SC 1000 Metabolic Chip) as for cell culturing. Cells were kept in Dulbecco's modified Eagle medium supplemented with penicillin/streptomycin and 10% FBS. Approximately  $1,75 \cdot 10^5$  cells were

seeded on the chip in 400  $\mu\text{L}$  and incubated over night at 37°C in 5%  $\text{CO}_2$  and 95% humidity until confluency was reached. The sensor chips with cells were then transferred to the Bionas 2500 Analyzing System.

### 2.2.5 Measurements with the cell based-sensor system

#### Experimental protocol

A pump system exchanges medium in 3 min cycles (3 min pump-go – 3 min pump-stop) with a flow rate of 56  $\mu\text{L}/\text{min}$ . During the stop periods the parameters were measured and updated after each measuring cycle each 10 seconds. The running medium (RM) consisting in DMEM was weakly buffered (1  $\text{mM}$  Hepes) during the analysis with reduced FBS (1%) and supplemented with penicillin/streptomycin.

Unless stated otherwise, the measurements were performed according to the following protocol: a) 5h equilibration time in order to let the cells adapt to the system and get stable physiological signals, b) 10h exposure to polluted samples in different concentrations, c) 7h recovering time with running medium to determine if effects are lasting or transient and d) removing of cells by addition of 0.2% Triton X-100 in running medium. This last step is necessary to obtain a basic signal without living cells on the sensor surface as a negative control.

#### Baseline measurement

A 0.2% solution of the detergent Triton-X 100 was pumped at the end of each experiment over the cells. This lead to the removal of the cells from the surface, either by destruction of the membrane or by detachment of the cells. The recorded data represent the sensor chip baseline (0% value) without cell adhesion, respiration, or metabolism.

#### Chip recovery

At the end of each experiment, the fluidic system was flushed for 10 min and a flow rate of 700  $\mu\text{L}/\text{min}$  with sterile water and 10 min with 70% ethanol (flow rate: 700  $\mu\text{L}/\text{min}$ ). With this step the residual medium was removed from the tubing system avoiding contaminations.

The chips were cleaned separately with a rubber scrubber using distilled water and 70% ethanol. Chips were checked under the microscope to ensure that the surface was clean and no signs of corrosion were present.

### Data analysis

The analysis of the recorded data was performed with the data analysis software “ORIGIN 8.5” (OriginLab Corp., Northampton, USA) and “EXCEL” (Microsoft Inc., Redmond, USA).

### 2.2.6 Cell viability assays

#### MTT proliferation assay

Cell viability after exposure to organic pollutants was compared to the results of the presented sensor system by measuring the reduction of the tetrazolium dye MTT [3-(4,5-dimethylthiazol-2-yl)-2,5-diphenyltetrazolium bromide] by mitochondrial succinate dehydrogenase (Mosmann, 1983). The MTT cell proliferation assay kit I (Roche Diagnostics, Mannheim, Germany) was used following manufacturer’s instructions. Approximately 5000 RLC-18 cells were seeded into each well of a 96-well plate (Greiner, Frickenhausen, Germany) and incubated over night to allow attachment to the plate surface. The medium was replaced with the test solutions, resulting in a volume of 100  $\mu\text{L}$  per well. Negative controls (DMEM with and without 1% DMSO) were also included in every experiment. After 12 h incubation, 10  $\mu\text{L}$  MTT solution was added to each well to get a final concentration of 0.5 mg/ml. After 4 h 100  $\mu\text{L}$  solubilization buffer were added to each well until the formazan salts were dissolved. Finally, the absorption was measured at 595 nm (test wavelength) and 640 nm (reference wavelength) using a FLUOstar microplate reader (BMG Labtechnologies, Offenburg, Germany).

#### Calcein AM cell viability assay

Calcein AM is membrane-permeant fluorescent cell marker. After being introduced to the cells calcein AM is hydrolyzed intracellularly by endogenous esterase into the green fluorescent dye calcein. Due to its negative charge calcein is retained in the cytoplasm of healthy cells (Wang et al., 1993).

Cells were seeded into a 96 well plate and incubated over night to allow attachment to the plate surface. The medium was replaced with the test solutions, resulting in a volume of 100  $\mu\text{L}$  per well. Negative controls (DMEM with and without 1% DMSO) were also included in every experiment. After incubation with the test compound the medium was aspirated and washed three times with PBS. 100  $\mu\text{L}$  2  $\mu\text{M}$  Calcein AM was added to each well and incubated for

30-60 min. The fluorescence was measured using a FLUOstar microplate reader (excitation wavelength 485 nm and emission wavelength 530 nm).

### **Immunohistochemistry againsts the $\alpha$ -estrogen receptor ( $\alpha$ ER)**

Aproximatelly 100.000 cells were plated into each well of 8 well chamber slides (Nalgene Nunc International, Rochester USA, cat. # 177402). Each well holds a volume of 200-500  $\mu$ L.

The medium was removed and cells were washed 3 times with PBS and fixed for 6 min in 4% paraformaldehyde. Cells were permeabilized and blocked for 2h at room temperature (RT) with 5% BSA and 0.3% TX in PBS. Afterwards the first antibody (Anti-Estrogen Receptor  $\alpha$  Antibody, rabbit monoclonal) was added in a PBS solution containing 1% bovine serum albumin (BSA) and 0.3% TX. Cells were incubated over night at 4°C and then washed 3 times with PBS. The secondary antibody was added (Alexa Fluor<sup>®</sup> 488 donkey anti-rabbit, 5 $\mu$ g/mL in PBS) and incubated for 2h at room temperature. Cells were washed 3 times with PBS and nuclei were counterstained with DAPI (5 min, room temperature, 1:5000 in PBS).

Slides were covered with mounting media (Clearmount Mounting Solution) and coversliped.

### **2.2.7 Functional data analysis, prediction of a chemical pollutant in a sample**

A statistical signal evaluation method was developed in order to predict the presence of a certain pollutant in an unknown sample. This method was designed for the case that only one contaminant is present but especially for those cases where a mixture of compounds is present in the sample.

The signals from the cell chips were analyzed with a functional generalized linear model (FGLM) for scalar responses, including a functional covariate and using basis expansions and maximization of the log-likelihood to estimate the model. This method is described in detail in Fuchs et al. (2015).

The responses  $y_i$  (with  $i = 1, \dots, N$ , number of measurements per signal) are assumed to be conditionally mutually independent and to follow a Bernoulli distribution of one trial and probabilities  $\pi_i$ .  $\eta^{1-13}$  is the linear predictor and takes into account the parameters/electrode types included in the function. It is possible to analyze only one parameter/electrode type ( $\eta^1 - \eta^3$ , data not shown), a combination of two parameters/electrode types ( $\eta^4 - \eta^{12}$ ), or a combination

of all 3 parameters/electrode types ( $\eta^{13}$ ).

$$y_i \sim B(1, \pi_i), \quad (2.1)$$

$$\text{with } \pi_i = \frac{\exp(\eta_i)}{1 + \exp(\eta_i)},$$

linear predictor  $\eta_i \in \{\eta_i^4, \eta_i^5, \eta_i^6, \eta_i^7, \eta_i^8, \eta_i^9, \eta_i^{10}, \eta_i^{11}, \eta_i^{12}, \eta_i^{13}\}$ ,

$$\eta^4 = \beta_0 + \int x_{isfet} \xi_{isfet} ds + \int x_{ides} \xi_{ides} dt$$

$$\eta^5 = \beta_0 + \int x_{isfet} x_{ides} \beta_1 ds dt,$$

$$\eta^6 = \beta_0 + \int x_{isfet} \xi_{isfet} ds + \int x_{ides} \xi_{ides} dt + \int x_{isfet} x_{ides} \beta_1 ds dt,$$

$$\eta^7 = \beta_0 + \int x_{isfet} \xi_{isfet} ds + \int x_{clark} \xi_{clark} dz,$$

$$\eta^8 = \beta_0 + \int x_{isfet} x_{clark} \beta_2 ds dz,$$

$$\eta^9 = \beta_0 + \int x_{isfet} \xi_{isfet} ds + \int x_{clark} \xi_{clark} dz + \int x_{isfet} x_{clark} \beta_2 ds dz,$$

$$\eta^{10} = \beta_0 + \int x_{ides} \xi_{ides} dt + \int x_{clark} \xi_{clark} dz,$$

$$\eta^{11} = \beta_0 + \int x_{ides} x_{clark} \beta_3 dt dz,$$

$$\eta^{12} = \beta_0 + \int x_{ides} \xi_{ides} dt + \int x_{clark} \xi_{clark} dz + \int x_{ides} x_{clark} \beta_3 dt dz,$$

$$\eta^{13} = \beta_0 + \int x_{isfet} \xi_{isfet} ds + \int x_{ides} \xi_{ides} dt + \int x_{clark} \xi_{clark} dz$$

$\beta_0$  is the intercept term, and  $x_{ides}$ ,  $x_{isfet}$  and  $x_{clark}$  are functional covariates, in our case the three signal types IDES, FET or CLARK. The data is, as usual, only available on a grid of equidistant measurement points. To account for this in the presented functional model the integrals are approximated by Riemann sums. The covariate functions as well as the coefficient functions ( $\xi_{ides}$ ,  $\xi_{isfet}$ ,  $\xi_{clark}$  and  $\beta_1$ ,  $\beta_2$ ,  $\beta_3$ ) are approximated by a tensor product of B-spline basis. The coefficient functions characterize the correlation between our response  $y_i$  and our signals. They have to be estimated. The term  $\beta(s, t)$  represents the functional covariate interaction term. This term incorporates possible information from the signals of two electrodes into the model. By this, signals that seem to be not or only slightly correlated to the response  $y_i$  when taken into account singly might show an increased correlation if they are combined with a second signal type.



# Chapter 3

## Results

### 3.1 Toxicity measurements using a cell-based sensor system

#### 3.1.1 Single measurements

In order to evaluate the sensitivity of the cellular detection layer and to gain insight into the mode of action of the above mentioned organic pollutants, the response of the physiological parameters, respiration and metabolic activity, and morphology was analyzed. The *IDES* electrode reflects the morphological status of the cells living on the surface of the chip and its changes. But not only the steadiness of the cytoskeleton, i.e. morphological change and adhesion properties, is read out, also cell to cell contacts as well as cell-matrix interactions are monitored.

Before the pollutant was applied to the medium a 5h adaptation time ensured the acclimation of the cells to the new environment. After the application, a recovering time of 7h was programmed in order to observe if damage is lasting or temporary. All compounds were solved in DMSO since they are water insoluble. Even if DMSO a wi DMSO is a widely used solvent. Nevertheless there are other possibilities of industrial relevance and naturally occurring. Appendix A show some of them and the repercussion to the cell layer.

#### Exposure of Chlorpyrifos to RLC-18 cells

Figure 3.1 A, B and C show the time dependent course of the physiological parameters of RLC-18 cells after the application of Chlorpyrifos in four different concentrations. All three parameters collapse immediately as soon as high concentrations, 500  $\mu\text{M}$  and 1000  $\mu\text{M}$ , of pesticide

### 3.1 Toxicity measurements using a cell-based sensor system

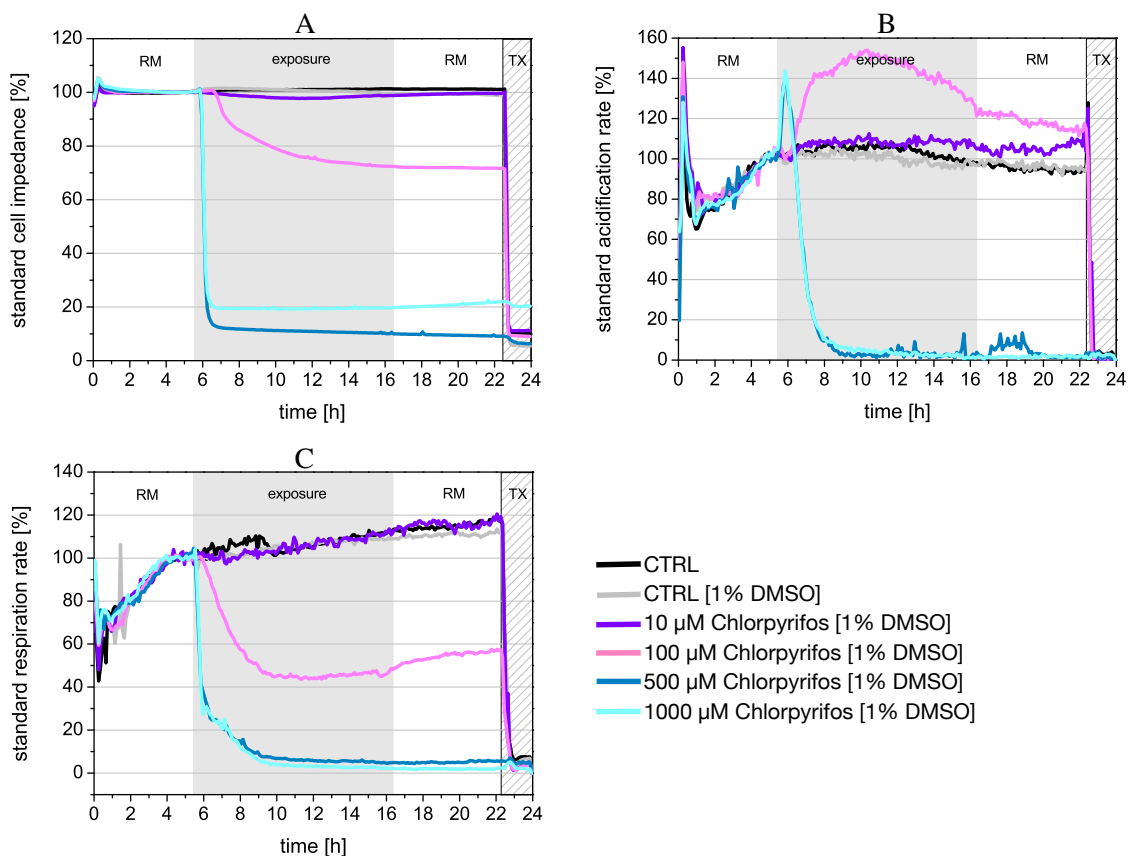


Figure 3.1: Impact of Chlorpyrifos on RLC-18 cells after 10h exposure time (shaded area) measured in Bionas Analyzing System followed by a recovering phase of 7h (white area). Cells were allowed to adapt to the system prior to exposure for 5h (white area). A) Standardized cell impedance, B) Standardized acidification rate, C) Standardized respiration rate. The results are reported as mean of three independent experiments.

are present. The fast decrease of the cell impedance down to 10% to 20% means the loss of attachment of the cellular layer to the chip surface and this in turn means cell death. The lowest concentration used (10  $\mu\text{M}$ ) is overcome by the cells since no difference with the control can be observed. 100  $\mu\text{M}$  Chlorpyrifos leads to a decrease in the respiration rate while the extracellular acidification rate increases and reaches a maximum after 10h measurement. Thereafter the acidification rate decreases and nearly recovers completely during the recovering phase. This opposing trends suggest an impairment in the respiration without causing a complete damage to the mitochondrial activity. The drop down in the ATP production is compensated by an increase in the glycolysis. This leads to an increased lactate production with the subsequent increased acidification rate.

### Exposure of TBBPA to RLC-18 cells

Figure 3.2 shows the physiological response of RLC-18 cells against the flame retardant TBBPA. Cells are susceptible even to the lowest concentration of TBBPA used,  $10 \mu\text{M}$ . The acidification rate increases up to 120% and the respiration rate decreases slightly (figure 3.2 B & C). Neither damage caused by TBBPA in this concentration is lasting. As soon as fresh medium is pumped during the recovering phase both parameters recuperate and attach to the course of the adaptation phase. The morphology of the cells remains constant during the application of  $10 \mu\text{M}$  TBBPA as well as the controls (figure 3.2 A). Concentrations higher than  $100 \mu\text{M}$  drive the cells to a complete physiological rest. The toxic effect for the cell layer is too high and all three parameters break down to 10%, which means cell death. Nevertheless, the velocity of this break down is concentration dependent. This can be better seen by observing the measured cell impedance (figure 3.2 A). The damage caused by  $1.000 \mu\text{M}$  TBBPA is almost immediately, 100

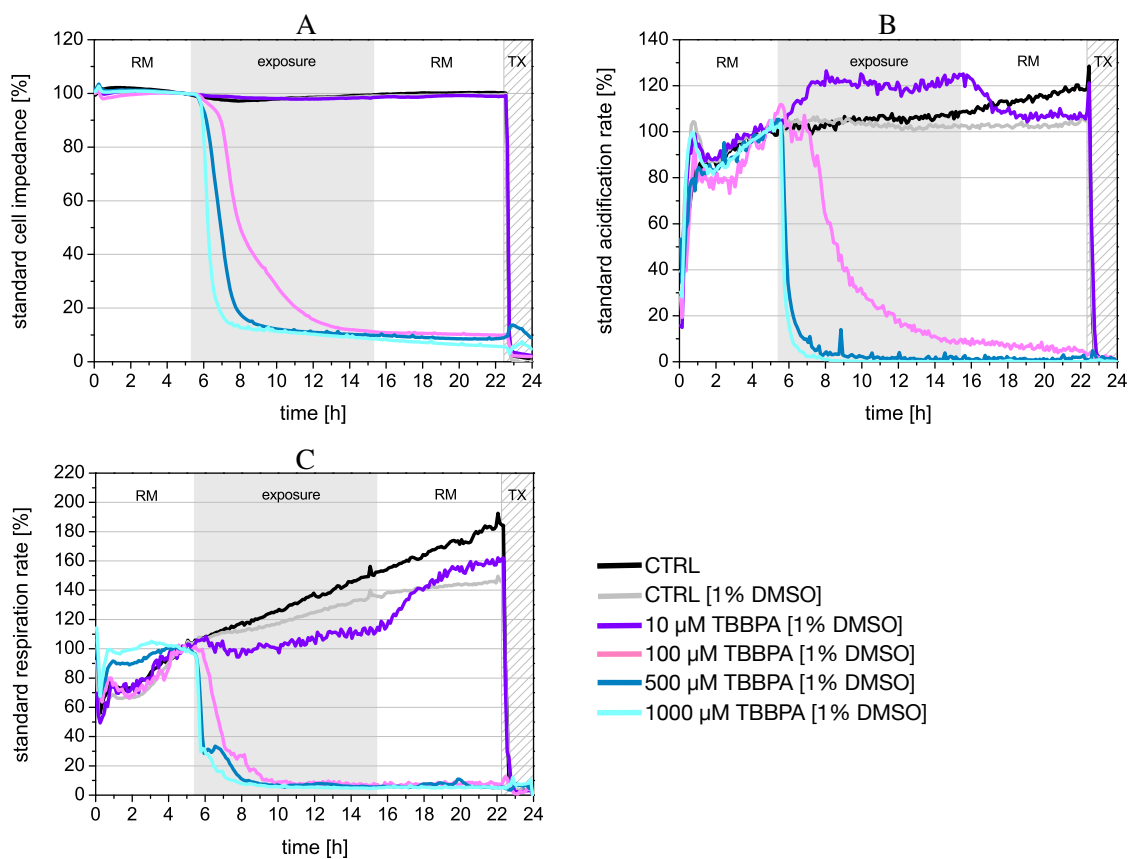


Figure 3.2: Impact of TBBPA on RLC-18 cells after 10h exposure time (shaded area) measured in Bionas Analyzing System followed by a recovering phase of 7h (white area). Cells were allowed to adapt to the system prior to exposure for 5h (white area). A) Standardized cell impedance, B) Standardized acidification rate, C) Standardized respiration rate. The results are reported as mean of three independent experiments.

$\mu M$  need more time until the effect is as strong as with  $1.000 \mu M$  and the time course after  $500 \mu M$  lies in between.

### Exposure of 4-MBC to RLC-18 cells

The UV filter 4-MBC is present in a variety of products from our daily use. Reason enough to analyze which consequences would be expectable if this chemical would enter the organism. In fact this substance is less toxic than the ones we studied before.  $10 \mu M$  4-MBC are perfectly overcome by the cells. All parameters behave as the controls (figure 3.3), meaning that there is no toxicity appreciable and no reason for concern.  $100 \mu M$  produces just little damage, nevertheless the toxic effect caused is lasting. Figure 3.3 C shows the respiration rate of the cellular layer. The addition of  $100 \mu M$  4-MBC leads to a decrease in the respiration rate of 10%. This slight decrease should not be ignored because the damage caused to the respiration chain persists after the compound has left the fluidic flow of the system. Concentrations higher

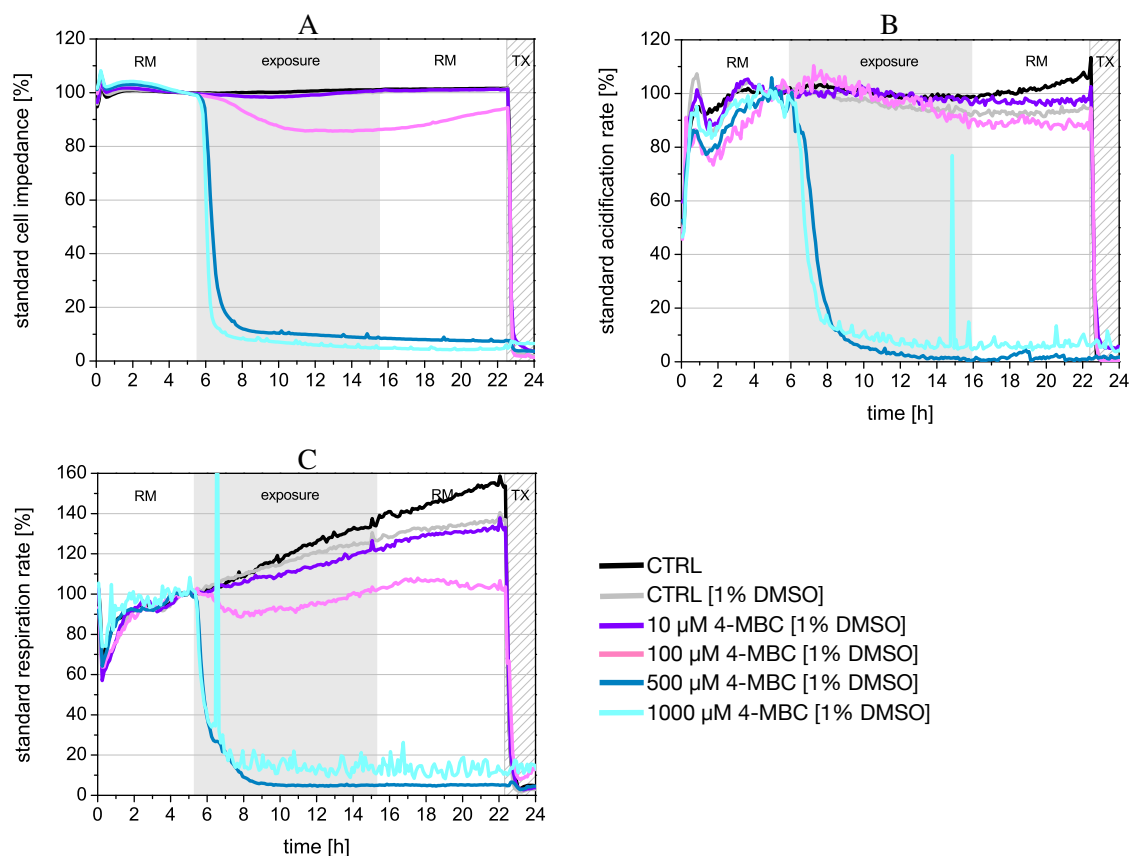


Figure 3.3: Impact of 4-MBC on RLC-18 cells after 10h exposure time (shaded area) measured in Bionas Analyzing System followed by a recovering phase of 7h (white area). Cells were allowed to adapt to the system prior to exposure for 5h (white area). A) Standardized cell impedance, B) Standardized acidification rate, C) Standardized respiration rate. The results are reported as mean of three independent experiments.

than 100  $\mu\text{M}$  lead to a fast decrease in all parameters, meaning that this concentrations (500  $\mu\text{M}$  and 1.000  $\mu\text{M}$ ) result in an irreparable damage and in consequence in cell death.

#### Exposure of 2-AA to RLC-18 cells

2-AA was chosen as a model substance representing the family of nitro-polycyclic aromatic hydrocarbons. This chemical is present in dyes, drugs, inks, plastics and agricultural chemicals (see chapter 1). Over the long term 2-AA is known to be a potential carcinogen causing mutations in eukaryotic as well as in prokaryotic cells. Figure 3.4 shows the toxicity of this organic compound in the short-term. The effect of 2-AA on the cellular layer is concentration dependent. Again, the lowest concentration (10  $\mu\text{M}$ ) remains nearly undetectable. Cells can handle this very low concentration without suffering any physiological alteration. Higher concentrations lead clearly to a visible impairment. The morphology changes as can be seen by the drop of the measured impedance (figure 3.4 A). This means that either cell to cell contacts

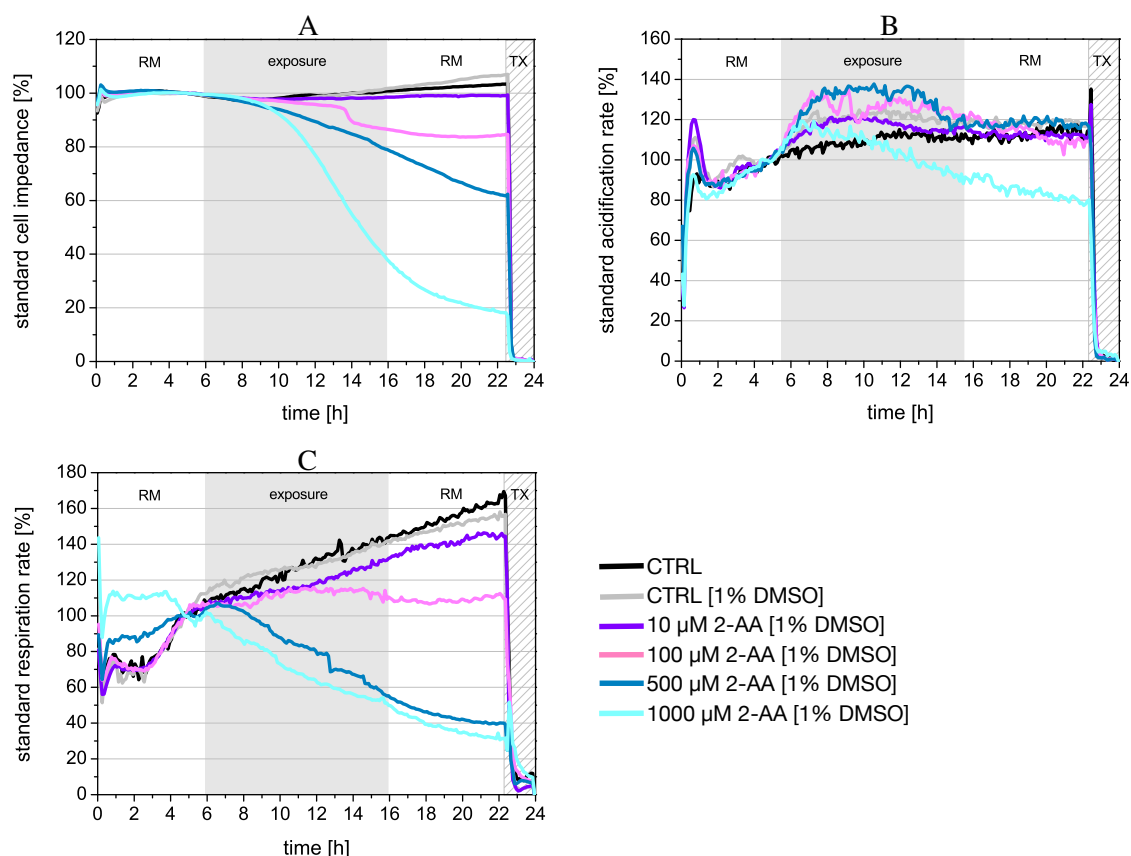


Figure 3.4: Impact of 2-AA on RLC-18 cells after 10h exposure time (shaded area) measured in Bionas Analyzing System followed by a recovering phase of 7h (white area). Cells were allowed to adapt to the system prior to exposure for 5h (white area). A) Standardized cell impedance, B) Standardized acidification rate, C) Standardized respiration rate. The results are reported as mean of three independent experiments.

are ceased or the cytoskeleton contracts leading to a round shaped cell form. The acidification rate increases if 100  $\mu M$  or 500  $\mu M$  2-AA is present in the sample but it recovers completely after exposure has ceased (figure 3.4 A). 1.000  $\mu M$  cause a short increase in the acidification rate but afterwards the metabolic rate diminishes. The slope of the respiration rate flattens after application of 100  $\mu M$  and falls constantly if higher concentrations are present. Previously, it was discussed that the loss of ATP synthesis by the respiration chain can be compensated by a higher glycolysis. Also feasible in this case is that the cells try to fight against the compound by activation carriers or accelerating the activity of metabolizing enzymes. All this appropriate measures would also lead to an increased extracellular acidification rate. Regardless of the reason, an alteration of a physiological parameters means that the cells are being hampered by the substance, what in turn means that the compound is bioactiv.

### 3.1.2 Cell viability measured by an end-point assay, prove of concept

The metabolic sensor system together with its electronic read-out provides a comprehensive evaluation of the cytotoxicity of a given chemical. Nowadays many assays are on the market and are used to determine the cellular chemosensitivity of a compound. There are several enzyme release assays (lactate dehydrogenase release assay, glucose-6-phosphate dehydrogenase release assay, glyceraldehyde-3-phosphate dehydrogenase release assay), cell viability assays (trypan blue and alamar blue assay, sulforhodamine B assay), cell survival assays (neutral red uptake assay, MTT assay, ATP assay), cell death assays (detection of caspases, membrane alterations, DNS fragmentation) (for a review see Sumantran (2011)). Each one analyzes the status of the cells by depicting a certain physiological or cellular process.

The MTT assay was chosen here for the comparison with the above presented multiparametric physiological sensor system. It is one of the most common and widely used end-point assays since it is easy, sensitive and rapid. It determines cell survival/cell viability by measuring mitochondrial activity (Scudiero et al. (1988)). A tetrazolium salt is reduced in the presence of an electron-coupling agent. This agent, NAD(P)H, is won through glycolysis and the cleavage is performed by the succinate-reductase from the respiratory chain of the mitochondria<sup>1</sup> (Mosmann (1983); van Meerloo et al. (2011)).

Figure 3.5 shows the impact of chlorpyrifos, TBBPA, 4-MBC and 2-AA to RLC-18 after 12h incubation measured by MTT. After the application of chlorpyrifos a toxic effect is first observed at 100  $\mu\text{M}$ . The viability decreases to 60% which is in line to the decrease in the respiration rate measured by the biosensor system (figure 3.1 C). Higher concentrations cause cell death and 10  $\mu\text{M}$  remain undetectable. In this case the toxicity is not high enough to cause acute damage in the respiration chain.

The flame retardant TBBPA provokes a dramatic increase in the cell viability in a concentration of 100  $\mu\text{M}$  and a decrease with concentrations higher than 500  $\mu\text{M}$ . The increase to 180% compared to the control could mean an induction in the proliferation of the cells. But more likely this is due to an increased metabolism in order to degrade TBBPA. Without success, as could be seen in figure 3.2, section 3.1.1. Probably this is the biggest disadvantage of end-point assays.

---

<sup>1</sup>Roche Applied Science, <http://www.roche-applied-science.com/shop/products/cell-proliferation-kit-i-mtt-#tab-3>

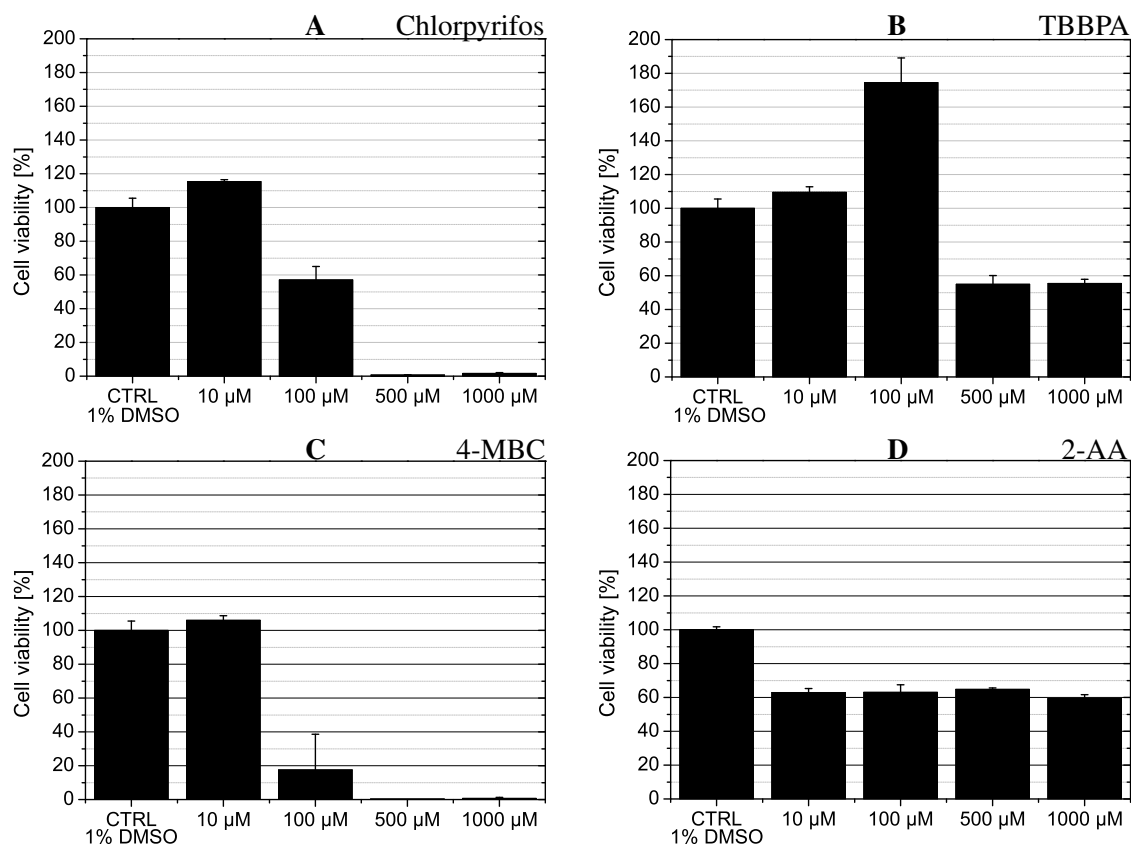


Figure 3.5: Cell viability of RLC-18 cells determined by MTT assay after compound exposure in different concentrations for 12h. Panel A: chlorpyrifos; Panel B: TBBPA; Panel C: 4-MBC; Panel D: 2-AA. The control containing 1% DMSO was set to 100%. The results are reported as mean  $\pm$  SD of three independent experiments.

There is no time scale to determine when a compound unfolds its toxicity and how the cell behaves or counteracts the effect, there is no information about pharmacokinetics available. More over the MTT assay can not differentiate between cytotoxicity and cytostatic drugs (Sumantran (2011)). Therefore, if cell viability decreases compared to the control it is either due to a toxic effect or because the substance inhibits cell division. Latter effect does not inherently mean toxicity.

A decrease in cell viability is observed after the application of 500  $\mu\text{M}$  and 1.000  $\mu\text{M}$  TBBPA, underlining the cell-based sensor measurements. Panel C in figure 3.5 describes the impact on RLC-18 after incubation with the UV-B filter 4-MBC. A high toxicity is observed if concentrations are higher than 100  $\mu\text{M}$ . Cell viability goes down to 20% after incubation with 100  $\mu\text{M}$  and to 0% with higher concentrations. In this case the assay is even more sensitive than the measurements performed with the cell sensor.

To round out the picture, 2-AA shows an concentration independent decrease in cell viabil-



ity down to 60% (figure 3.5 D). Remarkably this occurs for all concentrations, from 10  $\mu M$  to 1.000  $\mu M$ . If we claim that the MTT assay mirrors the integrity of the respiration chain, the damage caused here is independent of the amount of this chemical.

In the last two sections the impact of four model pollutants on RLC-18 cells was analyzed. They were applied into the fluidic system of the multiparametric physiological sensor system in different concentrations. The cellular detection layer is able to react to the presence of this chemicals in the medium. Moreover, the physiological response and the damage caused to the cells is, in general, concentration dependent. This results were also compared with a well established end-point assay. In general, the performed MTT assays were in line with the results obtained with the cell-based sensor. Merely TBBPA differed from the expectation, being considerably much less sensitive than the multiparametric sensor. 10  $\mu M$  passed unnoticed through the 96 well plate wells and 100  $\mu M$  TBBPA increased cell viability whereas the physiological parameters showed a doubtless toxic response which led to cell death after 3h.

There are, and this must not vanish into oblivion, huge differences in the experimental setups. An MTT assay is performed in 96 well plates and these are not connected to a fluidic system. This could reduce the toxic impairment since no “fresh” medium is supplied. During the time of the exposure the compound could be consumed by the cell. In this way the expected toxicity of the compound may be reduced. Moreover, the lack of a time scale makes it impossible to track the behavior of the cells. It is conceivable that cells recover after having been treated with a compound. If the MTT reagent is applied at this time point no toxicity would be perceptible.

A three parametric sensor coupled to a fluidic system with a data acquisition in real time has, in fact, advantages. The aim in the next section is to go one step further and figure out how the cells or more precisely the sensor behaves if a combination of the above studied chemicals becomes in contact to the cell layer.

#### **3.1.3 Simultaneous detection of organic pollutants**

It is rare that pollutants are present as single compound in a sample. Therefore it is crucial to elucidate how this cell-based system behaves if pollutants are present as a mixture. In this case,

not only the damage caused is crucial but also if the interaction between both compounds leads to a strengthen or additive effect or if the presence of one compound is able to outweigh or mitigate the effect of the second one.

The graphs shown in section 3.1.1 suggest a sensitivity threshold of the system for these chemicals ranging between 10  $\mu M$  and 100  $\mu M$ . 100  $\mu M$  is the concentration which led to a clearly visible signal without driving most of the cells to death. 10  $\mu M$  represents the beginning of a toxic effect in the case of TBBPA (figure 3.2) but not for the rest. Therefore the concentrations chosen for the coexposure of two compounds to RLC-18 cells are a combination of these two concentrations. Table 3.1 gives an overview of the protocol used.

Figure 3.6 shows the combinatorial measurement of chlorpyrifos and TBBPA. 100  $\mu M$  of both compounds lead to immediate cell death. The cell impedance, acidification rate as well as the respiration rate break down to 0-5%. In figure 3.2, section 3.1.1 the effect of 100  $\mu M$  TBBPA showed as well a fast decrease in all physiological parameters. Instead, 100  $\mu M$  Chlorpyrifos (figure 3.1) led to a clear signal but not to cell death. It is obvious here that a very toxic concentration of one compound outweighs the effect of the second one. 10  $\mu M$  of both chemicals show no alteration in the cell integrity (cell impedance, figure 3.6 A) but lead to an increase in the acidification rate in the same magnitude as in the case of TBBPA alone. The respiration rate is not altered in the combinatorial measurement which represents a mismatch compared to the single measurements, TBBPA causes a slight but noticeable decrease. Similarly, the toxic effect of 100  $\mu M$  Chlorpyrifos is attenuated if 10  $\mu M$  TBBPA is also present in the sample. A decrease in the cell impedance is present in the combinatorial treatment, also a decreased respiration rate with the subsequent increased acidification rate. But all these effects are not as pronounced as in the case where 100  $\mu M$  Chlorpyrifos was present as a single compound. In the

Compound combination	Chlorpyrifos 4-MBC	& &	TBBPA TBBPA
Concentration	10 $\mu M$		10 $\mu M$
	100 $\mu M$		100 $\mu M$
	10 $\mu M$		100 $\mu M$
	100 $\mu M$		10 $\mu M$

Table 3.1: Overview over the pollutant pairs and the employed concentrations

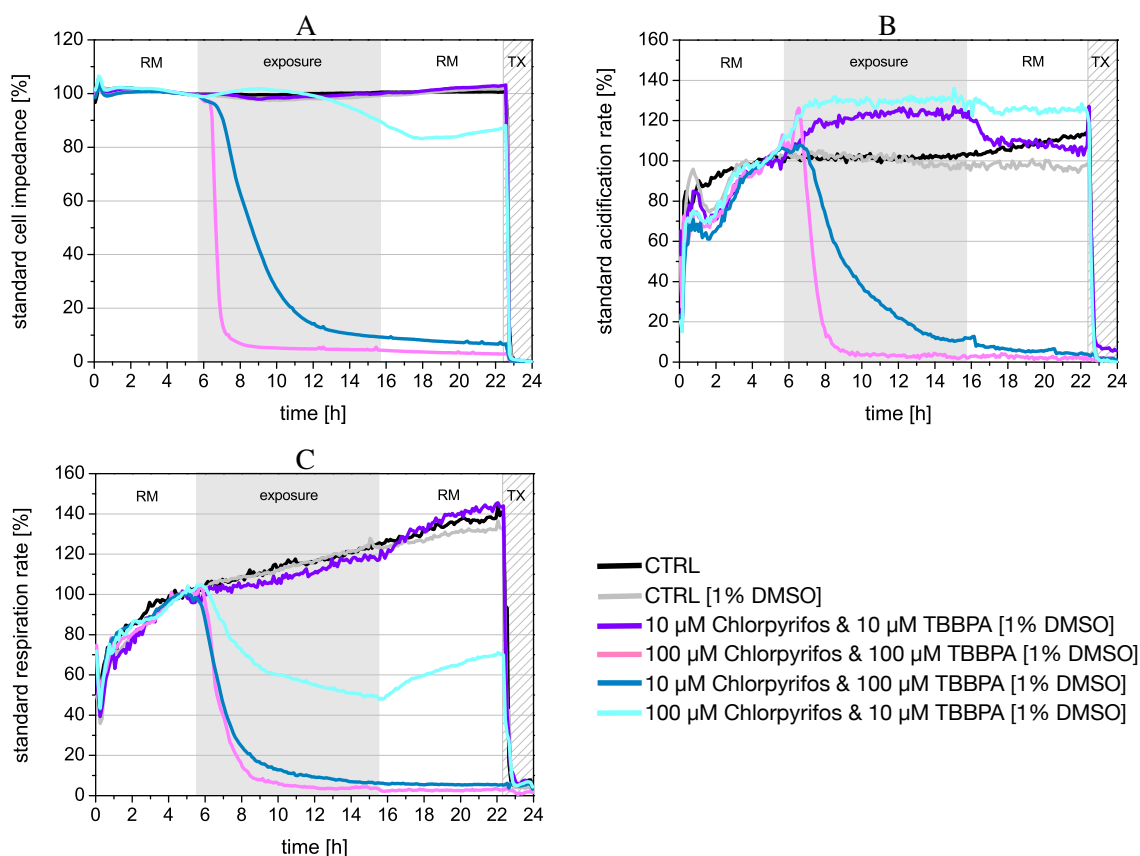


Figure 3.6: Impact of Chlorpyrifos and TBBPA on RLC-18 cells after 10h exposure time (shaded area) measured in Bionas Analyzing System followed by a recovering phase of 7h (white area). Cells were allowed to adapt to the system prior to exposure for 5h (white area). A) Standardized cell impedance, B) Standardized acidification rate, C) Standardized respiration rate. The results are reported as mean of three independent experiments.

combination the increase in the acidification rate reaches 130% instead of 150% and the slope of the acidification curve during the recovering phase is steeper as in Figure 3.1 C. This means that the cells are able to recover faster from the chemical exposure if 10  $\mu\text{M}$  TBBPA is also present in the sample. No mitigation effect is observed if 10  $\mu\text{M}$  Chlorpyrifos are combined with 100  $\mu\text{M}$  TBBPA. To the contrary, the effect of TBBPA predominates and all curves follow the same course as in the case of 100  $\mu\text{M}$  TBBPA alone.

The second coexposure studied was the combination of the UV-filter 4-MBC with TBBPA. The measurement corresponding to this experiment is shown in figure 3.7. After exposing the cells to 10  $\mu\text{M}$  4-MBC and 10  $\mu\text{M}$  TBBPA all physiological parameters decrease slightly down to 70-80%. The cells survive this exposure but the effect is lasting since the effect endures and the parameters do not reach 100% again after the recovering phase has finished.

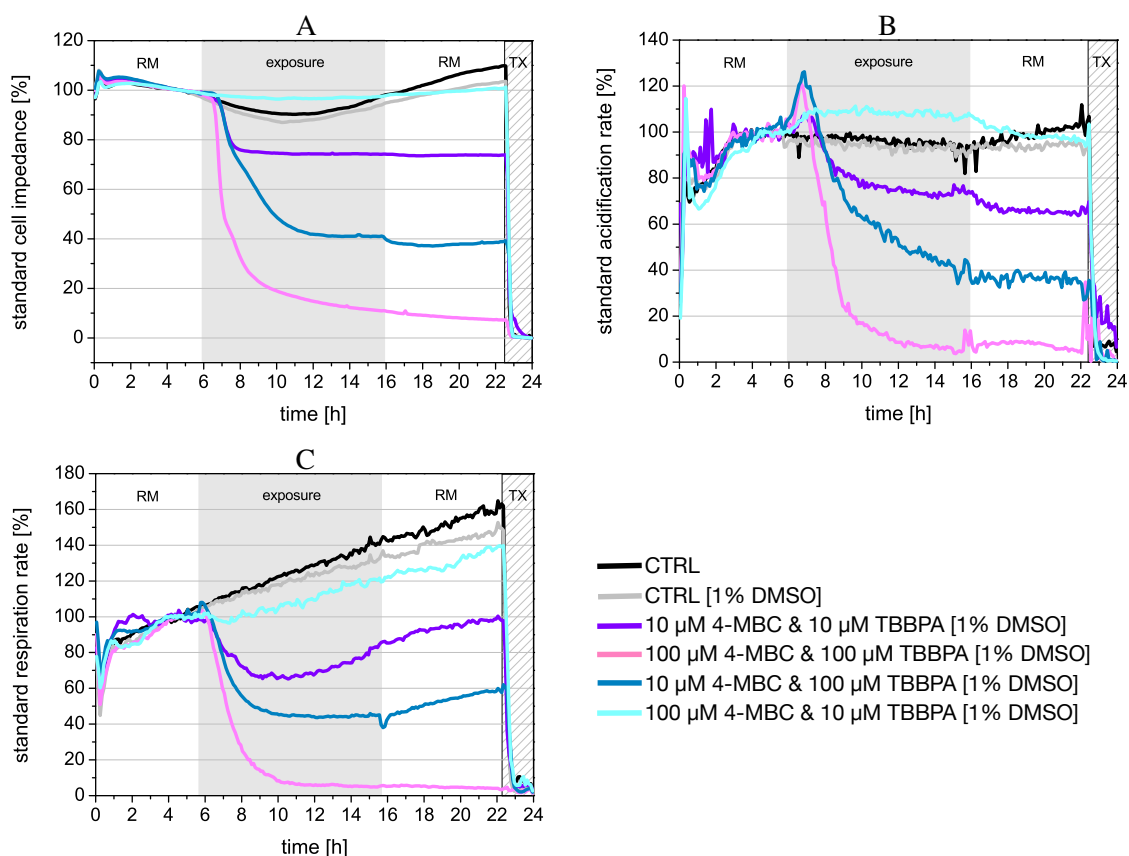


Figure 3.7: Impact of 4-MBC and TBBPA on RLC-18 cells after 10h exposure time (shaded area) measured in Bionas Analyzing System followed by a recovering phase of 7h (white area). Cells were allowed to adapt to the system prior to exposure for 5h (white area). A) Standardized cell impedance, B) Standardized acidification rate, C) Standardized respiration rate. The results were reported as mean of three independent experiments.

100  $\mu\text{M}$  4-MBC and 100  $\mu\text{M}$  TBBPA lead to a fast cell death and a physiological break down similar to the one observed in figure 3.2, where TBBPA was applied as a single compound. In terms of a toxicological effect, the combination of these two compounds in different concentrations is more interesting. After the application of 10  $\mu\text{M}$  4-MBC and 100  $\mu\text{M}$  TBBPA the cell impedance and the acidification rate decline to 40% and the respiration rate to 50-60% (figure 3.7). This is exactly in between of the values obtained after the single application of 4-MBC (figure 3.3) and TBBPA (figure 3.2). 100  $\mu\text{M}$  TBBPA led to a break down in all physiological parameters to 0-10%, which means cell death and 10  $\mu\text{M}$  4-MBC did not affect the cells. 4-MBC passed unnoticed through the system. If these chemicals appear together, the cells are hampered but still alive. Presumably the main effect is caused by TBBPA since this chemical in this concentration provokes rapid cell death. But the 10  $\mu\text{M}$  4-MBC are crucial for the cell survival, it mitigates the effect of TBBPA.

Figure 3.7 shows also the consequence of 100  $\mu\text{M}$  4-MBC and 10  $\mu\text{M}$  TBBPA. During the whole exposure the morphological status remains intact. This is reflected by the standardized cell impedance, which stays constant at 100%. The acidification rate increases slightly during the application and reaches 110%. This is in line with the decrease of the respiration rate (figure 3.7 C). The loss of ATP synthesis from the respiration chain is overcome by an increased glycolysis. This higher metabolic rate leads to the production of more waste products like lactate which acidify the extracellular medium. The decreased respiration rate is not visible as a systemic breakdown. Rather, it is appreciable as a slight decay in the slope of the curve.

If this combinatorial exposure is compared to the single treatments of 4-MBC (figure 3.3) and TBBPA (figure 3.2), it is possible to summarize the coexposure as a mitigation of the overall toxicity. 100  $\mu\text{M}$  4-MBC alone decreased the cell impedance by 10 to 15%. Also the respiration drifted from its original course. The cellular layer was very susceptible to 10  $\mu\text{M}$  TBBPA, the acidification rate increased to 120% and the respiration rate decreased significantly compared to the controls. All these effects are now attenuated if both compounds are presented to the cells. There is no morphological impairment to account for, the acidification rate increases by 10 but not by 20% and the respiration rate is only little affected.

As well as it was performed for the single measurements, the impact of the combined chemicals was analyzed also under the conditions of an MTT assays. This is going to be shown in the next section.

#### **3.1.4 Coexposure of organic pollutants to RLC-18 cells analyzed by MTT**

A mixture of Chlorpyrifos with TBBPA and 4-MBC with TBBPA in the same concentrations as in the analysis with the cell chip was added to the cells. The viability of the cells was then evaluated by MTT. Panel A in figure 3.8 shows the impact on RLC-18 cells after having been treated with Chlorpyrifos and TBBPA. No significant damage, compared to the control, is perceivable after the incubation with 10  $\mu\text{M}$  Chlorpyrifos/10  $\mu\text{M}$  TBBPA and 100  $\mu\text{M}$  Chlorpyrifos/10  $\mu\text{M}$  TBBPA. The incubation of compounds in the highest concentration (100  $\mu\text{M}$ ) leads to the death of the cells, whereas the combination 10  $\mu\text{M}$  Chlorpyrifos/100  $\mu\text{M}$  TBBPA increases cell viability up to 140%.

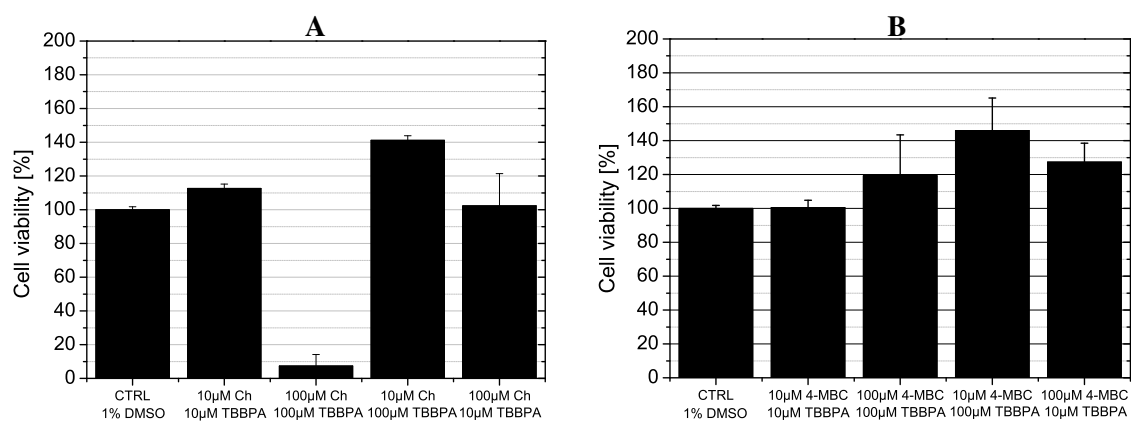


Figure 3.8: Cell viability of RLC-18 cells determined by MTT assay after compound coexposure in different concentrations for 12h. Panel A: chlorpyrifos and TBBPA; Panel B: 4-MBC and BBPA. The control containing 1% DMSO was set to 100%. The results were reported as mean  $\pm$  SD of three independent experiments.

There is a wide discrepancy between these data, obtained with MTT, and those acquired with the cell-based sensor system (3.6 in section 3.1.3). Only the combination with the highest concentration (100  $\mu$ M Chlorpyrifos and 100  $\mu$ M TBBPA) correlates with the data obtained with the metabolic chip. Sumantran (2011) assigns the outcome from the MTT assay with the integrity of the respiration chain. Therefore, if the sensor data show an impairment in the respiration rate, this damage should also be visible after having performed a MTT-assay. Nevertheless the damage caused by Chlorpyrifos and TBBPA (see figure 3.6) could not be reproduced by the MTT-assay.

A similar picture is obtained after having conducted the MTT assay with 4-MBC & TBBPA in combination. Similar in the sense that the result obtained with the MTT assay dissent from the data acquired with the cell-based sensor. The MTT assay (figure 3.8 B) reveals a perfect handling of these chemicals by the cells. The measured absorption for the combination 10  $\mu$ M 4-MBC/10  $\mu$ M TBBPA resides in the same range as the control after standardization of data. For all other combination cells even account for a viability improvement. 10  $\mu$ M 4-MBC/100  $\mu$ M TBBPA leads to an increase in viability up to 140% and 100  $\mu$ M 4-MBC/100  $\mu$ M TBBPA as well as 100  $\mu$ M 4-MBC/10  $\mu$ M TBBPA do not alter cellular healthiness. In contrast, the data acquired by the chip (figure 3.7) show an alteration in all combinations performed since the physiological status of the cells was influenced by these chemicals (figure 3.7).

It is conceivable, that the sensitivity of this assay does not allow small changes in cell

viability. More over, and probably more important is the fact that these two methods, a cell-based sensor and an end-point assays, are too distinct to make a valid comparison. There are several differences between these two techniques which should be kept in mind while comparing the data obtained from these experiments. Box 1 gives an overview about these differences.

#### Box 1: MTT & cell-based sensor

The MTT assay is a well established end-point assay to determine the toxicity of a substance. It was used in this study as a benchmark for the developed cell-based detection system. Before and after the performance of the assay several facts arose concerning the different setting of these two techniques. These differences are going to be explained here and should be kept in mind while evaluating MTT data or comparing these with cell-chip data.

- The cell based system accounts for a time-scale in real time. This narrows the gap between pharmacokinetics and pharmacodynamics, explaining when a compound unfolds its toxicity and how the cellular layer behaves and/or tries to counteract the cytotoxic effect produced.
- The lack of a time scale in the MTT assay makes it impossible to track the behavior of the cells. It is conceivable that cells recover after having been treated with the compound. If the MTT reagent is applied at this time point no toxicity would be perceptible.
- The MTT assay cannot differentiate between cytotoxicity and cytostatic drugs (Sumantran (2011)). Therefore, if cell viability decreases compared to the control it is either due to a toxic effect or because the substance inhibits cell division. Latter effect does not inherently mean toxicity.
- A fluidic system is coupled to the sensor. “Fresh” medium is supplied during the whole measurement, making the depletion of the compound due to metabolization impossible.

## 3.2 Prediction of chemicals in the sample, functional data analysis

It was shown that the used detection layer has the ability to notice the physiological damage caused by chlorpyrifos and TBBPA. The effect of these organic pollutants, if present simultaneously, is not merely additive. As shown in Figure 3.6 one chemical can overbalance the effect of the second one. Even more precarious for a valid risk assessment is the observation that one compound can mitigate the effect of the other one, which does not *a priori* mean that the sample is less dangerous. This fact makes it impossible to trace back the physiological response to a concrete compound. It is therefore of great interest to be able to decrypt the data collected by the cell-based sensor, in order to determine if the observed curve progression is due to one substance or if a second one is masking the effect of the first one. In this section a functional generalized linear model is being presented, which allows to determine if a certain pollutant is present in the sample or not.

In the functional binomial model used, the response  $y_i$  was classified into two classes, “0” if the pollutant is not present and “1” if it is present (Fuchs et al., 2015). Using this principle, five models were calculated, which are listed in Table 3.2. The first column defines the name of the model, the second the substances that have been taken into account in the response, this means the target compound which is wished to be ascertained.

Model	Substances
I	Undefined pollutant
II	Chlorpyrifos as single pollutant
III	TBBPA as single pollutant
IV	4-MBC as single pollutant
V	Chlorpyrifos single and in mixed samples with TBBPA
VI	TBBPA single and in mixed samples with Chlorpyrifos
VII	4-MBC single and in mixed samples with TBBPA
VIII	TBBPA single and in mixed samples with 4-MBC

Table 3.2: List of models.



Several versions of the functional generalized model were tested. Each of them include the data of different combinations of electrodes. Section 2 described the buildup of the model in detail and in this section the accuracy of this models will be presented. It is important to bear in mind or at least remember the versions of the model that had been designed. Box 2 recapitulates all the versions and summarizes the most important facts surrounding the functional generalized model (FGM).

Box 2: FGM and its versions

$$y_i \sim B(1, \pi_i), \quad (3.1)$$

with  $\pi_i = \frac{\exp(\eta_i)}{1+\exp(\eta_i)}$ ,

linear predictor  $\eta_i \in \{\eta_i^4, \eta_i^5, \eta_i^6, \eta_i^7, \eta_i^8, \eta_i^9, \eta_i^{10}, \eta_i^{11}, \eta_i^{12}, \eta_i^{13}\}$ ,

$\eta^4 = \beta_0 + \int x_{isfet} \xi_{isfet} ds + \int x_{ides} \xi_{ides} dt$ , acidification rate and cell impedance

$\eta^5 = \beta_0 + \iint x_{isfet} x_{ides} \beta_1 ds dt$ , interaction between acidification rate and cell impedance

$\eta^6 = \beta_0 + \int x_{isfet} \xi_{isfet} ds + \int x_{ides} \xi_{ides} dt + \iint x_{isfet} x_{ides} \beta_1 ds dt$ , acidification rate, cell impedance and their interaction

$\eta^7 = \beta_0 + \int x_{isfet} \xi_{isfet} ds + \int x_{clark} \xi_{clark} dz$ , acidification rate and respiration rate

$\eta^8 = \beta_0 + \iint x_{isfet} x_{clark} \beta_2 ds dz$ , interaction between acidification rate and respiration rate

$\eta^9 = \beta_0 + \int x_{isfet} \xi_{isfet} ds + \int x_{clark} \xi_{clark} dz + \iint x_{isfet} x_{clark} \beta_2 ds dz$ , acidification rate, respiration rate and their interaction

$\eta^{10} = \beta_0 + \int x_{ides} \xi_{ides} dt + \int x_{clark} \xi_{clark} dz$ , cell impedance and respiration rate

$\eta^{11} = \beta_0 + \iint x_{ides} x_{clark} \beta_3 dt dz$ , interaction between cell impedance and respiration rate

$\eta^{12} = \beta_0 + \int x_{ides} \xi_{ides} dt + \int x_{clark} \xi_{clark} dz + \iint x_{ides} x_{clark} \beta_3 dt dz$ , cell impedance, respiration rate and their interaction

$\eta^{13} = \beta_0 + \int x_{isfet} \xi_{isfet} ds + \int x_{ides} \xi_{ides} dt + \int x_{clark} \xi_{clark} dz$ , acidification rate, cell impedance and respiration rate

### 3.2.1 Identification of a polluted sample

The obligatory basis for the recognition of a certain substance in the sample is first, to make sure that the designed model is able to differentiate between a clean sample and a polluted one. No matter which pollutant is present in the sample, model I (figure 3.9) accounts for the detection of a chemical in a sample. To evaluate the goodness of a model the model quality  $R^2$  and the misclassification rates (MCR) of the data set were taken into account.  $R^2$  describes how well data points fit a statistical model and the missclassification rate describes how many samples were classed erroneously. It is possible to analyze only one parameter/electrode type ( $\eta^1 - \eta^3$ ), a combination of two parameters/electrode types ( $\eta^4 - \eta^{12}$ ), or a combination of all

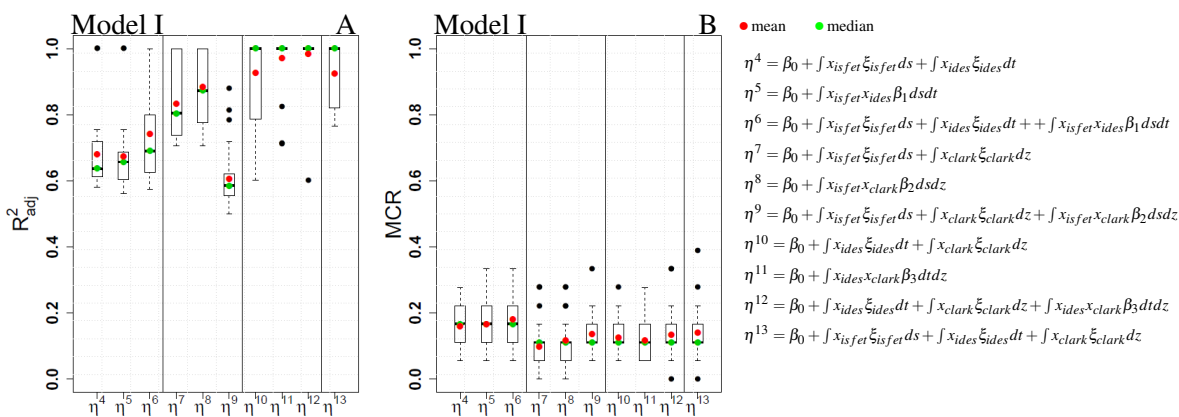


Figure 3.9: Prediction of an undefined pollutant in a sample, model quality and validation. The boxplots show 25 random draws out of the full data set. A) adjusted  $R^2$  of the model, B) misclassification rates of the validation data sets. The means and the medians are depicted as red and green dots respectively

3 parameters/electrode types ( $\eta^{13}$ ).

In this section all the model versions where at least the data sets of two electrodes are included in the functionals generalized I model will be presented, these are  $\eta^4 - \eta^{13}$ . The difference between these versions relies in the type and amount of electrodes taken into account for the model.  $\eta^5$ ,  $\eta^8$  and  $\eta^{11}$  represent the interaction term. It is the double integral of the product of two different electrode signals. This term describes how the signals of two electrodes behave relativ to each other. It accounts for the synchronous increase or decrease of the signals or for opposed trends, like the decrease of the respiration rate by simultaneous increase of the acidification rate. This term will become crucial for the identification of a certain pollutant in a sample.

The most basic scenario will be considered first, the identification of a polluted sample regardless the chemical contaminating it. The results for this model are shown in figure 3.9. The statistical model suits perfectly its purpose. For nearly all electrode combinations ( $\eta$ ), the adjusted  $R^2$  is close to 1 and the missclassification rates are in the range of 0.1 and 0.19. This means that only 10%-19% of the samples containing a pollutant are not recognized as contaminated.

A  $R^2$  of 0.6 is considered as a good fit for a model. All model variants have a  $R^2 \leq 0.6$  but there are slightly differences between the different  $\eta$ . The best results are archived with  $\eta^{10}$ - $\eta^{13}$ . In this case the information obtained from the IDES and clark electrodes are particularly relevant

for the detection of a polluted sample.

### 3.2.2 Identification of a concrete chemical in a polluted sample

Samples containing different concentrations<sup>2</sup> of the pesticide chlorpyrifos, the flame retardant TBBPA or the UV-filter 4-MBC were measured by the cell-based system. Afterwards, the obtained data were analyzed with the functional model in the expectation that the system would be able to ascertain the nature of the substance present in the sample or verify the good quality in case that the sample was unpolluted.

Figure 3.10 A & B shows the result for the detection of chlorpyrifos (model II). The high values for the adjusted  $R^2$  mean that the signals obtained during the measurements are very specific and characteristic providing the basis for a reliable model. The computational model can identify this substance with few false classifications, as reflected by the very low values of the misclassification rates (Figure 3.10 B). It starts to be important which electrode signal are taken into account. In general all versions ( $\eta$ ) are characterised by a  $R_{adj}^2 \geq 0.6$ . Nevertheless,  $\eta^7$ , which incorporates the signals from the IDES and the ISFET electrodes is not sufficient for a promising fit. The interaction term ( $\eta^8$ ) in contrast renders a nearly perfect fit. This shows the importance of the interaction term. Without incorporating another signal type, the interaction term improves the fit and the reliability of the model.

If TBBPA is set as the target compound (model III), the results are even more remarkable. Figure 3.10 C shows the adjusted  $R^2$  for all model variants. The  $R_{adj}^2$  is close to 1 for all model variants and in accord with this model quality, the misclassification rates are in the range of 0.1. This means that independently of the used electrode data, the algorithm detects easily the presence of TBBPA in a sample. Presumably this is because the impact on RLC-18 cells of TBBPA reflect a very characteristic alteration of the physiological parameters (see Figure 3.2), i.e. time dependence of the response and manner.

A misclassification rate between 0.19 and 0.2 characterizes the determination of the UV-screen 4-MBC (model IV, figure 3.10 F). Meaning that at least 80% of the 4-MBC containing samples are recognized. The model quality, figure 3.10 E, reflected by the  $R_{adj}^2$  however oscil-

---

<sup>2</sup>The concentrations used correspond to those presented in section 3.1.1:  $10\mu M$ ,  $100\mu M$ ,  $500\mu M$  and  $1.000\mu M$ .

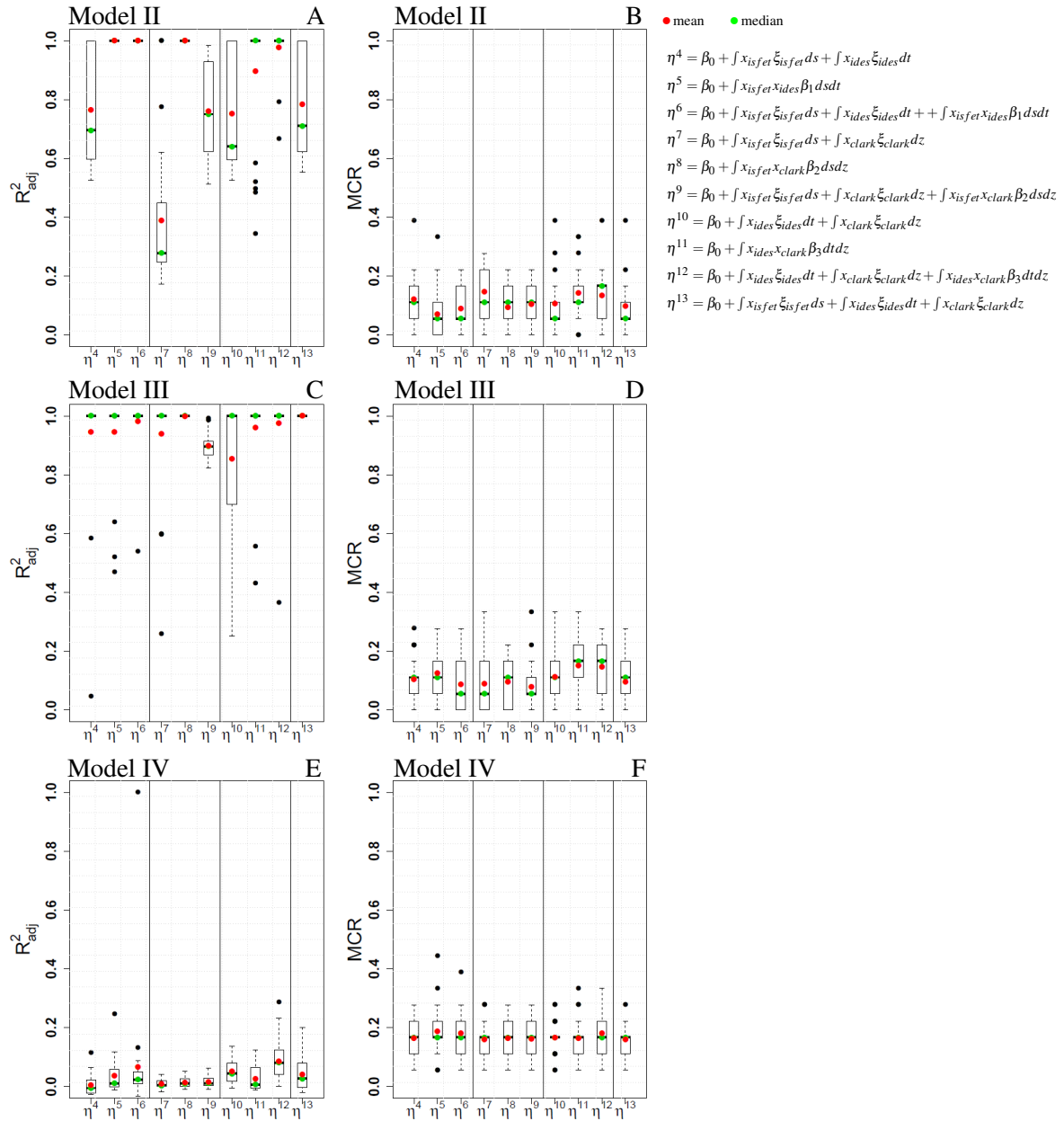


Figure 3.10: Panel A & B: Prediction of chlorpyrifos as single pollutant in a sample, model quality and validation. Panel C & D: Prediction of TBBPA as single pollutant in a sample, model quality and validation. Panel E & F: Prediction of 4-MBC as single pollutant in a sample, model quality and validation. The boxplots show 25 random draws out of the full data set. The left column shows the adjusted  $R^2$  of the model, the right the misclassification rates of the validation data sets. The means and the medians are depicted as red and green dots respectively

lates between 0 ( $\eta^8$ ) and 0.1 ( $\eta^{12}$ ). The low values for the  $R^2_{adj}$  can be explained by the low toxicity of this chemical. In figure 3.3 the response of the physiological parameters to 4-MBC were shown. Most of the concentrations used, show a curve progression close to the control. Therefore it is very difficult for the functional generalized model to fit the acquired data from the electrodes to an optimal model.

### 3.2.3 Identification of a concrete chemical in mixed samples

The biggest challenge for the statistical model is the recognition of a compound if this is present together with a second one. In model V (figure 3.11 A & B) the samples can contain no pollutant at all, only chlorpyrifos or a mixture of chlorpyrifos and TBBPA each in different concentrations. The response of the functional generalized model, that means the target compound, is still chlorpyrifos. The best model quality,  $R_{adj}^2$ , is achieved if the signals from the ISFET and IDES electrodes are considered together with the interaction term ( $\eta^6$ ), likewise the signals from the ISFET and Clark electrodes plus the interaction term ( $\eta^9$ ).

In model VI (figure 3.11 C & D) TBBPA is set as the response, so the target for the statistical model is the flame retardant in samples that can contain just this pollutant, a mixture of TBBPA with chlorpyrifos or nothing at all. As well as for the detection of chlorpyrifos in mixed samples, the choice of the adequate signal combination is a prerequisite for a high model

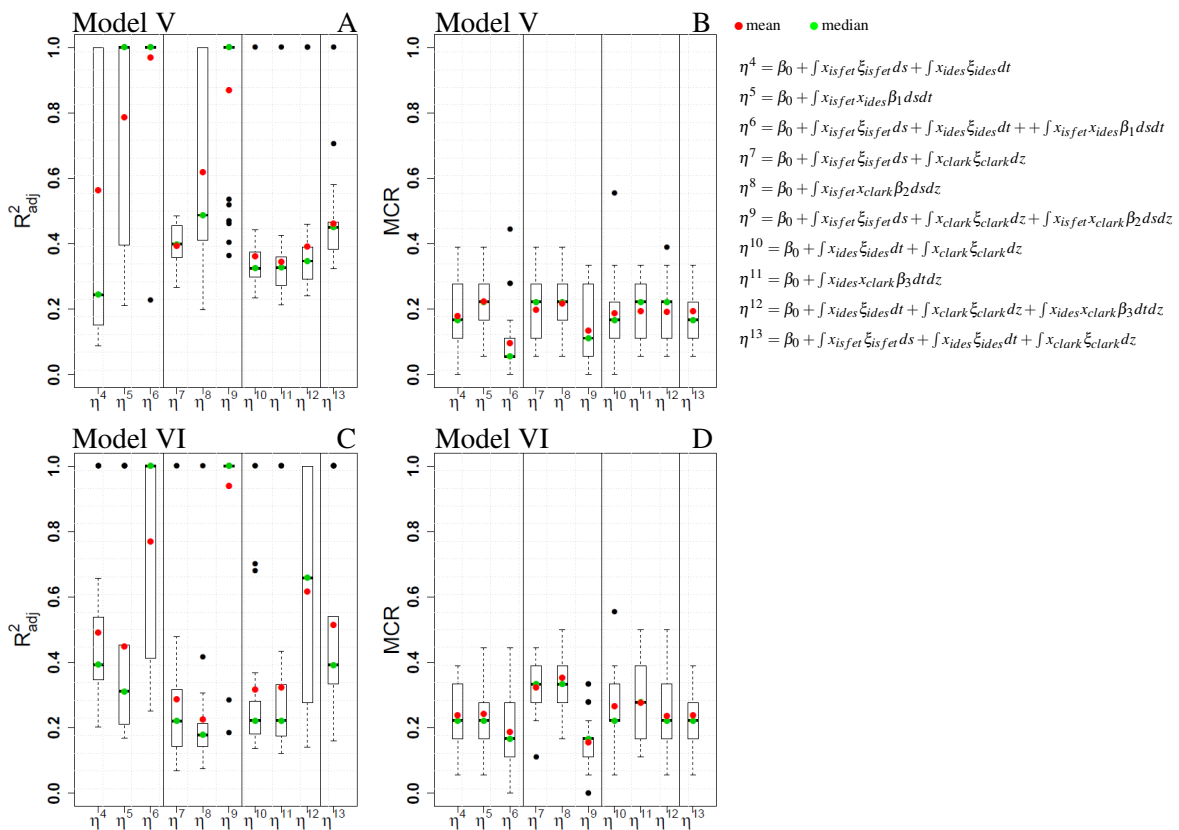


Figure 3.11: Panel A & B: Prediction of chlorpyrifos in samples mixed with TBBPA, model quality and validation. Panel C & D: Prediction of TBBPA in samples mixed with chlorpyrifos, model quality and validation. The boxplots show 25 random draws out of the full data set. The left column shows the adjusted  $R^2$  of the model, the right the misclassification rates of the validation data sets. The means and the medians are depicted as red and green dots respectively.

quality,  $R_{adj}^2$ , and a low missclassification rate,  $MCR$ . The best results are achieved with the model versions  $\eta^6$  and  $\eta^9$ :  $R_{\eta^6}^2 = 0.79$  &  $MCR_{\eta^6} = 0.19$  and  $R_{\eta^9}^2 = 0.95$  &  $MCR_{\eta^9} = 0.17$  (mean values, ●).

In the case of chlorpyrifos and TBBPA, the algorithm fulfills the expectations making it possible to detect these chemicals not only in single samples (figure 3.10) but also if they are present together as shown in this section. The high quality of latter detection is probably ascribed to a very characteristic impact of these two compounds to the physiology of RLC-18 cells. The most promising model versions,  $\eta^6$  and  $\eta^9$ , include the interactions term  $\iint x_{isfet}x_{ides}\beta_1 dsdt$  and  $\iint x_{isfet}x_{clark}\beta_2 dsdz$  respectively. In figure 3.6 the data acquired by the system after coexposure of chlorpyrifos and TBBPA to RLC-18 cells were shown. The signals of the IDES electrode and the ISFET electrodes as well as those from the Clark and ISFET electrodes are opposed, the decrease in one parameter is counteracted by an increase in the other one. The interaction accounts for this, since it implicates the product of both signals. Therefore the algorithm is so powerful in these two model versions.

The next two model versions focus on the recognition of the UV-screen 4-MBC and TBBPA if both can simultaneously be present in a polluted sample. The achieved results for model VII are represented in panels A & B in figure 3.12. The model quality  $R_{adj}^2$  reaches a maximal value of 0.5 for version  $\eta^8$ , which represents the interaction term  $\iint x_{isfet}x_{clark}\beta_2 dsdz$ . The  $R_{adj}^2$  of all other model versions remain below 0.5 and the missclassification rates range between 0.2 and 0.3. This is in accordance with the result presented in figure 3.10 panel E & F, where 4-MBC was present as a single compound. The difficulties to recognize 4-MBC rely probably on the low acute toxicity of this chemical. This leads to moderate changes in the physiological parameters of the detection layer.

Figure 3.12 C & D show the reverse case. The target compound in model VIII is TBBPA and it shall be recognized in samples with this chemical only and in those ones containing also 4-MBC. The fingerprint of TBBPA is a very characteristic one, therefore the fit features higher  $R_{adj}^2$  than in model VII. An  $R_{adj}^2 \geq 0.6$  is achieved with the model versions  $\eta^5$ ,  $\eta^6$ ,  $\eta^7$  and  $\eta^{13}$ . Moreover a perfect fit is obtained with  $\eta^8$ , the version where only the interaction term with IDES and ISFET signals are taken into account. Missclassification rates of around 0.2 for

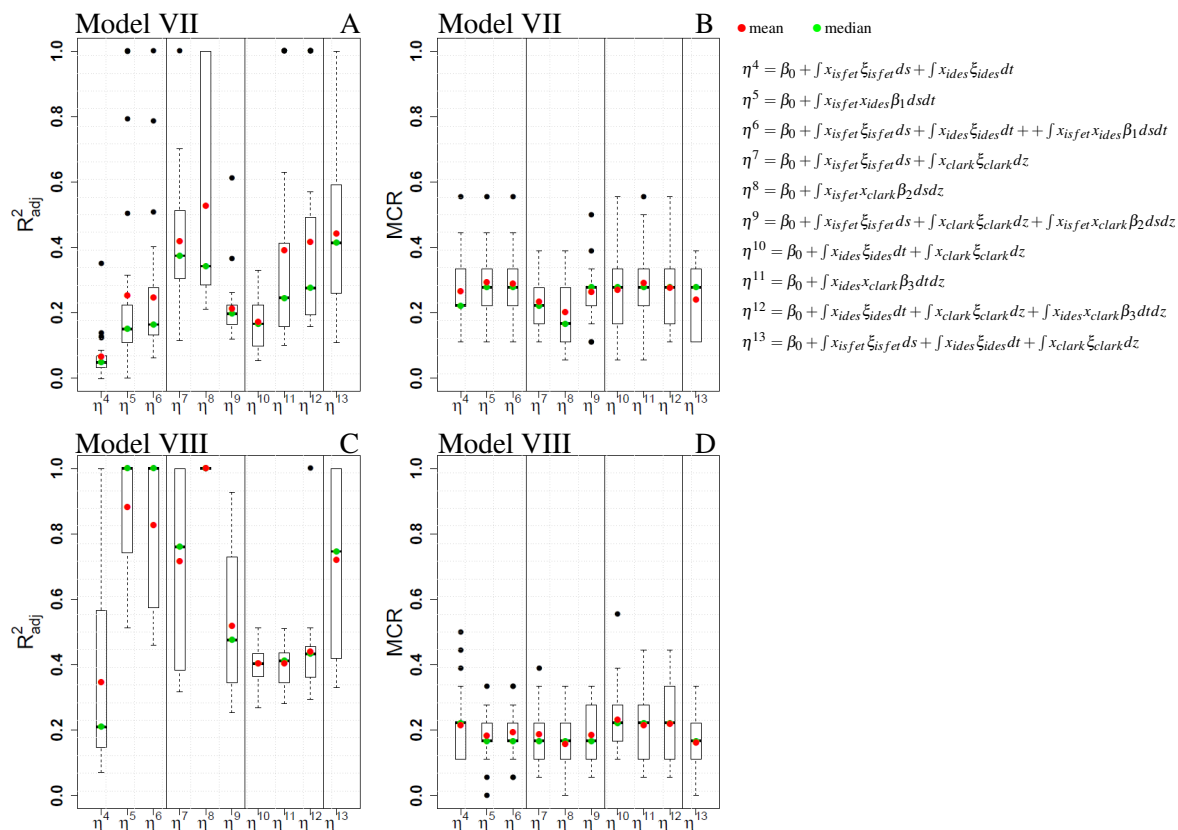


Figure 3.12: Panel A & B: Prediction of 4-MBC in samples mixed with TBBPA, model quality and validation. Panel C & D: Prediction of TBBPA in samples mixed with 4-MBC, model quality and validation. The boxplots show 25 random draws out of the full data set. The left column shows the adjusted  $R^2$  of the model, the right the misclassification rates of the validation data sets. The means and the medians are depicted as red and green dots respectively.

all versions round off the picture of this model.

The consistent further development of a system capable of detecting changes in cell viability by toxic pollutants is the recognition of the agent causing the pollution. The presented statistical model could represent the first step into this direction. The algorithm recognizes the alterations caused by a certain chemical after having been implemented with these signals and determines in this manner which chemical is present in a sample. The more data replications the systems gains the more accurate and precise the prediction is.

One reason for the hard recognition of 4-MBC in single and coexposed samples was probably, as already annotated, its low toxicity. But another reason could be minor or middle deviations from the signals of different measurements used to “teach” the model. We are confident that more measurements would improve the recognition capabilities of the algorithm. Higher  $R^2_{adj}$

and less scattering of the box plots (see figure 3.10 E & F and 3.11 A & B) would be the desired result.

The incorporation of the interaction term  $\iint x_{signal1}x_{signal2}\beta dsdz$  proved advantageous to the aim of this system. Model versions implementing this term showed, in general, a higher performance. Among these,  $\eta^6$  and  $\eta^9$  were the most favourable. In fact, they distinguished itself by an higher  $R_{adj}^2$  than model version  $\eta^{13} = \beta_0 + \int x_{isfet}\xi_{isfet}ds + \int x_{ides}\xi_{ides}dt + \int x_{clark}\xi_{clark}dz$ , which includes data from all three electrodes.



### 3.3 Proliferation promoting chemicals

Clean and safe water is in our society taken for granted. And in fact we are privileged, when we open our tap we can be sure that the outcoming water is drinkable and the majority of in-shore waters within the boundaries of the European Union are, at least, of acceptable quality. Nevertheless the risk of a sudden threat is always present, as happened in November 1, 1986. A storehouse at Schweizerhalle, an industrial area next to Basel, Switzerland burned down. More than thousand tons of chemical were destroyed and introduced into the atmosphere and into the River Rhine. The runoff of fire fighting water contributed also to this, leading to an even more dramatic contamination. River water, soil and ground water were affected (Giger, 2009). This biotop needed more than one decade to recover. This is an extrem example of an environmental crisis that happened overnight. Another, more recently occurred, was the burning and sinking of the oilplatform Deepwater Horizon in the Gulf of Mexico. 200 million gallons (750 million liters) of oil were released to the environment striking the atlantic sea and the adjacent coasts, like the one from Louisiana.<sup>3</sup>

One accident, one disaster, thousand instantly killed animals. A suddenly happened contamination is not the only problem, in fact a big one, but not the only one. There is a long-term matter of concern, as serious as the acute poisoning. We know that “chemicals not naturally belonging to or originating from a particular organism or an ecosystem” are called xenobiotics (Offermanns and Rosenthal, 2008). Industrial residues, pesticides, cosmetic products and many drugs are typical xenobiotics. Some of them have the ability to mimic endogenous ligands, activating hence their molecular pathways and causing, in some cases several damage to the organism since this activation is out of time.

The estrogen receptor (ER) is a common target receptor of xenobiotics. This is a matter of concern because:

1. The risk of breast cancer is increased by at least a twofold if serum levels of estrogen are increased (Yager and Davidson, 2006).
2. The risk of breast cancer is increased in postmenopausal women if high levels of estrogen are present in their breasts (Thomas et al., 1997).

---

<sup>3</sup>Source: National Geographic, <http://news.nationalgeographic.com/news/2014/04/140408-gulf-oil-spill-animals-anniversary-science-deepwater-horizon-science/> (23/06/2014).

In terms of environmental concern this means that a substance acting like estrogen could cause a similar damage as high levels of estrogen. This is, the promotion of growth and proliferation and suppression of apoptosis via activation of target genes directly or in cooperation with co-activator proteins or transactivation of growth receptors to boost receptor tyrosine kinase signaling (Caldon, 2014).

In this section it will be considered if the sensor system is able to detect proliferation due to estrogen signalling. The detection layer was switched from RLC-18 cells to MCF-7 cells, a human breast cancer cell line. The reason for this was the need of the occurrence of the estrogen receptor (ER) to bind estrogen or an estrogen-like chemical.

First the presence of the ER $\alpha$  was ensured. Second, the amount of cells on the chip and the used culture medium was customized for this purpose. These arrangements were made to enable proliferation and its possible visualization. Finally, measurements exposing the detection layer to 17 $\beta$ -estradiol and to estrogen-like chemicals were performed.

#### 3.3.1 Presence of the ER $\alpha$ in MCF-7 cells

The first step towards detecting proliferation is to make sure that the right receptor is expressed by the detection layer, the MCF-7 cells.

Estrogen signals through ER $\alpha$  and ER $\beta$ . Here, only ER $\alpha$  will be taken into account since proliferation promoting pathways and the risk of cancer arises mainly from the pathway activated by this receptor (Musgrove and Sutherland, 2009; Edwards, 2005).

Figure 3.13 shows an antibody staining against the intracellular ER $\alpha$ . The green fluorescence emitted by Alexa Fluor<sup>®</sup> 488 (figure 3.13 A) reveals the expression and presence of the target receptor. The Dapi staining (figure 3.13 B) together with the merging of both photos (figure 3.13 C) shows the intracellular localization of ER $\alpha$ .

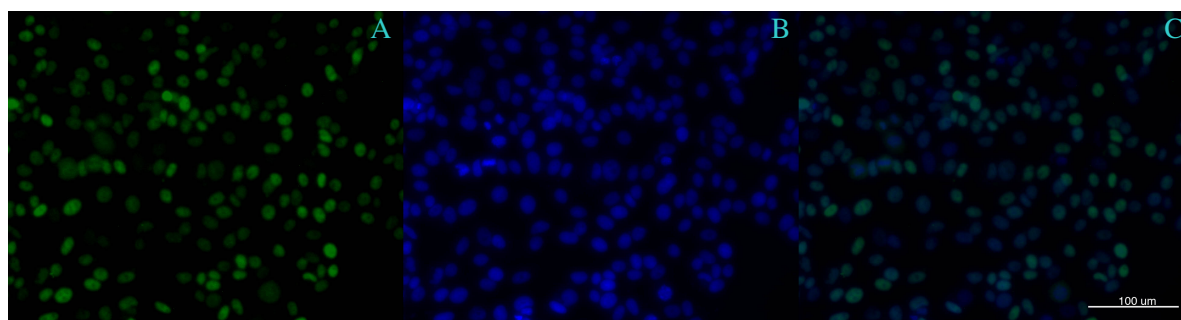


Figure 3.13: Presence of the estrogen receptor ( $\alpha$ -ER) in MCF-7 cells. A) Immunohistochemistry againsts the  $\alpha$ -ER (green), B) DAPI staining (blue), C) Merged picture of A and B.

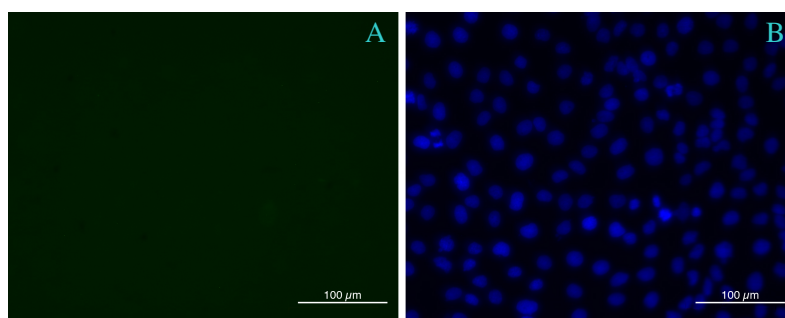


Figure 3.14: Presence of the estrogen receptor ( $\alpha$ -ER) in RLC-18 cells. A) Immunohistochemistry against the  $\alpha$ -ER (green), B) DAPI staining (blue).

The switching from RLC-18 to MCF-7 makes sense as can be seen in figure 3.14. The non-existence of the  $\alpha$ -ER in RLC-18 cells (figure 3.14 A) would have made it impossible to figure out if accelerated growth can be detected by an increased cell impedance of a higher respiration or acidification rate.

#### 3.3.2 Cell seeding for a proliferation analysis

Cells were cultivated in hormone free conditions before seeded on the chips. Moreover, and to ensure that no hormones or estrogen acting compound could impede the proper realization of this experiment cells were only used after having completed the third passage in hormone free and phenolred free medium (since this pH indicator is supposed to have estrogen-like character).

A cell density of about 70-80% was seeded on the biochips. A 100% confluency on the chip was not desired. Figure 3.15 shows how cells were seeded on the chip for a conventional measurement to determine the acute toxicity of a compound (figure 3.15 A) and for a prolif-

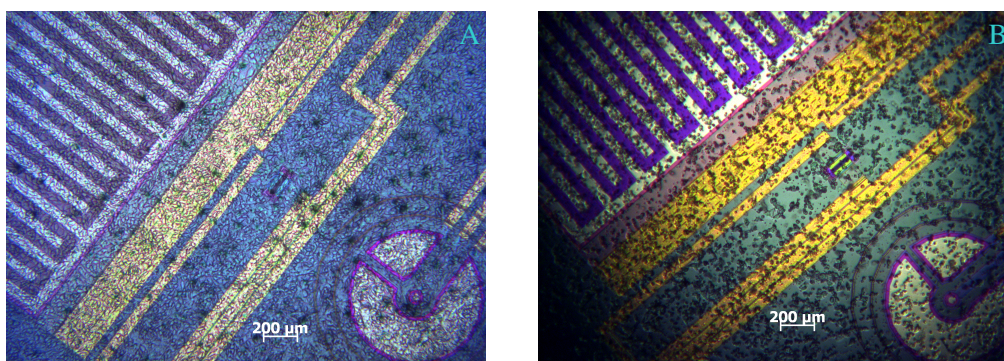


Figure 3.15: Comparison of the cell confluency between a chip ready to test the impact of a chemical and a proliferation analysis. A) A 100% confluency if cells are seeded to analyze the effect of a toxic compound, B) 70-80% confluency for cells seeded for a proliferation analysis.

eration analysis (figure 3.15 B). There should be enough space on the chip to allow growth on it. Very important was the free space on the IDES electrode. This electrode measures the cell impedance, the strongness of the attachment of the cells on the chip's surface. If the entire electrode is not covered from the beginning on but show a fast proliferating behaviour, the standardized cell impedance is expected to increase. Also the physiological parameters acidification and respiration rate could start to raise.

#### 3.3.3 Proliferation analysis of MCF-7 cells after exposure to estrogen ( $17\beta$ -estradiol)

In order to figure out if the sensor is able to detect an effect on the proliferation, MCF-7 cells were exposed to  $17\beta$ -estradiol.

The next two graphs will show one measurement where MCF-7 cells were exposed to estrogen, more precisely  $17\beta$ -estradiol, for 3 days and a second one where the cells were exposed for a longer time period, 6 days. Figure 3.16 shows the first measurement. The detection layer was exposed to  $17\beta$ -estradiol for 3 days. The cell impedance is presumably the most relevant electrode to sense growth. This electrode is not covered completely by cells. Should a substance stimulate their proliferation the cells would cover little by little its surface featuring, in the best case, a sigmoidal growth curve. Figure 3.16 A shows the standard cell impedance. In fact, after about 17 hours of exposure (24 hours measurement due to the preceded 7 hours adaptation time) 10 nM  $17\beta$ -estradiol seem to boost proliferation. A fast steep increase in the cell impedance can be observed. After 53 hours of exposure (60 hours measurement) the curve flattens giving rise to a sigmoidal growth curve. More over this graph shows also a concentration dependent toxicity of  $17\beta$ -estradiol for higher concentrations. 100 nM result in a decrease of the cell impedance after 30 hours measurement. The highest two concentrations (1.000 nM and 10.000 nM) lead to a decrease as soon as  $17\beta$ -estradiol gets in contact with the cell layer. This is consonant with the panels reflecting the acidification and respiration rate (figure 3.16 B and C respectively). Cells stop their metabolic activity. 100 nM is the concentration between proliferation stimulation and toxic behaviour. The cell viability is perturbed since the cell attachment is weakened. Nevertheless the acidification rate follows the level of the control (figure 3.16 B) and the respiration rate (figure 3.16 C) increases after 54 hours of measurement.

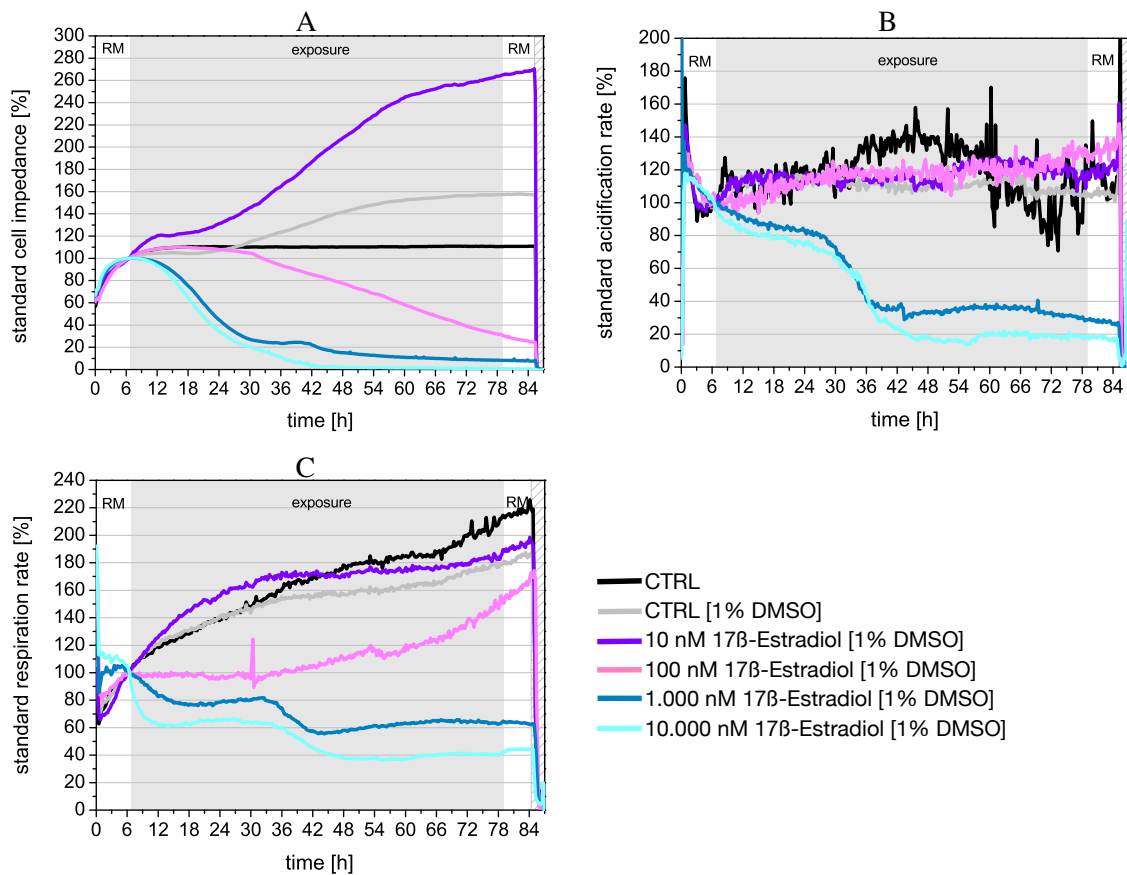


Figure 3.16: Detection of a proliferation promoting substance using MCF-7 as the sensitive layer.  $17\beta$ -estradiol was exposed for 72 hours (3 days, shaded area). The exposure time was preceded by and adaptation phase of 7 hours and a recovering of 5 hours (white area). A) Standardized cell impedance, B) Standardized acidification rate, C) Standardized respiration rate.

This measurement has shown that a faster proliferation becomes visible after about 17 hours of  $17\beta$ -estradiol application. If the exposure time is prolonged from 3 days to 6 days a similar time schedule should also be observed. Moreover this could also elucidate if the signals remain constant after 3 days or if changes in cell viability happen, not only for 10 nM  $17\beta$ -estradiol but also for all other, specially 100 nM. This concentration seemed not to provoke the death of the cells after 3 days but it could be possible that a longer time period leads to irreversible cell damage.

Figure 3.17 shows this measurement over 156 hours. The first 7 hours comprise the usual adaptation time were cells acclimate to the system and the last 5 were reserved for a recovering time for the case that a damage caused is reversible. 10 nM  $17\beta$ -estradiol stimulates growth, again after 17 hours exposure (24 hours measurement). The standardized cell impedance raises as depicted in figure 3.17. A growth that remains constant over several days and only slows

down after about 125 hours exposure (132 hours measurement). The maximal standardized cell impedance achieved here is 200% (see figure 3.17 A) whereas the maximum in figure 3.16 was 280%. This is due to the more complicated seeding of the cells. A confluency of 70-80% cannot be perfectly be achieved. And the variations from one seeding to another will be reflected in the cell impedance. The values of the y-axis should be interpreted as relative changes caused by a compound after exposure to the detection layer.

The acidification and respiration rates after exposure to 10 nM  $17\beta$ -estradiol (figure 3.16 B and C) follow the same trend as the control. This means that even if cell growth is accelerated, the cell concentration is not as high as cellular waste products could harm the cells.

The fate of the cells after exposure to the highest concentrations, 1.000 nM and 10.000 nM, is still the same as in figure 3.16. The cells perish by the toxicity of  $17\beta$ -estradiol if present in these high concentration. 100 nM provokes the loose of attachment of the cells to the surface

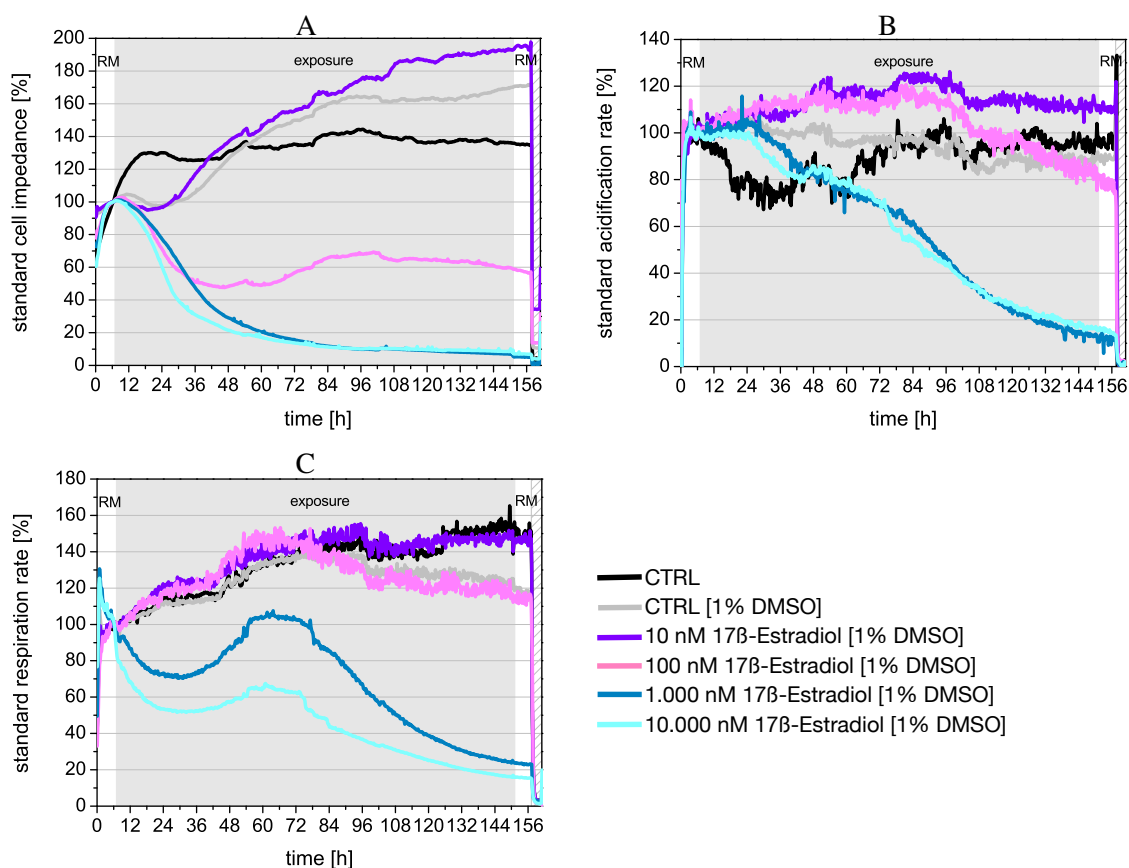


Figure 3.17: Detection of a proliferation promoting substance using MCF-7 as the sensitive layer.  $17\beta$ -Estradiol was exposed for 144 hours (6 days, shaded area). The exposure time was preceded by an adaptation phase of 7 hours and a recovering of 5 hours (white area). A) Standardized cell impedance, B) Standardized acidification rate, C) Standardized respiration rate.

after application (figure 3.16 A). Nevertheless the acidification and respiration rates (figure 3.16 B and C) remain constant for several days but finally tend to fall. So, this concentrations is presumably harmful if applied for too long time.

The observations obtained from the last experiments allow to state that this biosensor permits the detection and visualization of cell proliferation. The IDES electrode makes this possible, the electrode that measures the strength of cell attachment to the surface. While cells proliferate faster due to a chemical, in this case  $17\beta$ -Estradiol, the empty spaces on the chip's surface diminish leading to a rise in the standardized cell impedance. Once this could be clarified the next step is to test if the effect of a estrogen-like acting chemical can also be detected. The next section will show the results obtained after exposing MCF-7 cells to TBBPA.

#### 3.3.4 Proliferation analysis of MCF-7 cells after exposure to TBBPA

As described in section 1.4.3 TBBPA is suspected of promoting proliferation via binding to the  $\alpha$ -estrogen receptor. To figure out if this chemical has endocrine disrupting properties MCF-7 cells were cultivated under hormon free conditions and then exposed to TBBPA. In the case of a proliferating effect of TBBPA the standardized cell impedance should follow a trend similar to the one observed after the exposure of 10 nM  $17\beta$ -estradiol (figure 3.16). The potential proliferative effect of TBBPA was analyzed by exposing the cells to TBBPA for 66 hours while recording the physiological parameters with the cell-based sensor system. These results were compared with an end-point assay, the calcein test. Cell viability is ascertained by the hydrolyzation of the fluorescence dye calcein in healthy cells.

Figure 3.18 shows the reaction of the cell attachment, metabolism and respiration of MCF-7 when TBBPA is added to the medium. 10  $\mu$ M TBBPA does not evoke any notable alteration on the physiology on the cells. Compared to the control, the respiration rate (3.18 C) is decreased. The synthesis of ATP is being compensated by an increased glycolysis as can be seen by the increased acidification rate (3.18 B). A concentration dependent decrease in all parameters can be observed for higher concentrations, which lead to the death of the cellular detection layer. This results deny the assumption of TBBPA as an endocrine disrupting chemical. Or more precisely, in the case of endocrine disrupting properties the toxicity of this substance predominates.

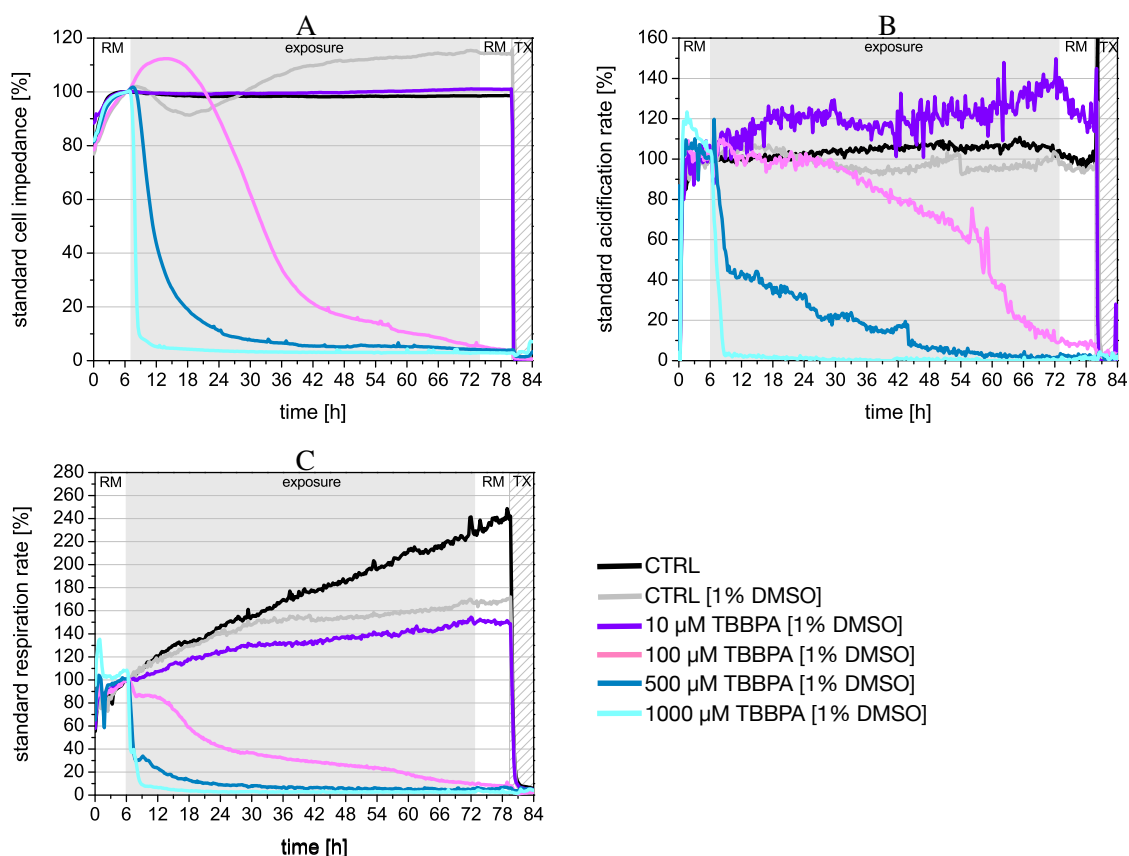


Figure 3.18: Detection of a proliferation promoting substance using MCF-7 as the sensitive layer. TBBPA was exposed for 66 hours (shaded area). The exposure time was preceded by and adaptation phase of 7 hours and a recovering of 5 hours (white area). A) Standardized cell impedance, B) Standardized acidification rate, C) Standardized respiration rate.

An estrogen sensitive detection layer like MCF-7 will suffer the harm of this chemical in the same way as a cell line without the  $\alpha$ -ER, like RLC-18 (see figure 3.2 for the effect of TBBPA on RLC-18 cells).

To compare the results shown above MCF-7 cells were cultured on a 96 well plate in a hormone-free manner and exposed for 60h to TBBPA. The concentrations used were the same as in the experiment performed with the biosensor: 10  $\mu$ M, 100  $\mu$ M, 500  $\mu$ M, and 1.000  $\mu$ M. Figure 3.19 A shows the measurement of the fluorescence intensity after performing the calcein assay. The bar diagramm is consistent with the results obtained with the biosensor in figure 3.18. 500  $\mu$ M and 1,000  $\mu$ M of TBBPA lead to cell death whereas 10  $\mu$ M does not affect cell viability. The consistency with 100  $\mu$ M is not so clear. The same problems as with the MTT assay appear here. The lack of a time resolution in an end-point assay makes it impossible to know when the compound unfolds its effect. Moreover it is possible that after some time the whole amount of compound is metabolized by the cells so that the solution is no longer toxic.



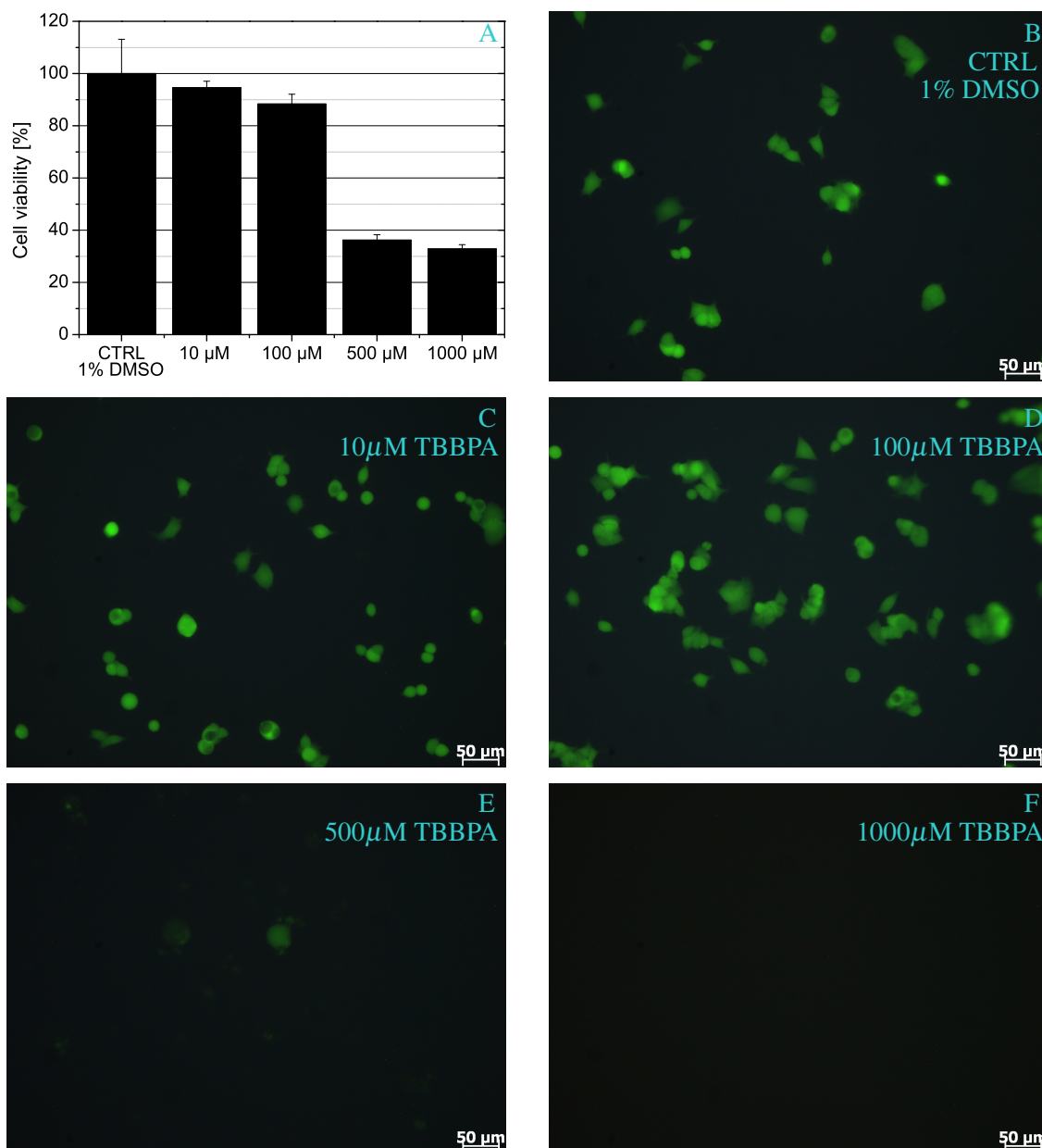


Figure 3.19: Cell viability of MCF-7 cells determined by calcein assay after exposure to TBBPA in different concentrations for 66h. Panel A: measurement of the fluorescence intensity. The results are reported as mean  $\pm$  SD of three independent experiments. Panel B-F: morphology of the cells after compound exposure.

In the calcein test 100  $\mu$ M TBBPA do nearly not harm the cells. There is a tendency towards a decrease in cell viability, as shown in figure 3.19 A. Nevertheless it is already known from figure 3.18 that cells die after exposure to 100  $\mu$ M TBBPA.

In this section the detection layer was exposed to different pollutants, alone and in combination. A software was developed to ascertain the composition of the contaminated by the aid of the data acquired from the measurements. And finally the application of this biosensor was

expanded from the detection of a pollutant to the detection of endocrine disrupting chemicals.

There are now some issues to overcome in order to bring this system closer to an application: the measurement of fresh water and how the transportation of a cell loaded chip can be done.

The next section will attend these two issues.

## 3.4 Overcoming challenges

The idea of this undertaking is that cell based sensor technology allows in a near future water quality assessment on site and in real time: one chip, one waterflow, a continuous signal. At the moment, however, this idea remains visionary and admittedly, presumptuous and pretentious. Nevertheless such a technique features so many advantages that merely the attempt is worthwhile. As described in section 1.6 the idea faces technical, biological and logistical challenges:

1. Cell-loaded chips have to be transported from the manufacturer to the customer.
2. A customer has to be able to store the cell-loaded chips for a certain time period without owning a laboratory equipment.
3. Pure water “kills” cells.

The next section will deal with the first two points, presenting an efficient and secure way to transport and store a cell-loaded chip and section 3.4.2 will show how it is possible to analyze a water probe without harming the cellular detection layer.

### 3.4.1 Preservation and transport of cell-loaded chips

A monolayer growing on the surface of the chip needs to survive the postal delivery at roomtemperature. After having arrived to its place of destination it is not guaranteed that the chip will be placed immediately into the system. Therefore, it should be possible that the chip can be stored at 4°C until the customer intends to use it. This means that the cells must be encapsulated in a medium or substance which shields impacts, provides them with enough nutrients and protects them from temperature fluctuations or dehydration.

In order to define a suitable medium porcine gelatine was solved in DMEM in different concentrations and checked for the viscous properties at different temperatures. 4°C represents the storage and preservation temperature, 25°C is room temperature representing thus transport temperature. Finally, 37°C: temperature at which the measurement systems works, gelatin is supposed to be in a liquid state under this condition since the fluidic system has to be able to suck the preservation substance out of the chip and replace it by running medium or a water sample. Table 3.3 shows the state of the gelatin depending on the temperature and the concentration. A too low concentrated preservation mixture leads to a nearly no existend solidification,

concentration	State		
	at 4°C	25°C	37°C
0.2%	liquid	liquid	liquid
0.5%	liquid	liquid	liquid
1%	solid	viscous	liquid
1.5%	solid	solid	liquid
2%	solid	solid	viscous

Table 3.3: State of gelatin/DMEM mixture dependent on the temperature

not even at 4°C. The gelatin remains in a liquid state in the temperature range between 4°C and 25°C. This was observed with the two lowest concentrations, 0.2% and 0.5%. Higher gelatin concentrations though, gained our attention. Specially 1% and 1.5% were of interest. With 1% it is possible to notice the temperature and concentration dependent physical phase of the gelatin. The lowest temperature (4°C) causes the solidification of the gelatin/DMEM solution upon the cell layer. The highest, 37°C, provokes the melting of the gelatin. At 25°C the solution remains in a viscous state. This represents a right step towards the goal but yet not the end of the road. 1.5% remains solid at 25°C, making this concentration particularly attractive since the lower and the upper edge of the set temperature limits keep the gelatin in the desired state, solid and liquid respectively. The highest concentration, 2% has also to be kept in mind as a solid state is also ensured at 4°C and 25°C. Nevertheless at 37°C, system temperature, it is not as liquid as a 1.5% concentration. The viscosity has to be kept in sight during the first minutes of a measurement since it is not guaranteed that the fluidic system is strong enough to pump it out from the chip and replace the gelatin with running medium.

After this preparing experiment the first measurement was run after having stored the cell chip for 1 day at 4°C in the mentioned gelatin concentrations. Figure 3.20 shows the physiological parameters of the cells after being stored for 1 day at 4°C. Different concentrations of gelatin were used to preserve and store the cells after having been seeded onto the chip. A measurement time of 24 hours was scheduled in order to analyze the physiological parameters of the biological detection layer and to figure out if the cells were able to withstand the exposure to a gelatin/DMEM preservation solution and the low temperature. Constant physiological parameters can be observed for all concentrations of gelatin during the whole measurement. The cell impedance (figure 3.20 A) is from beginning on at 100% which means a perfect attachment

to the chip surface and a healthy morphological status of the cells. The acidification and respiration rates (figure 3.20 B and C respectively) remain constant at or close to 100% suggesting a well functioning cellular metabolism. All in all the measurement reveal that cells survive the 24 hours at 4°C and that gelatin has no toxic effect on the cells. The 2% concentrated gelatin solution was sucked at 37°C by the pump without plugging the tubes of the fluidic system. Nevertheless, after removing the chips from the refrigerator, the chips loaded with 2% gelatin had to be incubated for 5-10 minutes at 37°C in order to ensure the melted status of the preservation solution. A 1.5% solution was in this sense more worthwhile since the melting procedure took place almost immediately.

The positive result and the affirmatory viability of the cellular detection layer after 1 preservation day led to the enlargement of the amount of storage days at 4°C. Figure 3.21 shows the physiological parameters, cell impedance, acidification and respiration rates after a storage time of 3 days. There is one striking observation straight away. The cells need more time to

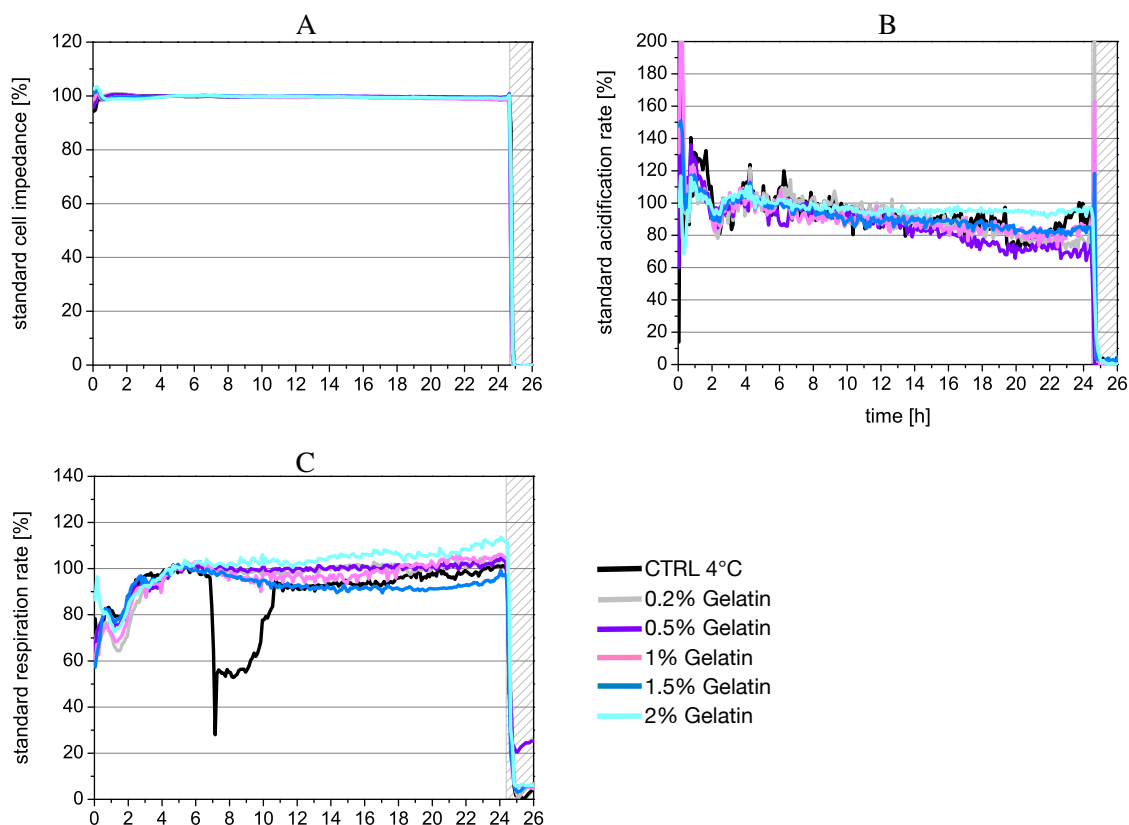


Figure 3.20: Representative measurement of the physiological viability of RLC-18 cells after **1 day** storage at 4°C encased by gelatin in different concentrations. A) Standardized cell impedance, B) Standardized acidification rate, C) Standardized respiration rate.

settle down and recover its full physiological function. Usually, cells need about 3 to 4 hours to adapt to the system. This means to deal with an atmosphere low in  $CO_2$  and a different medium as the cell culture medium (DMEM). After 4 days of preservation the cells need between 8 and 9 hours to reach 100% viability. The reason for this is that low temperatures slow down the metabolic activity of the cells (Pegg, 1976). So, the enlarged time to reach 100% is, in first line due to the longer recovering time needed to reactivate and retrieve the metabolic activity due to the low storage temperatures. After this adaptation time, signals remain constant over time.

The cells of all chips with different gelatin concentrations not only survived a 3 day long storage at  $4^\circ C$  but also recover its full metabolic function suggesting that they would be ready to detect pollutants in a contaminated water sample.

None of the used gelatin concentrations impaired or harmed the cells. Moreover, in both storage experiments, 1 day and 3 days storage (figure 3.20 and figure 3.21 respectively) a control was run in parallel with the gelatin preserved chips. The control was defined here as a chip

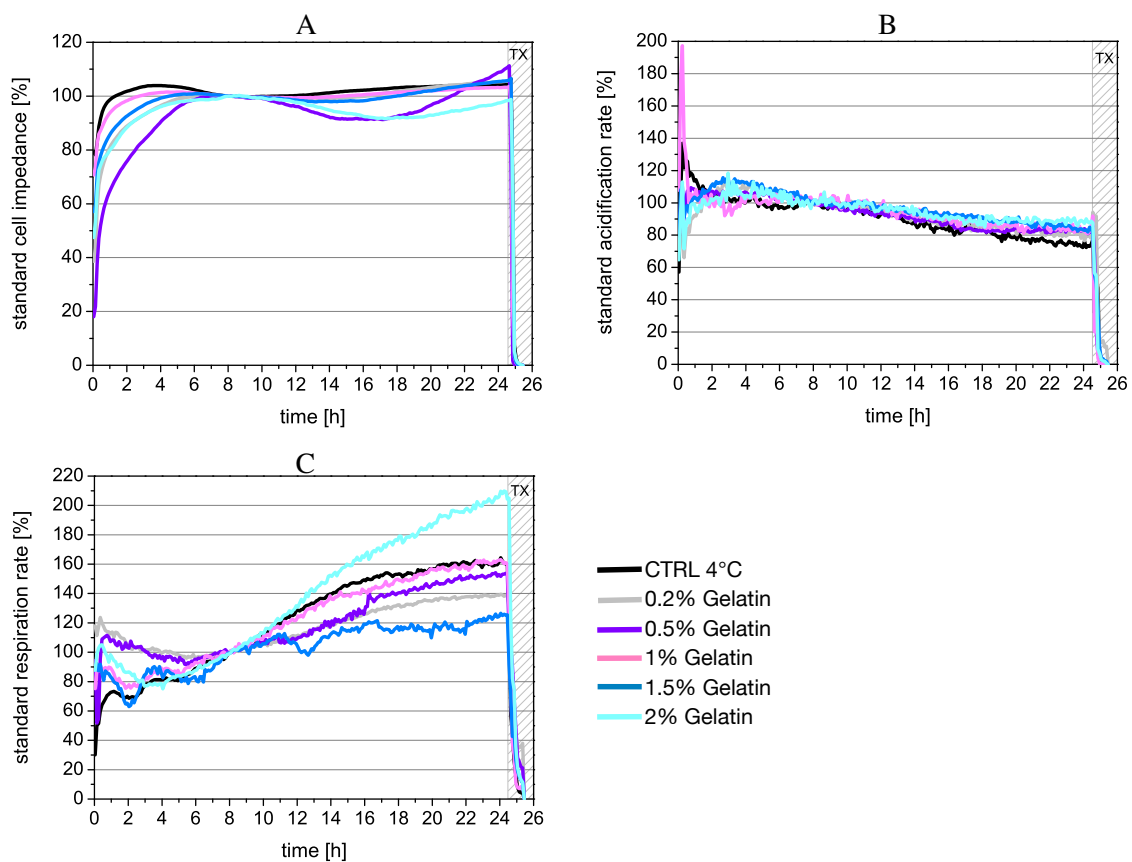


Figure 3.21: Representative measurement of the physiological viability of RLC-18 cells after **3 days** storage at  $4^\circ C$  encased by gelatin in different concentrations. A) Standardized cell impedance, B) Standardized acidification rate, C) Standardized respiration rate.

containing cells kept in DMEM, i.e. a chip loaded in the standard way as described in section 2.2.4. The only difference relied therein that this control chip was kept together with the test chips at 4°C. Interestingly, the cells on these control chips behaved in a similar manner as those kept in gelatin; featuring physiological paths close to all other cellular monolayers containing the gelatin based preservation substance. This suggests that the gelatin will mainly be advantageous for delaying the dry out of the cells since a refrigerator represents a low humidity environment is and to protect the detection layer against impacts.

Since all gelatin concentrations achieved positiv results the decision of which gelatin to choose for a delivery per mail was taken based upon the characteristics described in table 3.3. A 1.5% concentrated gelatin/DMEM solution seems to be the means of choice to prevent dehydration and impact protection. It solidifies fast at the desired temperature  $\geq 25^{\circ}\text{C}$  and liquidifies at system temperature, 37°C. For these reasons the next experiment was performed using only this gelatin concentrations.

The last two experiments showed that a two dimensional celllayer can be stored at 4°C in a conventional refrigerator at 4-10°C by slowing down their metabolic activity but maintaining them intact and enabling their complete recovery after a few hours at physiological temperature, 37°C. The next step was to increase the storage time up to 1 week.

The curves in figure 3.22 show the physiological status of the cell layer after having stored the cell-loaded chips at 4°C for 7 days. After this storage, the chips were sent from Munich to Heidelberg per mail. The delivery took around 24 hours in which grip of temperature control and a careful handling were lost. Once in Heidelberg the chips were stored again at 4°C for 3 days and afterwards the physiological parameters were measured.

Two chips were used to test this scenario. Figure 3.22 shows the results of this experiment. A dramatic increase of the cell impedance (figure 3.22 A) is the first observation that one can make. Either the long storage or the hits and impacts may detach the cells from the surface. After 24 hours the cell impedance reached a plateau and remained constant. The respiration rate (figure 3.22 C) kept constant from beginning on as well as the acidification rate (figure 3.22 B). Constant but with a slight downward drift. This can be due to the performed standardiza-

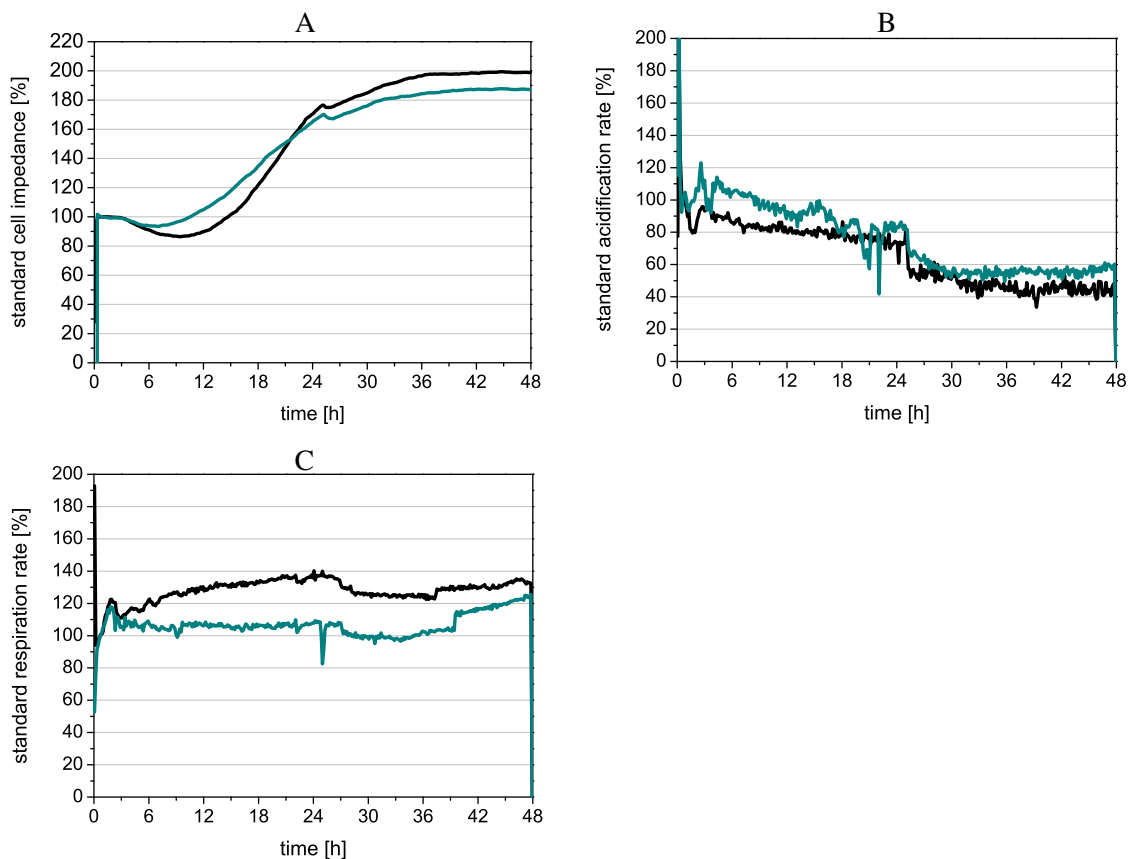


Figure 3.22: Physiological viability of RLC-18 cells after having been stored for **7 days** at 4°C, shipped from Munich to Heidelberg and stored for **3 days** again at 4°C. A) Standardized cell impedance, B) Standardized acidification rate, C) Standardized respiration rate.

tion. One point is set to 100% and all remaining measurement points are calculated relative to this one. This can cause a shift or a drift in the curve. Independently of the initial downward drift, also the acidification rate stays constant after 24 hours of measurement. In general it even does not matter if a rate goes up or down since the slope remains constant. In the case of a contamination the regarding physiological parameter would break down or increase suddenly.

In this section it was shown that a two dimensional cellular layer can be stored at low temperatures and transported over long distances. One question remains open, how can cells assess water quality if pure water is lethal for cells. This question will be the main subject in the next section.



#### 3.4.2 Water kills cells, *no longer*

Environmental monitoring faces the challenge of measuring an increasing number of analytes at ever-decreasing concentrations. Moreover new industrial processes, new materials to cope with the actual demand lead to an increasing number of chemical endproducts and intermediates. This means that the amount of potential pollutants in our environment is increasing constantly. Here relies the biggest advantage of whole-cell biosensors which outshines the drawbacks and transforms them into challenges still to overcome.

Analytical chemistry allows the detection of substances down to picograms. But only those components will be detected for which the person in charge is looking for. New chemicals or derivatives may go unnoticed. But the cells in a biosensor will notice the presence of any toxic compound in the water or whatever kind of aquatic medium. Nevertheless there is yet one fundamental open problem: pure water kills cells. Therefore this is one of the main challenges by developing a cell-based sensor for the detection of toxic chemicals in water samples.

The task is to find a way that permits cells to stay alive while a real water sample is being perfused through the system. Several attempts were performed and in this chapter the one that finally worked will be presented. The Appendix B offers one which looked promising since Bohrn et al. (2010, 2011) used a similar way for the detection of gases with cell-based biosensor.

One of the main problems is the different osmolarity between the cytoplasm of the cells and the water. Water represents a hypotonic solution compared to the inner cellular solution. This means that water will flow into the cell, increasing its volume and evoking the rupture of its membrane. Furthermore, cells need the presence of nutrients to survive.

All this led to the addition of DMEM in powder form to the water sample. This supply should reduce the difference in osmolarity and at the same time provide the cells with sufficient nutrients. The first experiment deals with the question if this way to adapt water to the cellular conditions is worthwhile. For this purpose water which is for sure clean and uncontaminated, deionized water from the laboratory and tap water, was used. The concept was then expanded to rain water and afterwards to water from the river Isar. The next issue to be shown in this section is the difference, if there is one, between the physiological reaction of the cells to a test compound, in this case  $\text{Ni}^{2+}$ , solved in tap water and in running medium (the preparation

protocol of running medium is described in section 2.2.5). The last graphic, which will close this section will be a long-term measurement. The sensor is supposed to run for at least one week without interruption.

Figure 3.23 shows the first measurement. Deionized water and tap water were treated with DMEM in powder form and exposed to the cells growing on a chip. The control was, as always, running medium. During the measurement two chips were exposed to deionized water and two to tap water. The cell impedance (figure 3.23 A) remains constant and at 100% for all chips and water types.

Concerning the acidification and respiration rate (B & C in figure 3.23) there is one striking fact which stands out. The slope of the curves during the application of tap water is higher than for deionized water. The acidification and respiration rates increase constantly. Probably a result to the different composition of the water which contains more ions and presumably more

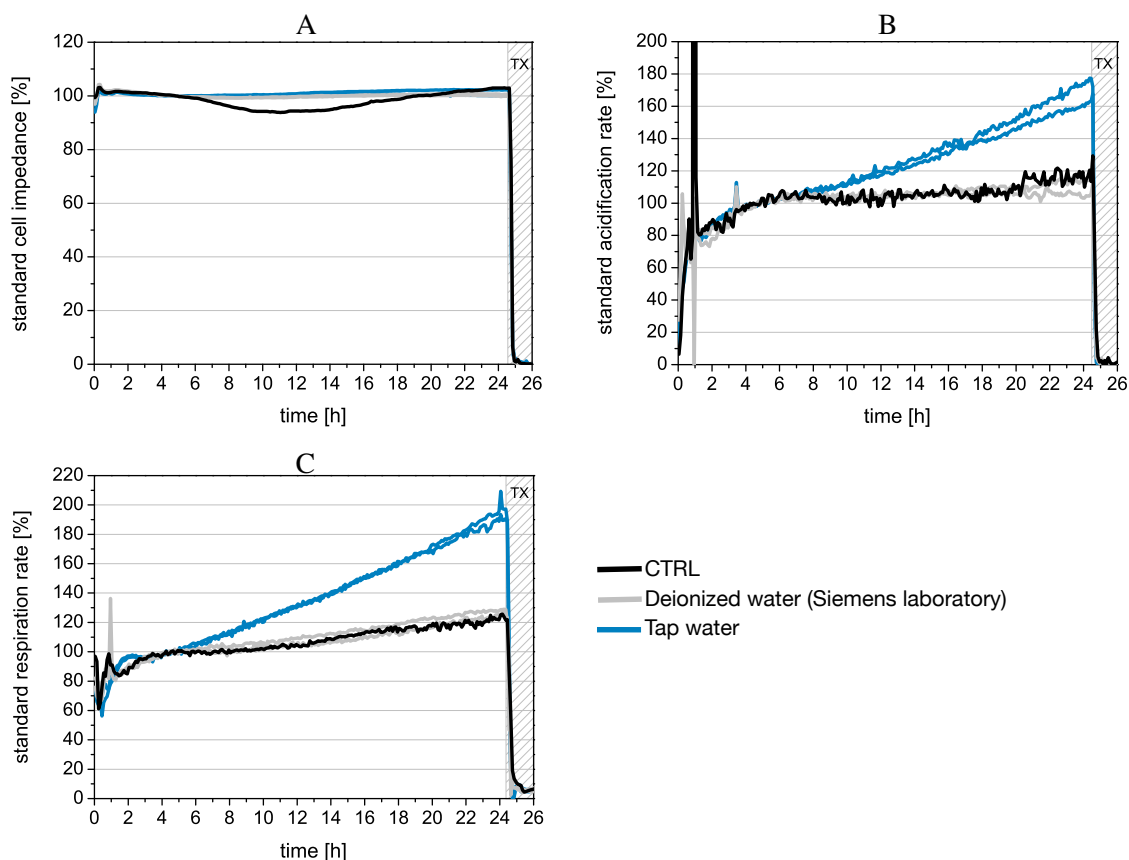


Figure 3.23: RLC-18 cells as biological detection layer for water quality control: survival analysis. Exposure of deionized water and tap water treated with DMEM (powder) to RLC-18 loaded chips. Two chips were exposed to each water sample. Water samples were applied from the beginning on to the cells. A) Standardized cell impedance, B) Standardized acidification rate, C) Standardized respiration rate.

oxygen than the treated deionized water or the commercially obtained high purified water (basis of running medium). It is an observation but basically not a matter of concern. The celllayer survives. Furthermore the metabolic rates are active and during the whole measurement over 100%. The slope is constant, *the curve is a line*. This means that the system would notice if a sudden pollutant would contaminate the water probe. A slope does not represent a problem, only varying curve shapes. This would impede a proper interpretation of the viability status of the cellular detection layer.

There is a quite simple and direct way to determine how tap water or water from another source, so far clean, affects and alters cellular metabolism but not kills the cells. The chips are exposed to tap and rain water after allowing an adaptation time with cell culture medium (running medium). The water samples are thus treated as a compound like in the experiments and figures shown in section 3.1.1 and 3.1.3, where RLC-18 were exposed to organic compounds. During the first 5 hours of the measurement cell culture medium is pumped through the system. This is the medium in which the cells are used to grow, hence this medium will not alter the metabolic properties of the cells. The medium is then replaced by tap and rain water. A different composition of these two water samples, for example in the concentrations of ions will presumably be reflected in at least one of the metabolic parameters of the cells.

The results of the attempt described here are shown in figure 3.24. For 10 hours the cellular layer of two chips was exposed to tap and rain water. A variation in the strongness of the attachment of the cells to the surface, reflected by the cell impedance (figure 3.24 A) is scarcely discernible. There is only a very slight increase after the application of rain water. But only the information provided by the cell impedance is too scarce to come to a conclusion. The panel B and C show the acidification and the respiration rate. There is more information allocated in here. First, as soon as the water probes passes through the fluidic system and comes in contact with the cell layer the cells react with a huge deflection in these two parameters. A deflection that was not observed in any experiments before. Only a physiological caused signal variation was observed after the application of chlorpyrifos, TBBPA, 4-MBC or 2-AA (figures 3.1, 3.2, 3.3 and 3.4) but not a shock like the ones observed here.

So, the cells notice a different composition of the water. The acidification and respiration

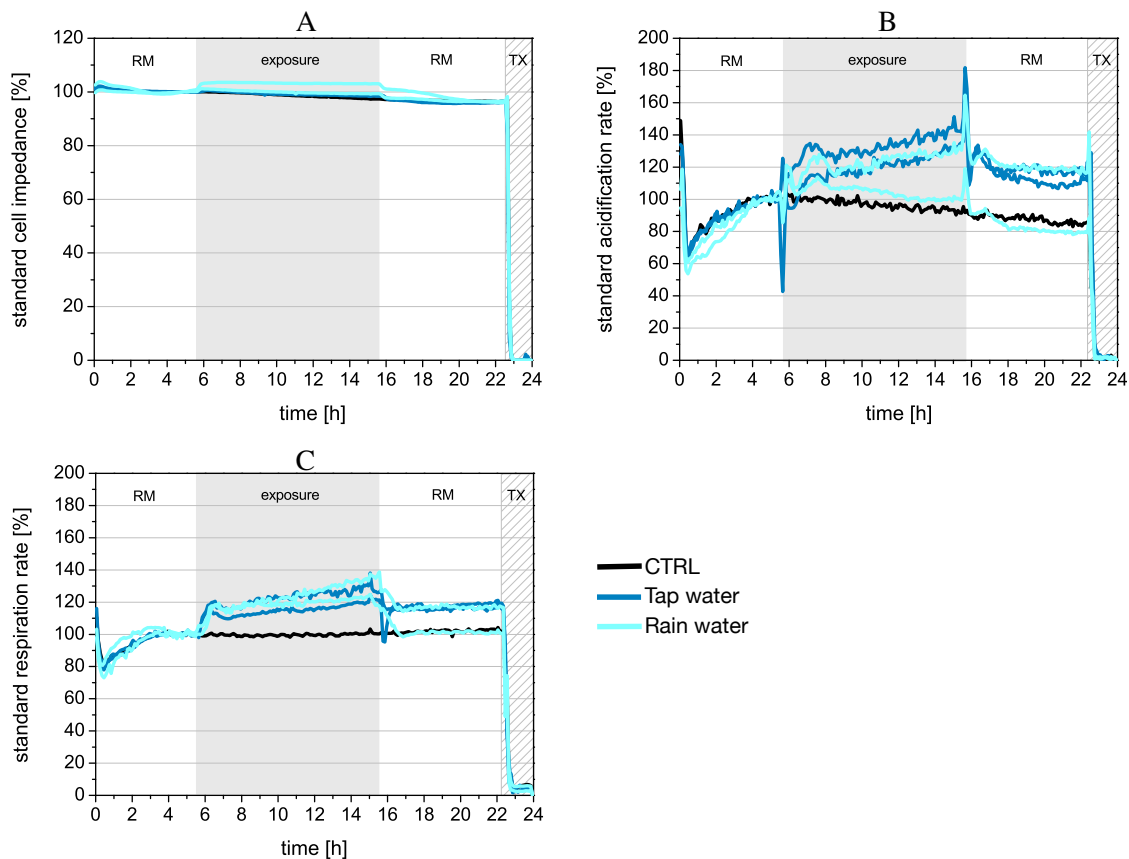


Figure 3.24: Impact of tap water and rain water on RLC-18 cells after 10h exposure time (shaded area) measured in Bionas Analyzing System followed by a recovering phase of 7h (white area). Cells were allowed to adapt to the system prior to exposure for 5h (white area). Two chips were exposed to each water sample. A) Standardized cell impedance, B) Standardized acidification rate, C) Standardized respiration rate.

rates go suddenly up and down but this effect endures only for a few minutes. It is just the consequence of the first contact. The two chips exposed to tap water show a constant increase in the acidification and respiration rates which lasts for the whole time of the exposure, an increase similar to the one observed in figure 3.23. After the application has ceased the metabolic parameters drop down to values close those measured during the adaptation phase or leastwise stop to increase and run parallel to the x-axis.

Rain water causes a similar effect as tap water. Merely one of the chips show, after an offset, a decrease in the acidification rate. It is conceivable that this is a chip dependent effect since the respiration rates follow in both cases the same increasing course. More over, as pointed out at the beginning of this characterization, there is in both chips a slight increase in the cell impedance. This could also be a consequence of the ions present in the water, in this case in the rain water sample. Cell adhesion proteins like integrins are  $\text{Ca}^{2+}$  dependent, a cation constantly

present in water. The decrease back to a 100% cell impedance after the rain water is replaced by cell culture medium is one argument more reinforcing this possibility.

The next step was to take a probe from the river Isar in Munich. The Isar river displays a waterquality of class II (marginally contaminated), being I the best class and V the worst, an ecological disaster<sup>4</sup>. This water is thus clean, even if not perfect. For sure, it does not feature drinking water quality. But the boundary to drinking water quality is not toxic water. There are several miles of different water qualities nuances in between. We do not expect this water to be harmful since it is allowed to swim in this river.

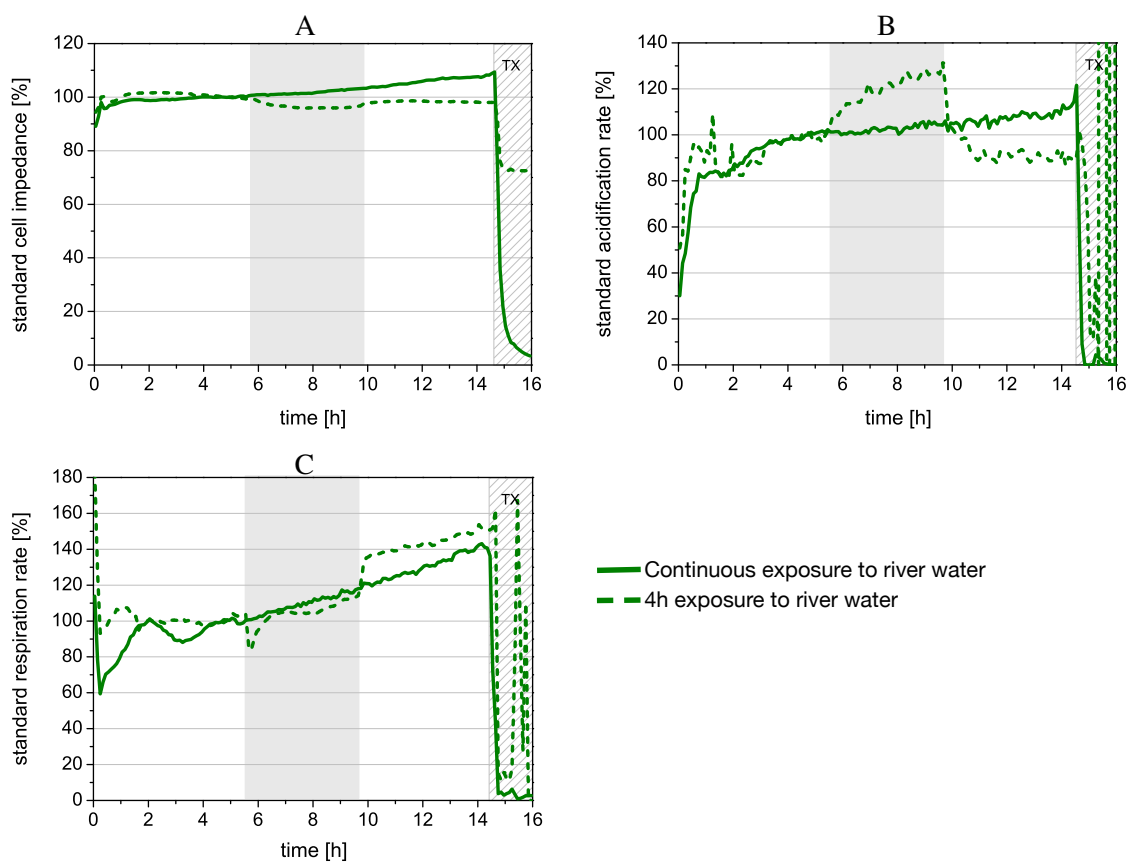


Figure 3.25: Impact of water from the river Isar (Munich) on RLC-18 cells. Continuous line represents a measurement where the river water was from the beginning on present in the fluidic of the system. Dashed line represents a measurement where the water probe was added for 4 hours preceded by an adaptation phase of 5 hours and followed by a recovering phase of 5 hours. A) Standardized cell impedance, B) Standardized acidification rate, C) Standardized respiration rate.

But it is questionable if the cells survive this water since they lack the clearance mechanism

<sup>4</sup>Source: Federal Ministry for Environment, Nature Conservation, Building and Nuclear Safety, <http://www.bmub.bund.de/themen/wasser-abfall-boden/binnengewasser/fluesse-und-seen/zustand-der-oberflaechengewasser/> (Jun. 6, 2014)

of an organism. As previously indicated, a constant signal, is desired for the purpose of water monitoring. Figure 3.25 combines the two concepts presented in the two above shown diagrams in one graph. The detection layer was exposed on the one hand from the beginning on with river water (continuous line) and on the other hand for 4 hours after allowing an adaptation time of 5 hours (dashed line).

No or little change can be recognized in the cell impedance after the application of river water as a compound (dashed line in figure 3.25 A). There is a slight decrease of about 2 to 3% during the 4 hours exposure time. The cells notice the difference in the composition of the medium but there is no morphological damage ascertainable. This is underpinned by exposing the cells during the whole measurement to the river water (continuous line in figure 3.25 A). The cell impedance remains constant through the whole measurement, as well as the acidification rate (continuous line in figure 3.25 B). Cells adapt to the given conditions of a different water composition than the one of culture medium. A constant glycolysis is a sign for a healthy status of the cells. Nevertheless the cells notice the presence of a different water composition if it is given after an adaptation phase with culture medium (dashed line in figure 3.25 B). The acidification rate increases up to 30% of the normal value. Also the respiration rate increases (panel C), slightly during the exposure time but does not recover. If applied from the beginning on, there is a constant increase (continuous line in figure 3.25 C).

Now, it would be interesting to know how the detection layer, the RLC-18 cells, reacts to a harmful chemical if it is present in tap water. This would represent or simulate a sudden contamination. In figure 3.26 the impact on the physiological parameters of  $\text{Ni}^{2+}$  solved in tap water (left column) and medium (right column) was compared. The used concentrations range for the cell culture medium from  $0.02 \mu\text{g/mL}$  to  $200 \mu\text{g/mL}$  in strides of a decimal power. From these measurements those concentrations which caused the biggest damage were depicted and used for another measurement, this time with tap water. There is a lot of information contained in this figure. RLC-18 cells act less sensitive if the  $\text{Ni}^{2+}$ -ions are present in tap water.

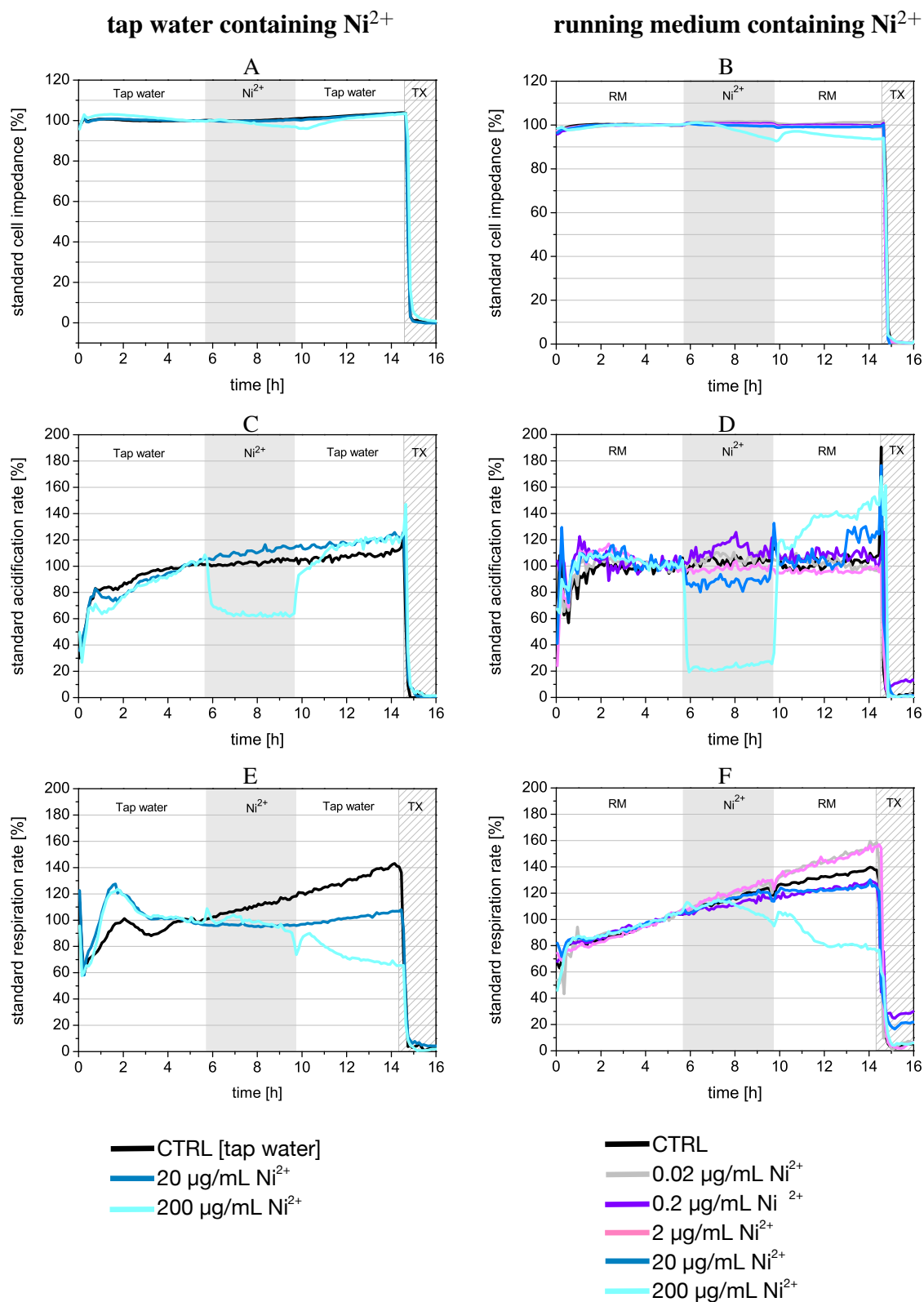


Figure 3.26: Detection of Ni<sup>2+</sup> in tap water using RLC-18 cells as the sensitive layer in comparison to cell culture medium. Left column represent the impact if Ni<sup>2+</sup> is present in tap water, right column if present in cell culture medium. The exposure time lasted for 5 hours (shaded area) preceded and followed by an adaptation and recovering phase of 5 hours (white area). A)B) Standardized cell impedance, C)D) Standardized acidification rate, E)F) Standardized respiration rate.

200  $\mu\text{g/mL}$   $\text{Ni}^{2+}$  provokes a clear impairment in the cellular physiology when present in cell culture medium. The cell impedance (figure 3.26 B) decreases by 10% and the acidification (figure 3.26 D) rate goes down to 20%. Despite this impact the acidification rate recovers completely after the sample containing  $\text{Ni}^{2+}$  is replaced by fresh medium. Also the respiration rate decreases during the time of the exposure but does not recover (figure 3.26 F). The respiration rate slows down to 80% where it stays constant.

The impact of 20  $\mu\text{g/mL}$  is less harmful and only visible by a reduction of the acidification rate by about 20%. Inferior concentrations seem not to harm the cells. Therefore these two concentrations, 20 and 200  $\mu\text{g/mL}$  were used to analyze if the impact produced by  $\text{Ni}^{2+}$  is similar if solved in tap water. 200  $\mu\text{g/mL}$   $\text{Ni}^{2+}$  present in tap water lead to a similar result than in cell culture medium. Nevertheless the effect is less pronounced. The acidification rate drops down to 60% (figure 3.26 C, but not to 20%) and the impairment in the respiration chain is similar to the one caused by  $\text{Ni}^{2+}$  in culture medium.

Unfortunately, the effect of 20  $\mu\text{g/mL}$  cannot be noticed. All rates remain constant. It is conceivable that the anions and cations present in tap water could attenuate the effect of the target ion  $\text{Ni}^{2+}$ . This effect has already been shown in section 3.1.3 and 3.2.3. Here the effect of two organic pollutants present in a sample at the same time was investigated. It was shown that if two pollutants are present at the same time in a sample, one can mitigate the toxicity of the second one. For example 10 $\mu\text{M}$  TBBPA masked the effect of 100 $\mu\text{M}$  Camphor (figure 3.7).

One last experiment will close this section. Since the life expectancy of a biosensor is problematic the next measurement was performed in order to determine if the biosensor survives a measurement time of 1 week. A collected rain water probe was used for this experiment. Figure 3.27 shows this measurement. There is a similarity with the 24 hours measurement using tap water shown in figure 3.23. The only difference is that the increase in the acidification and respiration rate (figure 3.27 B & C) is more prominent. This is due to the long time of the measurement. Both parameters increase constantly, the respiration rate from beginning on and the acidification rate after the second day. We know from the measurements already shown in this section that the composition of this water promotes this accelerated physiology. But another reason is here that the cells still proliferate. And more cells mean a higher metabolic rate.



Despite this, the parameters remain constant and a cell-chip can run and survive for at least one week.

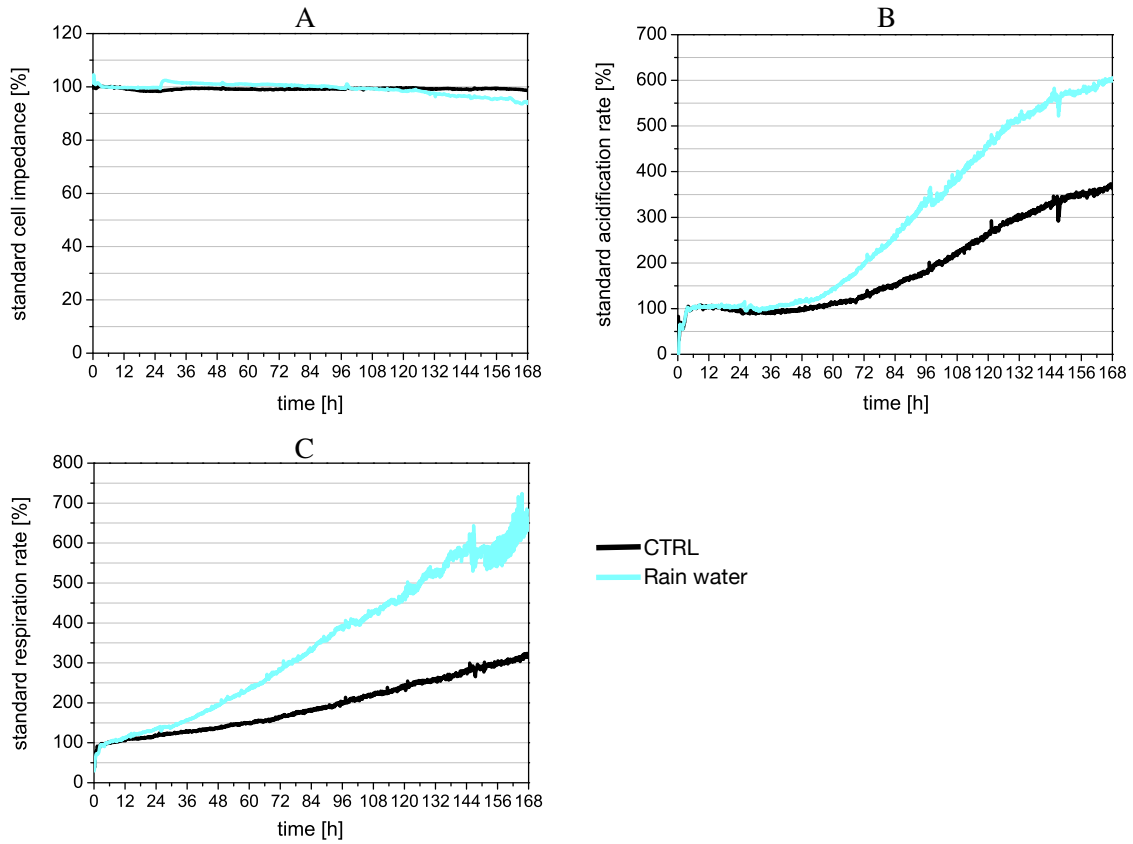


Figure 3.27: Suitability of RLC-18 as the detection layer for a 1 week long (rain) water measurement. A) Standardized cell impedance, B) Standardized acidification rate, C) Standardized respiration rate.

# Chapter 4

## Discussion

In this work the suitability of a cell-based sensor for the quality monitoring of aqueous media and the detection of hazardous chemicals in water was evaluated. Cultured eucaryotic cells react very sensitive to external influences with changes of their metabolism. The development of a sensor system which uses eucaryotic cells in order to detect bioactive substances takes advantage of this sensitivity.

### **4.1 Characteristics of a cell line to suit detection layer requirements**

The first step for the development of a cell-based biosensor is the choice of the right cell line. The highest possible sensitivity encompassed by a high robustness are the most desired characteristics to qualify as the detection layer for a biosensor. RLC-18 cells have shown to be an adequate cell line since after performing several measurements with the same test substance the electrical read-out shown by the physiological parameters cell impedance, acidification rate and respiration rate showed the highest reproducibility. More over, since the usage of cultured cells is finite in their passage and one stock can underlay several freeze and thaw processes it is crucial that the physiological properties of the cell line remain constant. For instance the use of HepG2 cells (human hepatocellular carcinoma) has been shown to be not appropriate for similar applications (Stütz, 2008). The physiological response varied after freezing and thawing of the cell line and from one passage to another.

Figure 4.1 shows the respiration rate of RLC-18 cells after having been exposed to 500  $\mu\text{M}$  chlorpyrifos. Each curve represents one measurement where different stocks of cells were used.

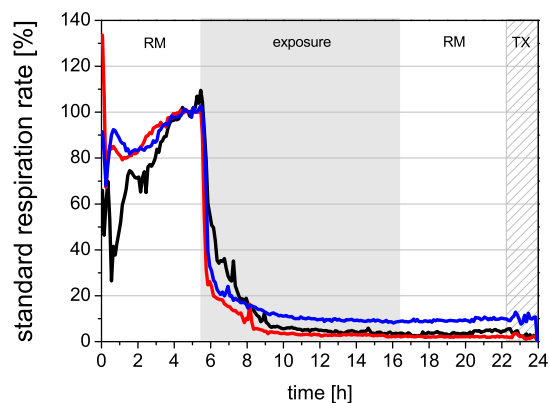


Figure 4.1: Reliability of RLC-18 cells as the detection layer for the detection of pollutants in aqueous media. In 3 independent measurements 500  $\mu\text{M}$  chlorpyrifos were applied to the detection layer for 10h. An adaptation time of 5h was preceded to the exposure and followed by 7h recovering time. The panel shows the impact of chlorpyrifos on the respiration rate.

The figure shows that for all measurements the respiration collapses at the same time and the decrease for all curves is simultaneous.

## 4.2 Solubility and Sensitivity

From the measurements performed with the four model compounds 2-Aminoanthracene (heterocyclic amine), chlorpyrifos (organophosphate insecticide), 3,3',5,5'-Tetrabromobisphenol A (flame retardant) and 4-methylbenzylidene camphor (UV-B filter) we know that the detection limits of this system ranges between 10 and 100  $\mu\text{M}$  in single applications. Converted into  $\mu\text{g/L}$ , this means that the cell layer is able to detect these chemicals starting from concentrations of 1000  $\mu\text{g/L}$  onwards. Now, if we compare this detection limit with the allowed or advised values within the boundaries of the European Union, we will see that there is a considerable gap to bridge. The *environmentally acceptable concentrations* declared by the WHO amount to 1  $\mu\text{g/L}$  and the maximal permitted concentration for organophosphate pesticides and polyaromatic hydrocarbons in drinking water amounts to 0.1  $\mu\text{g/L}$  (WHO, 2004).

Crucial for a toxicological effect of a chemical on the physiology of the cell is the binding of this chemical to a receptor or its internalization into the cell. If a compound is hardly soluble it will stay suspended in the aqueous phase or remain in the ground as a sediment. In its report about polyaromatic hydrocarbons like 2-AA, the World Health Organization accounted to this fact. First, because transportation remains local (section 1.4.1 and WHO (1998)) and

second, because toxicity may be reduced. Table 4.1 shows the solubilities of the used organic compounds in this PhD Thesis. They are all hardly soluble or insoluble. It is of course possi-

Chemical	Solubility	Reference
2-AA	0.073 mg/L	WHO (1998)
Chlorpyrifos	1.05 mg/L	European Union (2005)
TBBPA	4.16 mg/L	WHO (1995)
4-MBC	apparently not soluble	WHO (1998)

Table 4.1: Solubilities of 2-AA, Chlorpyrifos, TBBPA and 4-MBC in water.

ble to solve them in organic solvents like DMSO or Isopropanol but since the detection layer is based on cells it is necessary to use solvent concentrations below toxic values, this means a maximum of 2% DMSO. The consequence of this low solvent concentration is that not the entire portion of chemical used is solved and in turn biological active. This may explain why the detection limits of the here presented cell-based sensor are above those of standard methods like chromatographic techniques (Jimenez-Jorquera C, 2010).

This consideration is reinforced by the fact that the detection limits using soluble compounds is much lower. The German Water Framework Directive sets 0.02  $\mu\text{g/mL}$  as the maximal allowed concentration in drinking water and 0.2  $\mu\text{g/mL}$  in the environment for  $\text{Ni}^{2+}$  (Kubisch et al., 2012b). Figure 3.26 D in section 3.4.2 shows that the system is able to visualize an alteration of the acidification rate after application of 0.2  $\mu\text{g/mL}$   $\text{Ni}^{2+}$ . Since  $\text{Ni}^{2+}$  ions are soluble in water it can be assumed that the whole amount applied is biologically active.

The statement is now that this system detects the biological active portion of the contaminant in the medium. Bohrn et al. (2013) has shown this by comparing the physiological response of V79 cells (Chinese hamster lung fibroblasts cells) after being exposed to  $\text{Cr}^{6+}$  and  $\text{Cr}^{3+}$ .  $\text{Cr}^{6+}$  compounds have been shown to be 1000-fold more potent than  $\text{Cr}^{3+}$  compounds in inducing cytotoxicity and mutagenesis in the same cell type (Biedermann and Landolph, 1990).

There sensitivity of the detection layer can be improved by varying the composition of the used medium. In this study DMEM with 4.5 g/L glucose has been used. Stütz and Kubisch (2010) reported that the substitution of glucose by galactose improves the vulnerability of the cellular detection layer in certain cell lines. In a high glucose environment the ATP synthesized by the glycolysis is sufficient for the cells. If this high glucose disappears, energy production is

carried out by the more energy producing citric acid cycle. This leads to a higher susceptibility of cells against substances especially aiming at cellular respiration. Other factors like temperature may also play a role in calibrating the sensitivity of the detection layer.

## 4.3 Beyond acute toxicity of single exposure

Cells used as the detection layer in a biosensor have the advantage that they will notice any toxicity independently if there is one pollutant present in the sample or several. In Egging (2002); Subramanian (2004); Senveli and Tigli (2013) antibodies have been used as the sensing layer of a biosensor to bind chemicals. This allows the use of more than one antibody on the chip surface and in this manner many antigens can be detected. Nevertheless this method is constrained by the space on the chip since only a finite number of antibodies can be immobilized and by the fact that the synthesis of antibodies is expensive and time consuming. More over it is impossible to synthesize antibodies for all existing chemicals.

A cell-based sensor system allows the monitoring of the overall quality of a sample and independently of how many chemicals are present in the sample. Combined measurements of chlorpyrifos together with TBBPA and 4-MBC together with TBBPA have been shown in this work. In most of the concentration pairs used the system shows the expected result of a reinforced toxicity due to the presence of two toxic chemicals or at least that the system could show that there is “something” toxic in the sample. But also the unexpected result of the mitigation of the toxicity of one compound was observed. For example, the toxic effect of 100  $\mu\text{M}$  Chlorpyrifos is attenuated if 10  $\mu\text{M}$  TBBPA is also present in the sample. In this case not only the low solubility of the compounds may play a role. It is conceivable that transport mechanisms pump actively one compound out of the cell. Most eukaryotic ABC transporters export hydrophobic molecules from the cytoplasm (Locher, 2004) and this could lead to a decreased toxicity of the contaminated sample.

Due to the low solubility of apolar chemicals and cellular mechanisms diminishing toxicity a functional generalized linear model was developed to predict and ascertain the chemical/s present in the sample. The underlying data set is taken from the measurement and after a learning process the algorithm can determine which chemical is present in the sample. This method

has become increasingly important in the fields of health and biomedicine (Alborzinia et al., 2013; Ullah and Finch, 2013; Goldsmith and Scheipl, 2014) since it allows to analyze, model and predict most of the quasi-continuous data measured in various fields of research. For instance, in biomedicine the growth pattern of a tumor can be estimated as well as the severity of a disease (Sorensen et al., 2013). Even more recently, this method has been used to predict the heat value of a fossil fuel and the concentration of paracetamol in an aqueous medium using a biosensor (Fuchs et al., 2015).

Simultaneously to the detection of pollutants and the determination of their acute toxicity there is an increasing interest in detecting the presence of substances that may cause diseases in the long term. Among these, those that promote cell proliferation are of special interest since they are used in a variety of applications and also present in the environment (Jeffries et al., 2011; Schlumpf et al., 2001). The estrogen receptor is a main target of these chemicals and therefore the application of this biosensor for the detection of proliferating chemicals was a major task during this work. Under cell culture conditions 10 nM  $17\beta$ -estradiol has been shown to be the concentration leading to the highest expression of genes related with cell proliferation (Wang et al., 2004). Using MCF-7 cells which carry the estrogen receptor  $\alpha$  it was possible to visualize how  $17\beta$ -estradiol induce proliferation. Mainly the cell impedance allows the measurement of cell growth. Devices like the Roche xCELLigence have shown to be suitable for this applications. It consists on an electronic sensor analyzer carrying a 96-well plate. 80% of the bottom of the wells is covered by gold electrode sensors which measure the attachment of the cells to the surface (Bohrn et al., 2013). In this way a high resolution is ensured if cells proliferate or spread upon the surface. In the case of the here used sensor chip (SC 1000 Metabolic Chip) only a small portion is covered by the relevant IDES electrode (see table 2.5 in section 2.2.2). The augmentation of the surface covered by this electrode would improve the resolution of proliferation tests.

## 4.4 The long way towards an application

Besides the challenges of sensitivity and detection limits there are still some issues which have to be addressed in order to make a biosensor suitable for a field application for water quality monitoring. In this PhD two of them have been depicted out since they represent the most intu-

itive.

The right packaging of the sensor could be developed by studying how the medical and biotechnological field has managed to preserve and transport organs and tissues. The trend towards encapsulating cells and tissues in sponge-like materials has been crucial in this sense since they give shelter against mechanical stress and environmental fluctuations like temperature (Service, 2000; Hunt and Grover, 2010). A 1.5% concentrated solution of porcine gelatin was finally the most suitable medium to preserve and store the cell-loaded chip. This allowed us to store the chips in our lab in Munich at 4°C for one week and deliver them to Heidelberg, where they were stored again at 4°C for 3 days. The cells showed complete viability after this delivery and storage so that this technique can be used in the future for the transportation of a ready-to-use biosensor to a customer.

The measurement of tap water and from the river Isar in Munich reinforced the possibilities of this method to monitor the quality of water. The improvement done by solving DMEM in powder form is time consuming but until now the only way to allow the cellular detection layer to survive a water sample even if this is not contaminated.

# Chapter 5

## Outlook

A biosensor is not supposed to replace standard analyzing methods like chromatography or analytical chemistry but it could be used as a prescreen for toxic or bioactive substances in a sample. The challenge faced by the biosensors community is to fulfill the increasing requirements of environmental legislation. Sensitivity, selectivity, fast responses and costs are the main subjects. To assess this, the biological recognition element as well as the transducer have to be considered. At the moment they suffer from a lower robustness than many solid state sensors (Lagarde and Jaffrezic-Renault, 2011). This becomes crucial for outdoor applications where the sensor is exposed to temperature fluctuations or mechanical impacts.

The presented system is optimized for cell lines with a growth optimum at 37°C. Nevertheless, step by step, more and more complications are being overcome. In this study the transportation, storage and compensation of the osmolarity differences between water and the cytoplasm represented serious questions to account for. The huge work being done on this research field allows the rapid evolution of biosensors so that there is hope that soon one enters the market to monitor the quality of fresh water.



# Appendix A

## Using other solvents instead of DMSO

In the experiments shown in this PhD DMSO was used whenever a solvent was needed. DMSO is an established solvent in the world of science and due to its low toxicity below concentrations of 2%, the means of choice to carry out toxicity experiments. Nevertheless there were other solvents which came into question, some of them because they are used in industry or because they are naturally occurring. In both cases they could be present in fresh water and solving contaminants, reinforcing thus their toxicity.

In this part of the appendix two of them will be presented since they could replace DMSO in further studies.

### A.1 Polyethylene glycol (PEG)

Polyethylene glycol (PEG) is a polyether used in industrial manufacturing as well as in biology and medicine. It is present in skin creams and cosmetics, toothpastes, tattoos, etc... Depending on the molecular weight it is liquid at room temperature or a low-melting solid.

PEG-400 (different numbers are given depending on the chain size and therefore the molecular weight) was tested here because it is in a liquid state, it is strongly hydrophilic and has a very low toxicity (Maes et al., 2012).

In section 3.1.3 the toxicity of a mixture of 4-MBC and TBBPA was shown (see figure 3.6). The same measurements were performed using PEG-400 as a solvent instead of DMSO. Fig-

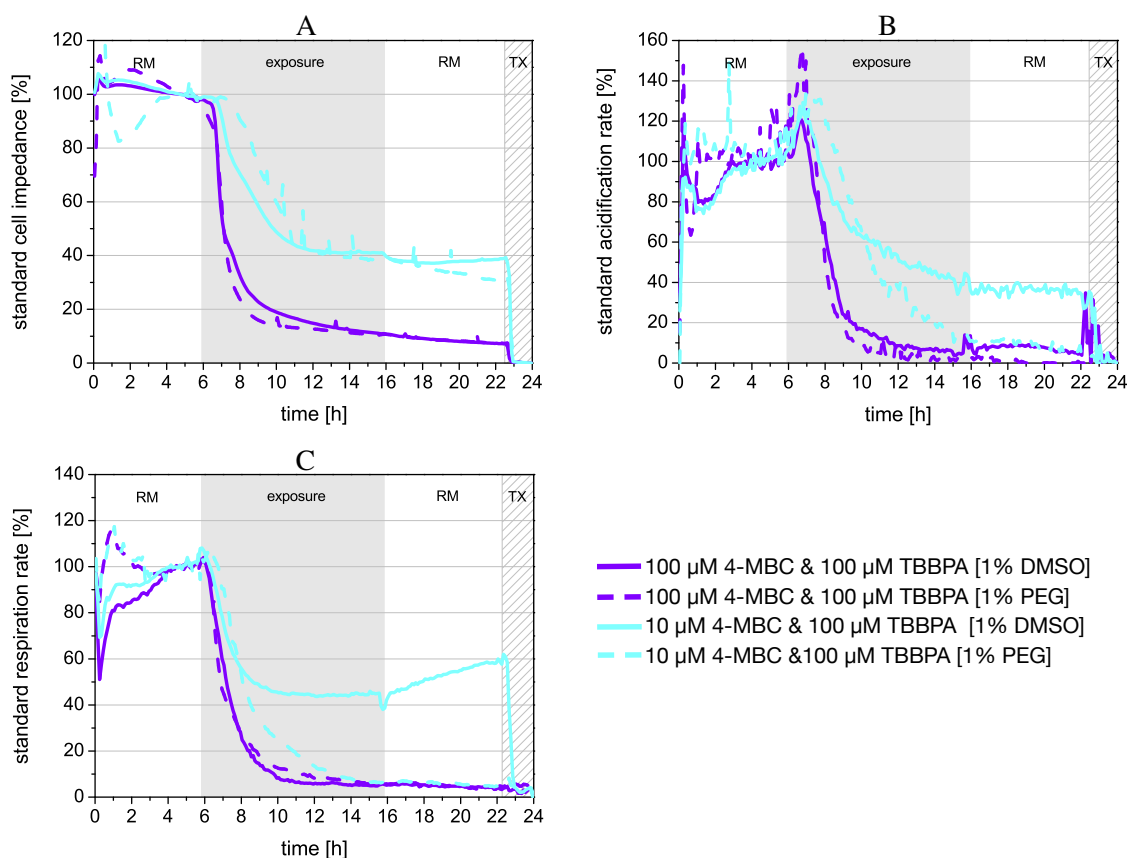


Figure A.1: Effect of the solvent PEG on the detection layer compared to DMSO. RLC-18 cells were exposed for 10h (shaded area) to 4-MBC and TBBPA solved in DMSO or in PEG in Bionas Analyzing System. The exposure was followed by a recovering phase of 7h (white area). Cells were allowed to adapt to the system prior to exposure for 5h (white area). A) Standardized cell impedance, B) Standardized acidification rate, C) Standardized respiration rate.

ure A.1 compares the results of two combinations with those obtained by using DMSO as a solvent. In the graphs, same colors represent the same concentrations of compound, the solid lines represent the samples where DMSO was used as a solvent and the dashed ones where PEG was used. The match between the different solvents is for all pairs nearly perfect. This means that PEG-400 could also be used as a solvent. More over, the wide applications of PEG makes it possible that it finds its way into rivers or lakes solving chemicals which can enter the food chain in this way.

## A.2 Saponin

Saponins are amphipathic glycosides synthesized by various plant species. Due to this amphipathic character they are able to solve apolar chemicals in water building miscelles. The fact that they are naturally occurring makes them particularly interesting because in this way pol-

luntants can be solved and transported for long distances.

In fact saponins are detergents and therefore toxic for organisms. Their application as a solvent might therefore be limited. Therefore it was tested if very low concentrations affect the healthiness of the cells. Figure A.2 shows the results of exposing RLC-18 cells to different concentration of saponin. All physiological parameters show the same devastating result. The cells die as soon as they come in contact with saponin. The toxicity of saponin is as high as the on of the detergent Triton-X. Even the lowest concentration tested, 0.01% leads to cell death.

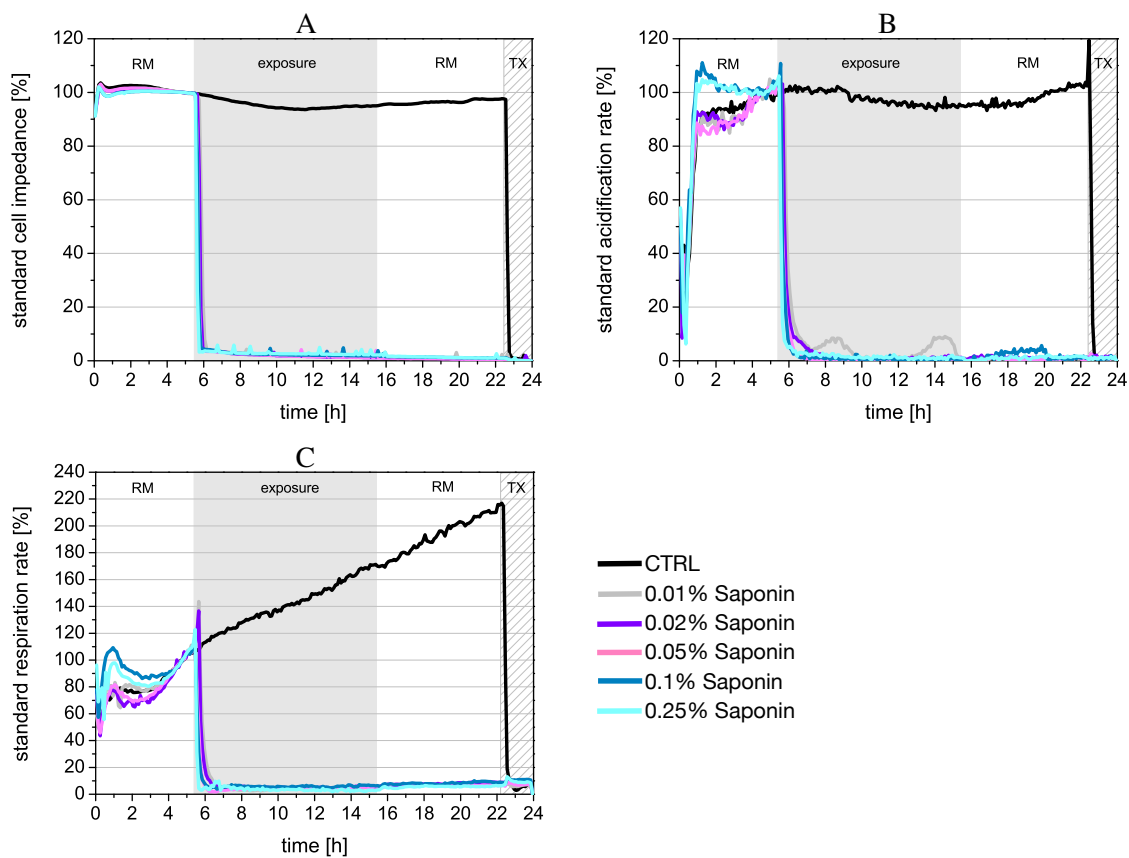


Figure A.2: Effect of the solvent saponin on RLC-18 cells. After an adaptation time of 5h (white area), cells were exposed to saponin for 10h (shaded area) and afterwards allowed to recover. A) Standardized cell impedance, B) Standardized acidification rate, C) Standardized respiration rate.

## Appendix B

### PBS to impede the toxic effect of water

One of the major problems by measuring water is that water represents a hypoosmotic environment for a cell. One idea to solve this problem would have been the addition of PBS to the water sample. At the same time, one has to keep in mind that the cells need the nutrients present in cell culture medium to survive. The sample containing PBS was therefore added only for 10 minutes. More over,  $\text{Ni}^{2+}$  solved in PBS was used as test substance in order to elucidate if it is possible to differentiate between the impact of nickel and the one of PBS alone. Figure B.1 shows the results corresponding to this experiment. The 2 grey dashed lines represent the 10 minutes where PBS or PBS with  $\text{Ni}^{2+}$  was added. In total the cells were exposed two times to the sample. The problem of this idea arises from the fact that the peaks caused by PBS are very similar the ones originated by PBS/ $\text{Ni}^{2+}$ . Even if the amplitude of the peak in the acidification rate is higher when  $\text{Ni}^{2+}$  is present (figure B.1 B) it is too easy to confound them. More over the signal obtained from the cell impedance and the respiration rates (figure B.1 A and C) are for both cases nearly the same.

For these reasons and from now on DMEM in powder form was diluted into the water sample (as described in section 3.4.2) to ensure the viability of the detection layer .

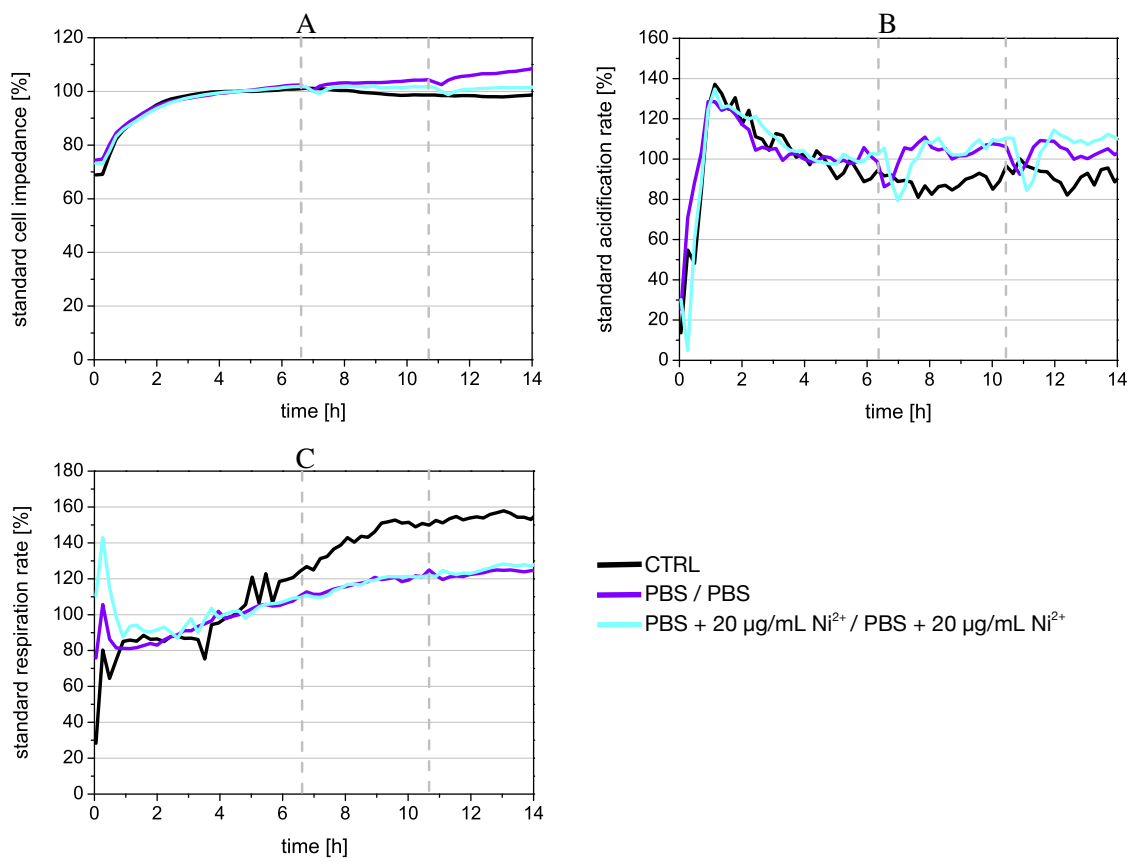


Figure B.1: Application of PBS with or without Ni<sup>2+</sup> for 10 minutes. The exposure was performed twice and is marked with a dashed grey line.

# Bibliography

- Aguilar, F., Autrup, H., Barlow, S., Castle, L., Crebelli, R., Dekant, W., Engel, K., Gontard, N., Gott, D., Grilli, S., Gürtler, R., Larsen, J., Leclercq, C., Leblanc, J., Malcata, X., Mennes, W., Milana, M., Pratt, I., Rietjens, I., Tobbyack, P., and Toldrá, F. (2008). Camphor in flavourings and other food ingredients with flavouring properties. *The EFSA Journal*, 729:1–15.
- Alaee, M., Arias, P., Sjödin, A., and Bergman, A. (2003). An overview of commercially used brominated flame retardants, their applications, their use patterns in different countries/regions and possible modes of release. *Environment International*, 29(6):683–9.
- Alborzina, H., Can, S., Holenya, P., Scholl, C., Lederer, E., Kitanovic, I., and Wöfl, S. (2011). Real-time monitoring of cisplatin-induced cell death. *PLOS one*, 6(5):e19714.
- Alborzina, H., Schmidt-Glenewinkel, H., Ilkavets, I., Breitkopf-Heinlein, K., X, X. C., Hortschansky, P., Dooley, S., and Wöfl, S. (2013). Quantitative kinetics analysis of bmp2 uptake into cells and its modulation by bmp antagonists. *Journal of Cell Science*, 126(Pt 1):117–27.
- Anh, T., Dzyadevych, S., Van, M., Renault, N., Duc, C., and Chovelon, J. (2004). Conductometric tyrosinase biosensor for the detection of diuron, atrazine and its main metabolites. *Talanta*, 63(3):365–370.
- Armitage, W. (1987). Cryopreservation of animal cells. *Symposia of the Society for Experimental Biology*, 41:379–393.
- Bagchi, A., Woods, E., and Critser, J. (2008). Cryopreservation and vitrification: recent advances in fertility preservation technologies. *Expert Review of Medical Devices*, 5(3):359–370.

- Baker, D., Taylor, H., Lee, S., Barker, S., Goad, M., and Means, J. (2001). Hepatic toxicity and recovery of fischer 344 rats following exposure to 2-aminoanthracene by intraperitoneal injection. *Toxicologic Pathology*, 29(3):328–32.
- Balmer, M., Buser, H., Müller, M., and Poiger, T. (2005). Occurrence of some organic uv filters in wastewater, in surface waters, and in fish from swiss lakes. *Environmental Science & Technology*, 39(4):953–62.
- Banerjee, M., Robbins, D., and Chen, T. (2013). Modulation of xenobiotic receptors by steroids. *Molecules*, 18(7):7389–7406.
- Bartlett, P., editor (2008). *Bioelectrochemistry Fundamentals, Experimental Techniques and Applications*. John Wiley & Sons, West Sussex, England.
- Belzer, F., Sollinger, H., Glass, N., Miller, D., Hoffmann, R., and Southard, J. (1983). Beneficial effects of adenosine and phosphate in kidney preservation. *Transplantation*, 36(6):633–635.
- Belzer, F. and Southard, J. (1980). The future of kidney preservation. *Transplantation*, 30(3):161–165.
- Betts, K. (2013). Molecular competition: flame retardants interact with key metabolism enzyme. *Environment Health Perspectives*, 121(10):A313.
- Bhattacharyya, J., Read, D., Amos, S., Dooley, S., Killham, K., and Paton, G. (2005). Biosensor-based diagnostics of contaminated groundwater: assessment and remediation strategy. *Environmental Pollution*, 134(3):485–492.
- Biedermann, K. and Landolph, J. (1990). Role of valence state and solubility of chromium compounds on induction of cytotoxicity, mutagenesis, and anchorage independence in diploid human fibroblasts. *Cancer Research*, 50(24):7835–7842.
- Birnbaum, L. S. and Staskal, D. F. (2004). Brominated flame retardants: Cause for concern? *Environmental Health Perspectives*, 112(1):9–17.
- Bohrn, U., Mucha, A., Werner, C., Trattner, B., Bäcker, M., Krumbe, C., Schienle, M., Stütz, E., Schmitt-Landsiedel, D., Fleischer, M., Wagner, P., and Schöning, M. (2013). A critical comparison of cell-based sensor systems for the detection of cr(vi) in aquatic environment. *Sensors and Actuators B*, 182:58–65.

- Bohrn, U., Stütz, E., Fleischer, M., Schöning, M., and Wagner, P. (2010). Real-time detection of co by eukaryotic cells. *Procedia Engineering*, 5:17–20.
- Bohrn, U., Stütz, E., Fleischer, M., Schöning, M., and Wagner, P. (2011). Eukaryotic cell lines as a sensitive layer for rapid monitoring of carbon monoxide. *Physica Status Solidi (A)*, 208(6):1345–1350.
- Bouchard, M., Chevrier, J., Harley, K., Kogut, K., Vedar, M., Calderon, N., Trujillo, C., Johnson, C., Bradman, A., Barr, D., and Eskenazi, B. (2011). Prenatal exposure to organophosphate pesticides and iq in 7-year-old children. *Environmental Health Perspectives*, 119(8):1189–95.
- Boudreau, M., Taylor, H., Baker, D., and Means, J. (2006). Dietary exposure to 2-aminoanthracene induces morphological and immunocytochemical changes in pancreatic tissues of fisher-344 rats. *Toxicological Sciences*, 93(1):50–61.
- Bousse, L. (1996). Whole cell biosensors. *Sensors and Actuators B: Chemical*, 34(1-3):270–275.
- Braunhut, S., McIntosh, D., Vorotnikova, E., Zhou, T., and Marx, K. (2005). Detection of apoptosis and drug resistance of human breast cancer cells to taxane treatments using quartz crystal microbalance biosensor technology. *Assay and Drug Development Technologies*, 3(1):77–88.
- Bruns, H., Kneser, U., Holzhüter, S., Roth, B., Kluth, J., Kaufmann, P., Kluth, D., and Fiegel, H. (2005). Injectable liver: A novel approach using fibrin gel as a matrix for culture and intrahepatic transplantation of hepatocytes. *Tissue Engineering*, 11-12:1718–26.
- Burbaum, J. and Sigal, N. (1997). New technologies for high-throughput screening. *Current Opinion in Chemical Biology*, 1(1):72–78.
- Caldon, C. (2014). Estrogen signaling and the dna damage response in hormone dependent breast cancers. *Frontiers in Oncology*, 4(106):eCollection.
- Carrière, V., de Waziers, I., Courtois, Y., Leroux, J., and Beaune, P. (1992). Cytochrome p450 induction and mutagenicity of 2-aminoanthracene (2aa) in rat liver and gut. *Mutation Research*, 268(1):11–20.



- Cerioti, L., Kob, A., Drechsler, S., Ponti, J., Thedinga, E., Colpo, P., Ehret, R., and Rossi, F. (2007). Online monitoring of balb/3t3 metabolism and adhesion with multiparametric chip-based system. *Analytical Biochemistry*, 371(1):92–104.
- Chen, W., Vermaak, I., and Viljoen, A. (2013). Camphor—a fumigant during the black death and a coveted fragrant wood in ancient egypt and babylon—a review. *Molecules*, 18(5):5434–54.
- Clark, L. and Lyons, C. (1962). Electrode systems for continuous monitoring in cardiovascular surgery. *Annals of the New York Academy of Sciences*, 102(1):29–45.
- Costa, L. (2006). Current issues in organophosphate toxicology. *Clinica Chimica Acta*, 366(1-2):1–13.
- Covington, A. (1994). Terminology and conventions for microelectronic ion-selective field effect transistor devices in electrochemistry. *Pure and Applied Chemistry*, 66(3):565–569.
- de Bolster, M. (1997). Glossary of terms used in bioinorganic chemistry (iupac recommendations 1997). *Pure and Applied Chemistry*, 69(6):1365–3075.
- de Wit, C., Herzke, D., and Vorkamp, K. (2010). Brominated flame retardants in the arctic environment—trends and new candidates. *Science of the Total Environment*, 408(15):2885–918.
- Deborah, C. and Smegal, M. (2000). *Human Health Risk Assessment; Chlorpyrifos*. U.S. Environmental Protection Agency.
- Dingemans, M., van den Bergand, M., and Westerink, R. (2011). Neurotoxicity of brominated flame retardants: (in)direct effects of parent and hydroxylated polybrominated diphenyl ethers on the (developing) nervous system. *Environmental Health Perspectives*, 119(7):900–7.
- Drew, D., Britton, W., Soderberg, D., Negrón-encarnación, I., Christensen, C., Liccione, J., Lowit, A., Irwin, W., Doherty, J., and Smegal, D. (2011). *Chlorpyrifos: Preliminary Human Health Risk Assessment for Registration Review*. U.S. Environmentam Protection Agency.
- Eaton, D., Daroff, R., Autrup, H., Bridges, J., Buffler, P., Costa, L., Coyle, J., McKhann, G., Mobley, W., Nadel, L., Neubert, D., Schulte-Hermann, R., and Spencer, P. (2008). Review of

- the toxicology of chlorpyrifos with an emphasis on human exposure and neurodevelopment. *Critical Reviews in Toxicology*, 38 Suppl 2:1–125.
- Edwards, D. (2005). Regulation of signal transduction pathways by estrogen and progesterone. *Annual Review of Physiology*, 67:335–376.
- Eggins, B. (2002). *Chemical Sensors and Biosensors*. John Wiley & Sons, West Sussex, England.
- Ehret, R., Baumann, W., Brischwein, M., Schwinde, A., and Wolf, B. (1998). On-line control of cellular adhesion with impedance measurements using interdigitated electrode structures. *Medical & Biological Engineering & Computing*, 36(3):365–370.
- Eltzov, E. and Marks, R. (2010). *Fiber-optic based cell sensors*. In: *Whole Cell Sensing Systems I*. Springer Berlin/Heidelberg.
- Eltzov, E. and Marks, R. (2011). Whole-cell aquatic biosensors. *Analytical and Bioanalytical Chemistry*, 400(4):895–913.
- Engel, S., Wetmur, J., Chen, J., Zhu, C., Barr, D., Canfield, R., and Wolff, M. (2011). Prenatal exposure to organophosphates, paraoxonase 1, and cognitive development in childhood. *Environment Health Perspectives*, 119(2):1182–89.
- European Food Safety Authority (2011). Conclusion on the peer review of the pesticide risk assessment of the active substance chlorpyrifos. *The EFSA Journal*, 9(1):1961.
- European Union (2000). Directive 2000/60/ec of the european parliament. and the council of 23 october 2000 establishing a framework for community action in the field of water policy. *Official Journal of the European Communities*, L 327/1.
- European Union (2001). *SCCNFP/0483/01; Final : Opinion on the evaluation of potentially estrogenic effects of UV filters, adopted by the SCCNFP during the 17<sup>th</sup> plenary meeting of 12 June 2001*. European Commission.
- European Union (2004). *SCCNFP/0779/04; Final : Opinion concerning 4-Methylbenzylidene Camphor, adopted by the SCCNFP during the 28<sup>th</sup> plenary meeting of 25 May 2004*. European Commission.

- European Union (2005). Commission directive 2005/72/ec of 21 october 2005. amending council directive 91/414/eec to include chlorpyrifos, chlorpyrifos-methyl, mancozeb, maneb, and metiram as active substances. *Official Journal of the European Communities*, L 279/63.
- European Union (2006). *SCCP/1042/06; Final : Opinion concerning 4-Methylbenzylidene Camphor, Adopted by the SCCP during the 9<sup>th</sup> plenary meeting of 10 October 2006*. European Commission.
- European Union (2013). Commission implementing regulation (eu) no 762/2013 of 7 august 2013. amending implementing regulation (eu) no 540/2011 as regards the extension of the approval periods of the active substances chlorpyrifos, chlorpyrifos-methyl, mancozeb, maneb, mcpa, mcpb and metiram. *Official Journal of the European Communities*, L 213/14.
- Evans, M., Muir, D., Lockhart, L., Stern, G., Ryan, M., and Roach, P. (2005). Persistent organic pollutants and metals in the freshwater biota of the canadian subarctic and arctic: an overview. *Science of the Total Environment*, 351-352:94–147.
- Fahy, G., Wowk, B., Pagotan, R., Chang, A., Phan, J., Thomson, B., and Phan, L. (2009). Physical and biological aspects of renal vitrification. *Organogenesis*, 5(3):167–175.
- FDA (1983). *Proposed rules: external analgesic drug products for over-the-counter human use; tentative final monograph*. Fed Reg 48, 5852 – 5869.
- Foxenberg, R., Ellison, C., Knaak, J., Ma, C., and Olson, J. (2011). Cytochrome p450-specific human pbpk/pd models for the organophosphorus pesticides: Chlorpyrifos and parathion. *Toxicology*, 285(1-2):57–66.
- Fremes, S., Furukawa, R., Li, R., RD, R. W., Mickle, D., and Tumiati, L. (1991a). Prolonged preservation with university of wisconsin solution. *Journal of Surgical Research*, 50(4):330–334.
- Fremes, S., Li, R., RD, W., DA, D. M., and Tumiati, L. (1991b). Prolonged hypothermic cardiac storage with university of wisconsin solution. an assessment with human cell cultures. *Journal of Thoracic and Cardiovascular Surgery*, 102(5):666–672.
- Fremes, S., Li, R., Weisel, R., Mickle, D., Furukawa, R., and Tumiati, L. (1991c). The limits of cardiac preservation with university of wisconsin solution. *Annals of Thoracic Surgery*, 52(4):1021–1025.

- Fuchs, K., Scheipl, F., and Greven, S. (2015). Penalized scalar-on-functions regression with interaction term. *Computational Statistics and Data Analysis*, 81:38–51.
- Fuerhacker, M. (2009). Eu water framework directive and stockholm convention: can we reach the targets for priority substances and persistent organic pollutants? *Environmental Science and Pollution Research International*, 16 Suppl 1:S92–7.
- García, S., Seidler, F., and Slotkin, T. (2005). Developmental neurotoxicity of chlorpyrifos: targeting glial cells. *Environmental Toxicology and Pharmacology*, 19(3):455–61.
- García, V., García-Pérez, E., Belyakova, E., Llames, S., Pevida, M., Tevar, F., Otero, J., and Meana, A. (2008). Room temperature storage of cultured human articular chondrocytes. *Cell Preservation Technology*, 6(3):199–206.
- Gato, W., Halesand, D., and Means, J. (2012). Hepatic gene expression analysis of 2-aminoanthracene exposed fisher-344 rats reveal patterns indicative of liver carcinoma and type 2 diabetes. *Journal of Toxicological Sciences*, 37(5):1001–16.
- Giaever, I. and Keese, C. (1993). A morphological biosensor for mammalian cells. *Nature*, 366(6455):591–592.
- Giger, W. (2009). The rhine red, the fish dead—the 1986 schweizerhalle disaster, a retrospect and long-term impact assessment. *Environmental Science and Pollution Research International*, 16 Suppl 1:S98–111.
- Goldsmith, J. and Scheipl, F. (2014). Estimator selection and combination in scalar-on-function regression. *Computational Statistics and Data Analysis*, 70:363–372.
- Han, B. and Bischof, J. (2004). Engineering challenges in tissue preservation. *Cell Preservation Technology*, 2(2):91–112.
- Hendriks, H., van Kleef, R., van den Berg, M., and Westerink, R. (2012). Multiple novel modes of action involved in the in vitro neurotoxic effects of tetrabromobisphenol-a. *Toxicological Sciences*, 128(1):235–46.
- Ho, C., Robinson, A., Miller, D., and Davis, M. (2005). Overview of sensors and needs for environmental monitoring. *Sensors*, 5(1):4–37.

- Holenya, P., Can, S., Rubbiani, R., Alborzina, J., Jünger, A., Cheng, X., Ott, I., and Wöfl, S. (2014). Detailed analysis of pro-apoptotic signaling and metabolic adaptation triggered by a n-heterocyclic carbene-gold(i) complex. *Metallomics*, 6(9):1591–601.
- Hong, J., Kandasamy, K., Marimuthu, M., Choi, C., and Kim, S. (2011). Electrical cell-substrate impedance sensing as a non-invasive tool for cancer cell study. *Analyst*, 136(2):237–45.
- Hsieh, B., Deng, J., Ger, J., and Tsai, W. (2001). Acetylcholinesterase inhibition and the extrapyramidal syndrome: A review of the neurotoxicity of organophosphate. *Neurotoxicology*, 22(4):423–27.
- Hunt, N. and Grover, L. (2010). Cell encapsulation using biopolymer gels for regenerative medicine. *Biotechnology Letters*, 36(6):733–742.
- Hunt, N., Smith, A., Gbureck, U., Shelton, R., and Grover, L. (2010). Encapsulation of fibroblasts causes accelerated alginate hydrogel degradation. *Acta Biomaterialia*, 6(9):3649–56.
- Jamieson, N., Sundberg, R., Lindell, S., Claesson, K., Moen, J., Vreugdenhil, P., Wight, D., Southard, J., and Belzer, F. (1988). Preservation of the canine liver for 24-48 hours using simple cold storage with uw solution. *Transplantation*, 46(4):517–522.
- Janjua, N., Mogensen, B., Andersson, A., Petersen, J., Henriksen, M., Skakkebaek, N., and Wulf, H. (2004). Systemic absorption of the sunscreens benzophenone-3, octylmethoxycinnamate, and 3-(4-methyl-benzylidene) camphor after whole-body topical application and reproductive hormone levels in humans. *Journal of Investigative Dermatology*, 123(1):57–61.
- Jeffries, M. S., Conoanb, N., Cox, M., Sangster, J., Balsiger, H., Bridges, A., Cowman, T., Knight, L., Bartelt-Hunt, S., and Koloka, A. (2011). The anti-estrogenic activity of sediments from agriculturally intense watersheds: assessment using in vivo and in vitro assays. *Aquatic Toxicology*, 105(1-2):189–198.
- Jemnitz, K., Veres, Z., Torok, G., Toth, E., and Vereczkey, L. (2004). Comparative study in the Ames test of benzo[a]pyrene and 2-aminoanthracene metabolic activation using rat hepatic S9 and hepatocytes following in vivo or in vitro induction. *Mutagenesis*, 19(3):245–250.

- Jimenez-Jorquera C, Orozco J, B. A. (2010). Isfet based microsensors for environmental monitoring. *Sensors*, 10:61–83.
- Jochen, G. and Theis, M. (1995). Camphorated oil: still endangering the lives of canadian children. *Canadian Medical Association Journal*, 152(11):1821–1824.
- Jokanović, M. and Kosanović, M. (2010). Neurotoxic effects in patients poisoned with organophosphorus pesticides. *Environmental Toxicology and Pharmacology*, 29(3):195–201.
- Kawamura, Y., Ogawa, Y., Nishimura, T., Kikuchi, Y., Nishikawa, J., and Nishihara, T. (2003). Estrogenic activities of uv stabilizers used in food contact plastics and benzophenone derivatives tested by the yeast two-hybrid assay. *Journal of Health Science*, 49:205–12.
- Khine, H., Weiss, D., Graber, N., Hoffman, R., and Esteban-Cruciani, N. (2009). A cluster of children with seizures caused by camphor poisoning. *Pediatrics*, 123:1269.
- Khokhar, J. and Tyndale, R. (2012). Rat brain cyp2b-enzymatic activation of chlorpyrifos to the oxon mediates cholinergic neurotoxicity. *Toxicological Sciences*, 126(2):325–35.
- Kim, B. and Gu, M. (2003). A bioluminescent sensor for high throughput toxicity classification. *Biosensors and Bioelectronics*, 18(8):1015–1021.
- Klammer, H., Schlecht, C., Wuttke, W., and Jarry, H. (2005). Multi-organic risk assessment of estrogenic properties of octyl-methoxycinnamate in vivo a 5-day sub-acute pharmacodynamic study with ovariectomized rats. *Toxicology*, 215(1-2):90–6.
- Kubisch, R., Bohrn, U., Fleischer, M., and Stütz, E. (2012a). Cell-based sensor system using 16 cells for broad band continuous pollutant monitoring in aquatic environments. *Sensors*, 12(3):3370–3393.
- Kubisch, R., Bohrn, U., Fleischer, M., and Stütz, E. (2012b). Cell-based sensor system using 16 cells for broad band continuous pollutant monitoring in aquatic environments. *Sensors*, 12(3):3370–3393.
- Kunz, P., Galicia, H., and Fent, K. (2006). Comparison of in vitro and in vivo estrogenic activity of uv filters in fish. *International Journal of Andrology*, 90(2):349–61.
- Lagarde, F. and Jaffrezic-Renault, N. (2011). Cell-based electrochemical biosensors for water quality assessment. *Analytical and Bioanalytical Chemistry*, 400(4):947–964.

- Lee, K. and Mooney, D. (2001). Hydrogels for tissue engineering. *Chemical Reviews*, 101(7):1869–1880.
- Leung, H., Jin, L., Wei, S., Tsui, M., Zhou, B., Jiao, L., Cheung, P., Chun, Y., Murphy, M., and Lam, P. (2013). Pharmaceuticals in tap water: Human health risk assessment and proposed monitoring framework in china. *Environmental Health Perspectives*, 121(7)(7):839–846.
- Lieberzeit, P. and Dickert, F. (2007). Sensor technology and its application in environmental analysis. *Anal. Bioanal. Chem.*, 387:237–247.
- Lieberzeit, P. and Dickert, F. (2009). Chemosensors in environmental monitoring: challenges in ruggedness and selectivity. *Anal. Bioanal. Chem.*, 393:467–472.
- Locher, K. (2004). Structure and mechanism of abc transporters. *Current Opinion in Structural Biology*, 14(4):426–431.
- Ma, R., Cotton, B., Lichtensteiger, W., and Schlumpf, M. (2003). Uv filters with antagonistic action at androgen receptors in the mda-kb2 cell transcriptional-activation assay. *Toxicological Sciences*, 74(1):43–50.
- Maerkel, K., Durrer, S., Hensel, M., Schlumpf, M., and Lichtensteiger, W. (2007). Sexually dimorphic gene regulation in brain as a target for endocrine disrupters: developmental exposure of rats to 4-methylbenzylidene camphor. *Toxicology and Applied Pharmacology*, 218(2):152–65.
- Maes, J., Verlooy, L., Buenafe, O., de Witte, P., Esguerra, C., and Crawford, A. (2012). Evaluation of 14 organic solvents and carriers for screening applications in zebrafish embryos and larvae. *PLOS one*, 7(10):1–9.
- Manoguerra, A., Erdman, A., Wax, P., Nelson, L., Caravati, E., Cobaugh, D., Chyka, P., Olson, K., Woolf, L., Keyes, D., Christianson, G., Scharman, E., and Troutman, W. (2006). Camphor poisoning: an evidence-based practice guideline for out-of-hospital management. *Clinical Toxicology (Philadelphia)*, 44(4):357–70.
- Marler, J., Upton, J., Langer, R., and Vacantic, J. (1998). Transplantation of cells in matrices for tissue regeneration. *Advanced Drug Delivery Reviews*, 33(1-2):165–182.

- Marxer, C., Coen, M., Greber, T., Greber, U., and Schlapbach, L. (2003). Cell spreading on quartz crystal microbalance elicits positive frequency shifts indicative of viscosity changes. *Analytical and Bioanalytical Chemistry*, 377(3):578–586.
- Mauro, R. and Zhang, L. (2007). Unique insights into the actions of CNS agents: lessons from studies of chlorpyrifos and other common pesticides. *Central Nervous System Agents in Medicinal Chemistry*, 7:183–99.
- Meijer, H. H. M., Muilwijk, M., van den Berg, M., and Westerink, R. (2014). A comparison of the in vitro cyto- and neurotoxicity of brominated and halogen-free flame retardants: prioritization in search for safe(r) alternatives. *Archives of Toxicology*, X:X–Y.
- Mosmann, T. (1983). Rapid colorimetric assay for cellular growth and survival: application to proliferation and cytotoxicity assays. *Journal of Immunological Methods*, 65(1-2):55–63.
- Muhammad-Tahir, Z. and Alocilja, E. (2003). A conductometric biosensor for biosecurity. *Biosensors and Bioelectronics*, 18(5-6):813–819.
- Musgrove, E. and Sutherland, R. ((2009)). Biological determinants of endocrine resistance in breastcancer. *Nature Reviews Cancer*, 9(9):631–643.
- Nicholls, J., Martin, A., Wallace, B., and Fuchs, P. (2001. p. 248-251). *From Neuron to Brain*. Sinauer Associates, Inc.
- Offermanns, S. and Rosenthal, W., editors (2008). *Encyclopedia of Molecular Pharmacology*. Springer-Verlag Berlin Heidelberg New York 2008.
- Ono, K., Gondo, N., Arita, M., Fozzard, H., Hadama, T., and Uchida, Y. (1995). University of Wisconsin solution preserves myocardial calcium current response to isoproterenol in isolated canine ventricular myocytes. *Circulation*, 92(9 Suppl):452–457.
- Pegg, D. (1976). Long-term preservation of cells and tissues: a review. *Journal of Clinical Pathology*, 29(4):271–285.
- Pegg, D. (2002). The history and principles of cryopreservation. *Seminars in Reproductive Medicine*, 20(1):5–13.
- Pegg, D. (2007). Principles of cryopreservation. *Methods in Molecular Biology*, 368:39–57.



- Plagellat, C., Kupper, Furrer, R., de Alencastro, L., Grandjean, D., and Tarradellas, J. (2006). Concentrations and specific loads of uv filters in sewage sludge originating from a monitoring network in switzerland. *Chemosphere*, 62(6):915–25.
- Ploeg, R., Goossens, D., McAnulty, J., and JH Southard JH, B. F. (1988). Successful 72-hour cold storage of dog kidneys with uw solution. *Transplantation*, 46(2):191–196.
- Ramanathan, S., Shi, W., Rosen, B., and Daunert, S. (1998). Bacteria-based chemiluminescence sensing system using  $\beta$ -galactosidase under the control of the arsr regulatory protein of the ars operon. *Analytica Chimica Acta*, 369(3):189–195.
- Rauh, V., Arunajadai, S., Horton, M., Perera, F., Hoepner, L., Barr, D., and Whyatt, R. (2011). Seven-year neurodevelopmental scores and prenatal exposure to chlorpyrifos, a common agricultural pesticide. *Environmental Health Perspectives*, 119(8):1196–1201.
- Rauh, V., Perera, F., Horton, M., Whyatt, R., Bansal, R., Hao, X., Liu, J., Barr, D., Slotkin, T., and Peterson, B. (2012). Brain anomalies in children exposed prenatally to a common organophosphate pesticide. *Proceedings of the National Academy of Sciences*, 109(20):7871–76.
- Reistad, T., Mariussen, E., and Fonnum, F. (2005). The effect of a brominated flame retardant, tetrabromobisphenol-a, on free radical formation in human neutrophil granulocytes: The involvement of the map kinase pathway and protein kinase c. *Toxicological Sciences*, 83(1):89–100.
- Reistad, T., Mariussen, E., Ring, A., and Fonnum, F. (2007). *In Vitro* toxicity of tetrabromobisphenol-a on cerebellar granule cells: Cell death, free radical formation, calcium influx and extracellular glutamate. *Toxicological Sciences*, 96(2):268–278.
- Ritter, L., Solomon, K., Sibley, P., Hall, K., Keen, P., Mattu, G., and Linton, B. (2002). Sources, pathways, and relative risks of contaminants in surface water and groundwater: a perspective prepared for the walkerton inquiry. *Journal of Toxicology and Environmental Health, Part A: Current Issues*, 65(1):1–142.
- Ronkainen, N., Halsall, H., and Heineman, W. (2010). Electrochemical biosensors. *Chemical Society Reviews*, 39(5):1747–1763.

- Roy, T., Sharma, V., Seidler, F., and Slotkin, T. (2005). Quantitative morphological assessment reveals neuronal and glial deficits in hippocampus after a brief subtoxic exposure to chlorpyrifos in neonatal rats. *Developmental Brain Research*, 155(1):71–80.
- Saitakis, M. and Gizeli, E. (2012). Acoustic sensors as a biophysical tool for probing cell attachment and cell/surface interactions. *Cellular and Molecular Life Sciences*, 69(3):357–371.
- Samuelsen, M., Olsen, C., Holme, J., Meussen-Elholm, E., Bergmann, A., and Hongslo, J. (2001). Estrogen-like properties of brominated analogs of bisphenol a in the mcf-7 human breast cancer cell line. *Cell Biology and Toxicology*, 17:139–51.
- Scheirer, W. (1997). *Reporter gene assay applications*. In: *High throughput screening: The discovery of bioactive substances*. Marcel Dekker, Inc., New York, Dekker.
- Schlumpf, M., Cotton, B., Conscience, M., Haller, V., Steinmann, B., and Lichtensteiger, W. (2001). In vitro and in vivo estrogenicity of uv screens. *Environment Health Perspectives*, 109(3):239–44.
- Schlumpf, M., Harry, H., Wuttke, W., Ma, R., and Lichtensteiger, W. (2004a). Estrogenic activity and estrogen receptor  $\beta$  binding of the uv filter 3-benzylidene camphor. comparison with 4-methylbenzylidene camphor. *Toxicology*, 199(2-3):109–20.
- Schlumpf, M., Schmid, P., Durrer, S., Conscience, M., Maerkel, K., Henseler, M., Gruetter, M., Herzog, I., Reolon, S., Ceccatelli, R., Faass, O., Stutz, E., and W Wuttke, H. H., and Lichtensteiger, W. (2004). Endocrine activity and developmental toxicity of cosmetic uv filters – an update. *Toxicology*, 205(1-2):133–22.
- Schreurs, R., Sonneveld, E., Jansen, J., Seinen, W., and van de Burg, B. (2005). Interaction of polycyclic musks and uv filters with the estrogen receptor (er), androgen receptor (ar), and progesterone receptor (pr) in reporter gene bioassays. *Toxicological Sciences*, 83(2):264–72.
- Scudiero, D., Shoemaker, R., Paull, K., Monks, A., Tierney, S., Nofziger, T., Currens, M., Seniff, D., and Boyd, M. (1988). Evaluation of a soluble tetrazolium/formazan assay for cell growth and drug sensitivity in culture using human and other tumor cell lines. *Cancer Research*, 48(17):4827–4833.
- Senveli, S. and Tigli, O. (2013). Biosensors in the small scale: methods and technology trends. *IET Nanobiotechnology*, 7(1):7–21.

- Service, R. (2000). Tissue engineers build new bone. *Science*, 289(5484):1498–1500.
- Shen, M., Cheng, J., Wu, R., Zhang, S., Mao, L., and Gao, S. (2012). Metabolism of polybrominated diphenyl ethers and tetrabromobisphenol a by fish liver subcellular fractions in vitro. *Aquatic Toxicology*, 114-115:73–9.
- Shimada, T. and Fujii-Kuriyama, Y. (2004). Metabolic activation of polycyclic aromatic hydrocarbons to carcinogens by cytochromes p450 1a1 and 1b1. *Cancer Science*, 95(1):1–6.
- Slotkin, T. (2004). Cholinergic systems in brain development and disruption by neurotoxicants: nicotine, environmental tobacco smoke, organophosphates. *Toxicology and Applied Pharmacology*, 198(2):132–51.
- Slotkin, T. and Seidler, F. (2012). Developmental neurotoxicity of organophosphates targets cell cycle and apoptosis, revealed by transcriptional profiles in vivo and in vitro. *Neurotoxicology and Teratology*, 34(2):232–41.
- Sorensen, H., Goldsmith, J., and Sangalli, L. (2013). An introduction with medical applications to functional data analysis. *Statistics in Medicine*, 32:5222–5340.
- Southard, J. and Belzer, F. (1995). Organ preservation. *Annual Review of Medicine*, 46:235–247.
- Stütz, E. (2008). Analyse von metabolischen effekten von cucl, cucl<sub>2</sub> im vergleich zu cuso<sub>4</sub> auf hepg2-zellen. Technical report, Siemens AG.
- Stütz, E. and Kubisch, R. (2010). Zellkulturoptimierung am beispiel der v/) zellen, sowie testung mit (zwei) ausgewählten substanzen. Technical report, Siemens AG.
- Su, L., Jia, W., Hou, C., and Lei, Y. (2011). Microbial biosensors: A review. *Biosensors and Bioelectronics*, 26(5):1788–1799.
- Subramanian, G., editor (2004). *Antibodies: Volume 1: Production and Purification*. Springer, New York, NY, USA.
- Sumantran, V. (2011). Cellular chemosensitivity assays: an overview. *Methods in Molecular Biology*, 731:219–236.

- Sun, T., Tsuda, S., Zauner, K., and Morgan, H. (2010). On-chip electrical impedance tomography for imaging biological cells. *Biosensors and Bioelectronics*, 25(5):1109–1115.
- Takenaka, S., Yamashita, K., Takagi, M., Uto, Y., and Kondo, H. (2000). Dna sensing on a dna probe-modified electrode using ferrocenylnaphthalene diimide as the electrochemically active ligand. *Analytical Chemistry*, 72(6):1334–1341.
- Tang, J., Cao, Y., Rose, R., Brimfield, A., Dai, D., Goldstein, J., and Hodgson, E. (2001). Metabolism of chlorpyrifos by human cytochrome p450 isoforms and human, mouse and rat liver microsomes. *Drug Metabolism and Disposition*, 29(9):1201–4.
- Thévenot, D., Toth, K., Durst, R., and Wilson, G. (2001). Electrochemical biosensors: recommended definitions and classification. *Biosensors and Bioelectronics*, 16(1-2):121–131.
- Thomas, H., Reeves, G., and Key, T. ((1997)). Endogenousestrogenandpostmenopausal breast cancer: aquantitative review. *Cancer Causes and Control*, 8(6):922–928.
- Ullah, S. and Finch, C. (2013). Applications of functional data analysis: A systematic review. *BMC Medical Research Methodology*, 13(43).
- van Meerloo, J., Kaspers, G., and Cloos, J. (2011). Cell sensitivity assays: the mtt assay. *Methods in Molecular Biology*, 731:237–245.
- Wahlberg, J., Love, R., Landegaard, L., Southard, J., and Belzer, F. (1987). 72-hour preservation of the canine pancreas. *Transplantation*, 43(1):5–8.
- Wang, D., Fulthorpe, R., Liss, S., and Edwards, E. (2004). Identification of estrogen-responsive genes by complementary deoxyribonucleic acid microarray and characterization of a novel early estrogen-induced gene: Eeig1. *Molecular Endocrinology*, 18(2):402–411.
- Wang, X., Terasaki, P., Rankin, G., Chia, D., Zhong, H., and Hardy, S. (1993). A new micro-cellular cytotoxicity test based on calcein am release. *Human Immunology*, 37(4):264–270.
- WHO (1995). *Environmental health criteria 172. Tetrabromobisphenol A and derivatives*. World Health Organization, Geneva, Switzerland.
- WHO (1997). *Environmental health criteria 192. Flame retardants: A general introduction*. World Health Organization, Geneva, Switzerland.

- WHO (1998). *Environmental Health Criteria 229. Selected Nitro- and Nitrooxy-polycyclic aromatic Hydrocarbons*. World Health Organization, Geneva, Switzerland.
- WHO (2004). *WHO Specifications and Evaluations for Public Health Pesticides*. World Health Organization, Geneva, Switzerland.
- Windmill, K., McKinnon, R., Zhu, X., Gaedigk, A., Grant, D., and McManus, M. (1997). The role of xenobiotic metabolizing enzymes in arylamine toxicity and carcinogenesis: Functional and localization studies. *Mutation Research / Fundamental and Molecular Mechanisms of Mutagenesis*, 376(1-2):153–160.
- Wolf, B., Brischwein, M., Baumann, W., Ehret, R., and Kraus, M. (1998). Monitoring of cellular signalling and metabolism with modular sensor-technique: The physiocontrol-microsystem (pcm<sup>®</sup>). *Biosens. Bioelectron.*, 13:501–509.
- Xiao, C. and Luong, J. (2003). On-line monitoring of cell growth and cytotoxicity using electric cell-substrate impedance sensing (ecis). *Biotechnology Progress*, 19(3):1000–1005.
- Xu, H., Blair, N., and Clapham, D. (2005). Camphor activates and strongly desensitizes the transient receptor potential vanilloid subtype 1 channel in a vanilloid-independent mechanism. *Journal of Neuroscience*, 25(39):8924–37.
- Yager, J. and Davidson, N. ((2006)). Estrogencarcinogenesisinbreastcancer. *New England Journal of Medicine*, 354(3):270–282.
- Yagiuda, K., Hemmi, A., Ito, S., Asano, Y., Fushinuki, Y., Chen, C., and Karube, I. (1996). Development of a conductivity-based immunosensor for sensitive detection of methamphetamine (stimulant drug) in human urine. *Biosensors and Bioelectronics*, 11(8):703–707.
- Ye, Q., Zünd, G., Benedikt, P., Jockenhoevel, S., Hoerstrup, S., Sakyama, S., Hubbell, J., and Turina, M. (2000). Fibrin gel as a three dimensional matrix in cardiovascular tissue engineering. *European Journal Cardio-Thoracic Surgery*, 17(5):587–591.
- Young, S., Wong, M., Tabata, Y., and Mikos, A. (2005). Gelatin as a delivery vehicle for the controlled release of bioactive molecules. *Journal of Controlled Release*, 109(1-3):256–274.
- Zuccarini, P. (2009). Camphor: risks and benefits of a widely used natural product. *Journal of Applied Sciences and Environmental Management*, 12(2):69–74.

## Acknowledgment

Evamaria Stütz has made this PhD position at Siemens in Munich possible. It was a great experience to work with her. During the first two years of my thesis Ulrich Bohrn was also doing his PhD in Evi's lab. Thanks to Ulrich Born for the invaluable discussion.

Karen Fuchs made the mathematical part of this thesis possible.

Thanks to my first advisor Prof. Stefan Wölfl for his constant guidance and support and to Prof. Michael Wink for his great advice.

My parents Gabriel and Jarmila and my sister, Jarmi, have always been there for everything. Thanks for your patience and love

Thanks to Karl Hacker and Pauble Maurey for helping me relax.

Julia and Rocky, thanks for being there.



Rocky, simply the best